

NIGHTFALL
Special Report

MAGELLANIC MYSTERY

A photograph of a dark, wooded path leading into the distance. The path is illuminated by a bright light source at the far end, creating a strong perspective effect. The surrounding trees are silhouetted against a dark sky.

ABSTRACT

Magellan's Ghost, to paraphrase Winston Churchill, is a riddle wrapped in a mystery inside an enigma. Between 2005 and 2017 a small group of nine experienced amateur astronomers have reported a band of visually faint emission which begins at the base of the LMC, parallels the long axis of Chameleon, brightens somewhat as it nears Apus, and finally fades from view in Triangulum Australe. It is variously described as a 'broad, even band of emission,' 'a stripe 3° to 4° wide,' 'a cometary tail streaming from the LMC,' 'as wide as the LMC itself,' 'about as bright as the the Zodiacial light 50° above the horizon,' and 'resembles an elongated form of the gegenschein.'

Yet despite all the avid sky gazers who reside in the southern hemisphere, plus visitors from the north, no one else has mentioned it. Historically, it has been imaged only twice: once in 1955 and again in 2010. The two references to the emission in the historical literature are vague at best. Only one professional astronomer has reported seeing the emission. It has been ignored by the larger professional community. There is no mention of it in the literature.

The various observations can be summarised as a broad swath with a surface brightness about 24 – 25 MPSAS that extends about 30° from the leading edge of the LMC in Mensa as far as Apus. All the observations were made in exceptionally dark, non light-polluted seeing conditions in remote locations in the Chilean Andes, Namibia, the Karoo of South Africa, and the Outback in Australia. At the observers' latitudes the Large Magellanic Cloud at meridian is 45° to 55° elevation during the darkest hours of the night. The observers commonly report that they able to see the Chameleon Dark Clouds and the Dark Doodad filament in Musca without optical aid.

The emission has not been much pursued by amateur astro-imagers. Only a handful of images show it at all. It is simply too big and too faint. If it does appear in an image, it is usually taken as noise to be processed out of the view. The three images recorded by Colin Robson specifically for this report suggest a structure of three clumpy soft-edged patches about 3° to 4° each on the long axis, beginning in the LMC southeastern quadrant. It passes through Mensa, briefly fades under the central part of Chameleon, brightens a bit in Apus, and finally vanishes into Triangulum Austral.

The described morphology of the patches differs from the filamentary, striated Galactic cirrus (GC) that pervades the region. The numerous Galactic cirrus patches in the Chameleon/Apus/Octans region seldom exceed a surface brightness of <26.5 MPSAS, while the emission observers report is ± 24.5 MPSAS.

A literature search was conducted to discover whether the LMC-SMC self-interactions or the ongoing Magellanic interaction with the Galactic disc might explain the observed emission. The results were nil. The phenomenon observers report is too big and too bright to be associated with any disturbance of Magellanic matter by ram pressure or tidal forces.

In sum, we have a series of observations of an optical structure which cannot be traced definitely to a probable cause, situated in a region whose complexity provides multiple false leads.

But since we are on the subject of false leads, here is the most piquant clue of all: 357 years ago Johannes Bayer's 1661 *Uranometria* was the first star map to depict his freshly invented asterisms to put a human stamp on the starry sky. For the first time ever, we knew of Tucana, Ara, Grus, Pavo, Apus, Musca, Chameleon.

Look carefully at Bayer's map on the next page. You just might see the first Galactic clue ever recorded by humankind: Apus's feathery tail wafts beneath Chameleon before fading into what is now Mensa. It is actually a fair approximation of where Magellan's Ghost lies in that part of the sky today. Bayer could not have possibly seen Magellan's Ghost. Yet there it is, in plain sight, the smoking gun on the table so astutely noticed by Sherlock Bayer. Is Apus's tail a clue? Or false lead?

The Churchillian riddle is this: Have nine observers with credible histories been collectively seized with averted imagination? Are all the other observers simply not paying attention? Are observing conditions simply not good enough elsewhere?

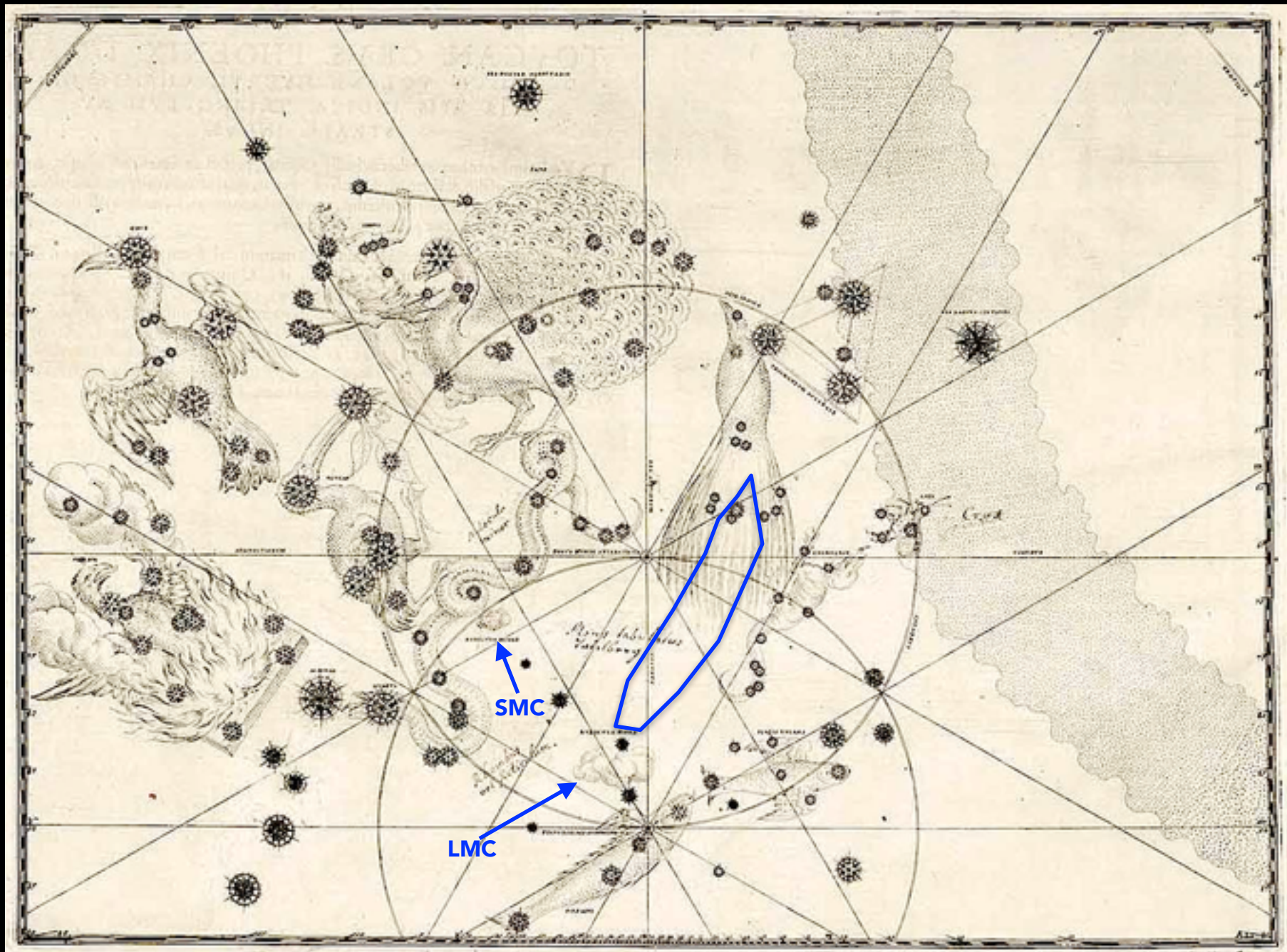
The mystery is this: What are we seeing?

And now the enigma. What astrophysical phenomenon could cause such a spatially huge structure to shine just brightly enough to be seen with the human eye?

Let's find out.

=[Douglas Bullis, Nightfall, Deep-Sky Observers Section of the Astronomical Society of South Africa \(ASSA\)](#)

- [Dave Riddle](#)
- [Timo Karhula](#)
- [Brian Skiff](#)
- [Hisayoshi Kato](#)
- [Chris Beere](#)
- [Dana De Zoysa](#)
- [Robin Hegenbarth](#)
- [Colin Robson](#)



Johann Bayer's 1661 *Uranometria* invented twelve new constellations in the southern hemisphere sky unknown to ancient Greece and Rome. His Chart 49 plotted Phoenix, Tucana, Grus, Pavo, Hydrus, Apus, Tri. Australe, Crux, Chameleon, Volans, Dorado. At the risk of cartosphemery, the LMC and SMC are identified, and the approx. position of Magellan's Ghost has been outlined with a blue swatch.

Magellanic Mystery

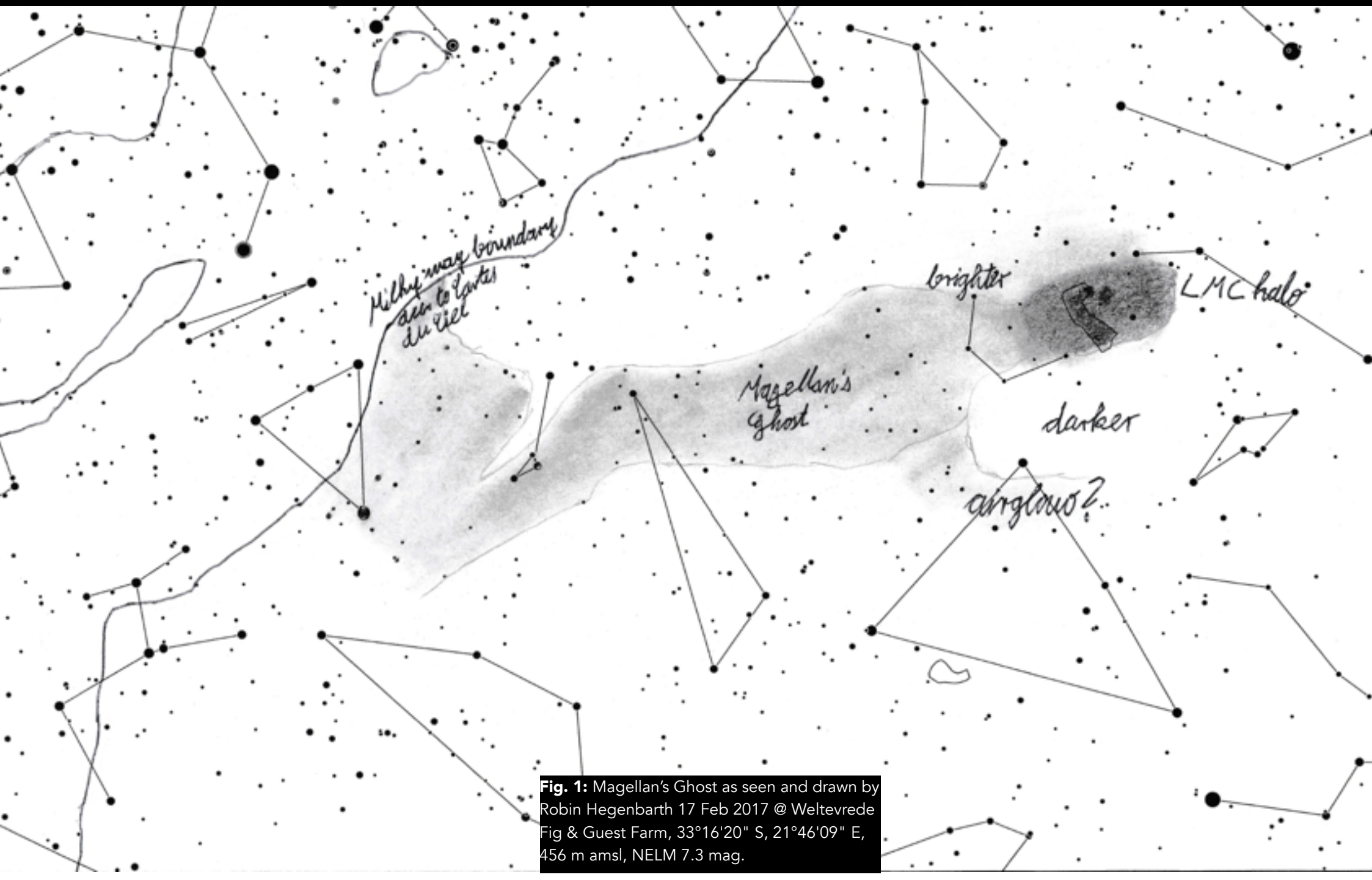


Fig. 1: Magellan's Ghost as seen and drawn by Robin Hegenbarth 17 Feb 2017 @ Weltevreden Farm, 33°16'20" S, 21°46'09" E, 456 m amsl, NELM 7.3 mag.

Figment or Filament?

As far back as Pannekoek 1928 sporadic reports in the literature mention a faint, inexplicable, “ghost streamer” in the southern skies, seemingly associated with the Large Magellanic Cloud. The emission is described as about the same surface brightness as the faint ends of the Zodiacal light, the gegenschein, or the Sculptor Dwarf galaxy in a six-inch telescope.

For this report we adopt the name “Magellan’s Ghost” as an easy to remember rubric.

Three reports in the professional literature between 1928 and 1957 vaguely refer to the emission but do not examine whether it is real or what it is made of.

The reports from the amateur community come from only nine experienced visual observers. The first mention was in 1989 and detailed observer reports were published sporadically between 2005 and 2018. All observers mention serendipitous first sightings in which the Ghost appeared as a band of light bright enough to be noticed at first glance and without optical aid, but only in the darkest skies.

The professional astronomer Brian Skiff, presently with Lowell Observatory near Flagstaff, Arizona USA, discussed the emission in a Yahoo *Amastro* post in 2011. Skiff reports that he first noticed it at Las Campanas in the Chilean Andes in 1989, and had noted it several times since.

This is a rather small sample considering the purported size and brightness of the emission and the ease with which was seen. Given the large number of enthusiastic stargazers who live under Southern skies but have never reported the emission, it seems odd that only visitors from Europe and the USA somehow manage to see what the locals routinely miss. Only one observer who has reported the Ghost actually lives in the Southern hemisphere, Dana De Zoysa in South Africa. One northern observer, Timo Karhula of Sweden, is fortunate enough to own a family holiday home in a remote small town in the Western Outback of Australia. Hence he has been able to log the Ghost numerous time over the years.

Foreigners who visit southern skies for the stargazing typically lodge in one of the Southern Hemisphere’s astronomy-specific guest farms, e.g.,

[Hakos Farm](#) or [Tivoli Guest Farm](#) in Namibia. These establishments are located in exceptionally dark locales far from human-originated lights. They target the sophisticated deep-sky astrophotographer/observer market with sophisticated pro-am telescopes, cameras, and tracking gear. Few astrophotographers are equipped to image 30° fields or extended sub-Mv 25 objects.

More germane is the sky quality where the observations occur. If it seems odd that so few have seen this faint emission but so many experienced observers have not, there are several plausible explanations:

- Skies have to be nearly SQM 22.00 perfect. Very few people have access to such skies.
- Light pollution has to be essentially zero, which means high-altitude remote countryside. High desert is best, but who wants to live there? All observers agree that even small amounts of light pollution renders observing the emission difficult to impossible.
- Observers have to be alert enough to stop, look, and ask, "Is that faint flare a real phenomenon or an illusion caused by the proximity of the LMC to the Galactic disc?"
- At roughly 3° wide and 30° long (**Fig. 1**), the Ghost is so extended and unusual that no one really expects to see it. It's easy to shrug off something that's improbable in the first place. How many observers expect to come across a 30-degree long comet tail without a comet attached?

Most observers agree that the minimum naked-eye visible magnitude is 7.2. Few skies on earth are that dark. In the southern hemisphere this means the Chilean Andes, Namibia, the Karoo region of South Africa, and several locales in Australia.

First Reports, June 2005

The first to see and describe this mysterious Ghost in a public forum was the amateur astronomer David Riddle. [On 4 June 2005 he reported](#),

I recorded three separate observations in my notebook. The filament is a surprisingly easy naked-eye object. After making an adjustment for the different altitudes of the filament and the Zodiacal Band, I judged the objects to be of about equal brightness. To my eye, the combination of the Large Magellanic Cloud and the "LMC filament" makes one of the more bizarre sights in the entire sky -- the LMC appearing as a brilliant cometic "coma" with a ghostly "tail" (~ 30° reaching towards the Milky Way. This "deep-sky comet" is certainly an unusual combination of galactic and extragalactic objects!

The nature of the filament remained a puzzle until I had a few evenings of extraordinary atmospheric transparency to look closely and carefully at the object. Using my 70 mm "Pronto" refractor with a 31 mm Nagler and a pair of excellent (borrowed) 8 x 42 Swarovski binoculars, I concluded the filament was not a product of massed groups of faint stars or an unusually elongated "absorption hole." The Chameleon I and II molecular clouds were easily seen with the unaided eye on these evenings, so I'm fairly confident that dark nebulae do not play a role in defining the filament.

I noted that the filament "touched" the LMC but the part of the filament closest to the Magellanic Cloud might be a part of a halo surrounding (and belonging to) the LMC. The other end (near Beta Apodis, HD 149324) blended into the Milky Way. I thought the (relatively) brightest part of the filament to be in the vicinity of Eta Octantis (HD 96124).

After making my notes, I turned to the MegaStar program and my nebulae "atlas" to see if the observed positions really lined up with the catalogued nebulae. I was delighted to see that observation and theory matched up very well.

I've concluded that the "LMC Filament" is most likely an unusually bright (albeit low surface brightness), extended reflection nebula. It does indeed seem possible that a 30 degree long nebular complex runs from the LMC to the Milky Way. Nothing else seems to explain its visibility so well.

[\Dave Riddle, reporting in Amastro in June 2005](#)

[Reply on same thread by Brian Skiff](#), Lowell Observatory, 4 June 2005:

Very interesting if this is indeed the case. I guess I'm surprised since my impression of it was that it was very uniform in brightness, much like the zodiacal band (as you describe) between the gegenschein and the more conical part of the zodiacal light. At least I'm glad I haven't been imagining it!

\Brian

Dave Riddle responded the next day:

Brian:

You certainly weren't imagining this thing! An unintended test of the filament's visibility happened one night while I walking to my room from the Sossusvlei Mountain Lodge observatory. A quick look skyward before calling it quits for the night revealed the filament before I had time to orient myself to the sky and before the familiar constellation patterns fell into place. No "wishful seeing" here – the filament was visible at a glance.

\Dave Riddle

The most important points in these posts are (a) the immediate obviousness of the object; (b) its relatively uniform structure, brightness, and size; and (c) Dave Riddle's correct guess that the object was Galactic cirrus made somehow brighter than the average 26.5–28.0 MPSAS surface brightness of Galactic cirrus in the S. equatorial polar region. Hence the question raised by these initial sightings is, "How does the background cirrus become illuminated to 24–25 MPSAS to be visible to the unaided eye?"

Subsequent reports, 2007–2018

Four years later, Dave Riddle recalled his early sightings of the emission on the Yahoo Amateur Astronomy Mailing List *Amastro*:

The "bridge" that runs from the Milky Way to the LMC is, in my opinion, one of the most spectacular naked-eye objects in the heavens. Resembling a deep-sky comet with the LMC as the coma and a faint tail stretching in the direction of Triangulum Australe. I made few notes on this object when I was in Namibia a few years ago:

On two different evenings, I noted the object to be a little brighter in the area of Eta Octantis (the approximate position of the extended reflection nebula GN 13.23.0.01). The bridge was difficult to trace any closer to the Milky Way than the area of Beta, Gamma and Delta Apodis due to the faint extensions of the Galaxy. I thought this low surface brightness filament to be about as bright as the Zodiacal Band (in other words, not all that hard to see if the sky is dark).

I am pretty confident that this thing is composed of galactic cirrus clouds. It can be demonstrated that a number of obscure bright nebulosities (from the *Atlas of Galactic Nebulae*) compose the filament.

Brian Skiff thereupon recalled his own early memories of the emission:

I saw it 20 years ago from Chile [1989]. . . it is about as bright as the zodiacal band on either side of the gegenschein, and makes a bee-line from the LMC toward the galactic center. If you trace this on a wide-field sky chart, you'll see that it goes right over the south celestial pole then merges with the Milky Way somewhere in the vicinity of alpha TrA. Its texture is very smooth, not unlike the zodiacal band. From Las Campanas on those February/March evenings, with the LMC on the meridian at dusk, it was obvious as a band heading straight down to the horizon. By morning at around 12h sidereal time, it was better placed — the LMC setting in the southwest, and the merge-point well

up in the southeast. It might be worth noting that patchy strands of the Milky Way connect (almost) the LMC to the galactic plane from the direction of the False Cross (delta Vel/IC 2391 area). That was described by de Vaucouleurs back in the 1950s when he was at Mount Stromlo. This feature is rather patchy, and is clearly just extended Milky Way star clouds.

In another undated post in that same thread came from the Swedish astronomer Timo Karhula, visiting Australia at the time:

I and two prominent Finnish amateur astronomers [Iiro Sairanen and Esko Luukkonen] had the privilege to visit and stay in a distant farm in the Outback, Western Australia. The nearest town worth mentioning was 130 km away. The skies were overwhelming! Both SQM meters showed 22.08 and 22.09. Limiting magnitude naked eye was between 7.6 and 7.9. When Omega Centauri rose, I could see 1000s of stars in its outskirts with only 25x100 binoculars.

The Gegenschein in eastern Taurus could be seen just sitting next to the Milky Way. The zodiacal band was bright and went from horizon to horizon. I found a bridge of light connecting the Large Magellanic Cloud with the Milky Way. It was a rather faint lane of light, as wide as LMC and about as faint as the zodiacal band on both sides of the Gegenschein

I asked Brian Skiff about the material between LMC and Milky Way. Brian confirmed my observation about this light between LMC and the Norma Cloud.

A few posts later in the same thread Timo Karhula elaborated on his Australia observation:

This light-bridge was not that particularly difficult to spot in these conditions. After midnight it was pointing more or less south. It looked like a waterfall tumbling from LMC. Later in the night, this feature had turned clock-wise so I was sure it was a real thing.

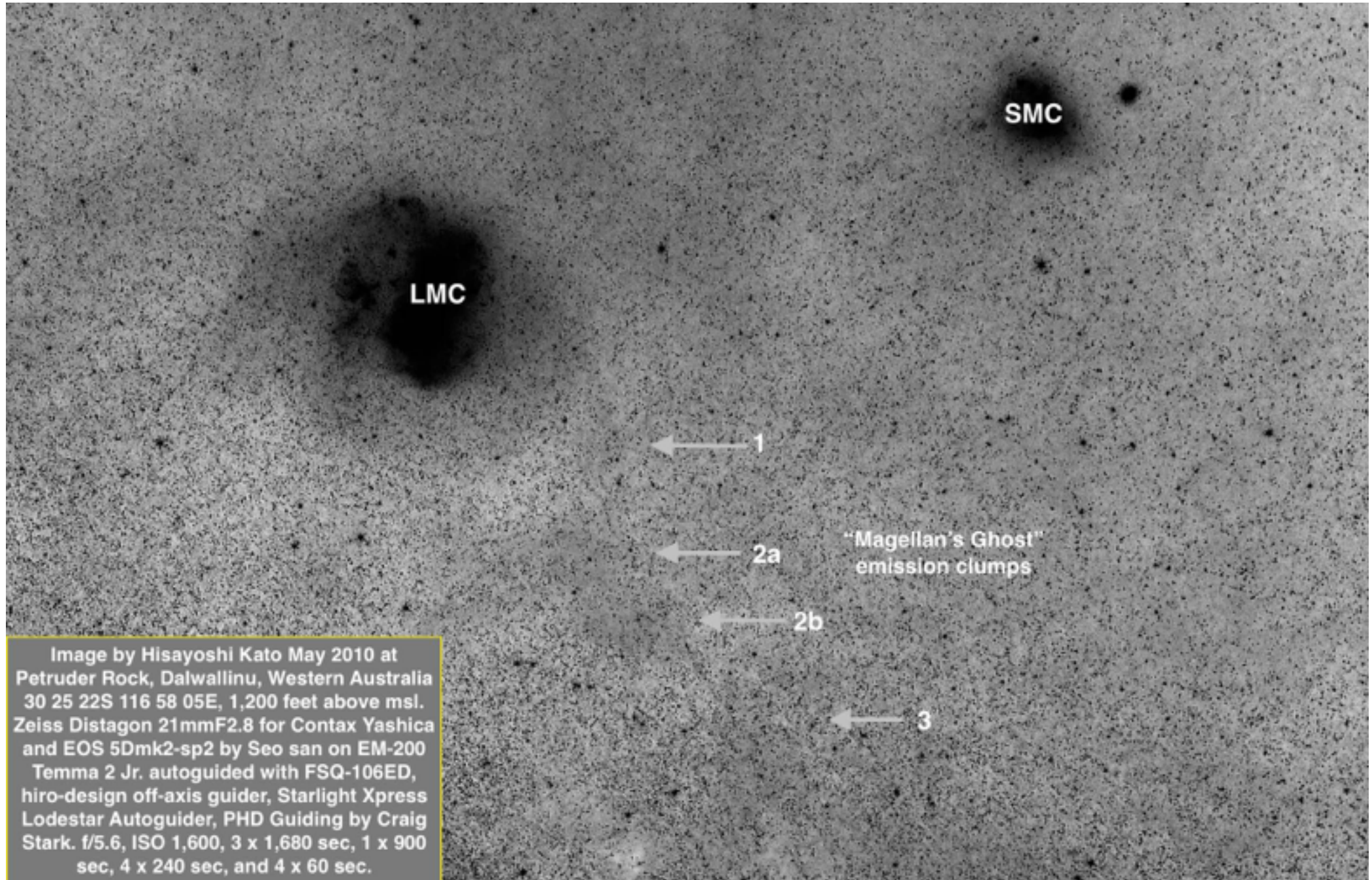


Fig. 2: Large-field mosaic imaged by [Hisayoshi Kato 2010](#). The [original image](#) has been rotated 180° and processed to emphasise the green band. First published in the [Australian amateur forum IcelnSpace 12 Apr 2010](#) in post by IIS forum member [Bert Van Donkelaar](#). For a technical discussion of the processing that produced this image, [see here](#). Hisayoshi Kato's other images are located [here](#) and [here](#).

Our SQM-L and another SQM was about 22.0 right after the end of my galaxy challenges were successful with 25x100 binoculars. These were the Sculptor Dwarf, Fornax Dwarf, and IC 1613 in Cetus. All of these were definitive sightings and their sizes and orientations corresponded very well with *Uranometria*.

Brian Skiff informed me on December 19, 2009, that he had once seen an image of the LMC bridge taken with a "parking lot" fish-eye lens at Las Campanas, Chile:

"Greetings Timo. The bridge from the LMC toward the galactic center that you describe is just what I saw on both of my trips to Las Campanas in Chile. It basically extends straight south from the LMC to the south celestial pole, then follows a great-circle approximately to the Norma starcloud (or, alpha TrA, as you say) — it runs into the Milky Way, so you lose it much like the zodiacal band close to the Milky Way. I, too, have wondered why it is not mentioned anywhere that I know of. I remember once seeing an image taken at CTIO using what they called the "parking lot camera", a wide-field lens + CCD. This image showed the feature, but I do not know where to find that image again."

\Timo

Reports in the popular astronomy forums

The visibility of Galactic cirrus to the unaided eye has been an occasional topic on the popular amateur astronomy forums [Cloudy Nights](#) and [IceInSpace](#). The subject was first raised in 2005 when the American enthusiast [Steve Mandel](#) compiled his [The Unexplored Nebula Project](#). When descriptions of a large, bright band of mysterious light seemingly emanating from the LMC first appeared in 2010, interest in barely visible extended objects acquired fresh energy, e.g. [Cloudy Nights 26 Dec 2009](#); [Cloudy Nights 27 May 2011](#), [IceInSpace](#) (Australia) 11 Nov 2010; this thread links to [the only three images of the Ghost](#) prior to new images made for this study by Australian astrophotographer [Colin Robson](#) in 2018.

Timo Karhula 11 Nov 2010 writing in [IceInSpace](#).

With our unaided eyes, we noted how the light band reached from the LMC, went due south, passed the south celestial pole and continued along a great circle towards the Norma star cloud in the Milky Way. The materia bridge was nearly as wide as LMC itself and more than 40° long. In surface brightness it was comparable to the faintest part of the zodiacal band and maybe half of the gegenschein's. In the beginning of the night, it reminded me of a waterfall that disappeared into the airglow near the horizon. Later in the night, this phenomenon had rotated clock-wise around the south celestial pole which proved that this was indeed an astronomical feature that followed the earth's rotation. The materia bridge disappeared in Triangulum Australe, near its alpha star, Atria. It is most remarkable that nobody (as far as I know) has taken photographs of the light bridge! It is neither visible on Axel Mellinger's panorama of the Milky Way which reaches the surface brightness level of about 24 magnitudes per square arc-second. This phenomenon should not be confused with the Magellanic Stream, which is only visible in radio wavelengths and streams in opposite direction from the SMC to the outskirts of the constellation Andromeda. One theory is that the observed light bridge is the combined light from millions of faint stars or gas that Milky Way has stripped from our satellite galaxy due to tidal effects at an earlier close passage. The light might also originate from intergalactic cirrus like the clouds that can be seen near M81 in extremely deep photographic exposures. Spectroscopic analyses of the light should settle this matter. Curiously enough, the southern celestial pole is involved in a faint band of light while the northern pole, near Polaris, is the starting point of a dark lane in the Milky Way. I suspect a sky capable of showing stars to magnitude 7.5 or has a darkness of about SQM 21.9 is necessary to show the light bridge between the LMC and the Norma Star Cloud. Has anyone on this forum seen the bridge of light? It would be very strange if nothing more is known of this naked-eye feature!

Timo Karhula writing in IceInSpace 8 April 2011

I recently saw another glimpse of the LMC "light bridge" — on TV! It was in a nature program from the Atacama desert. On a time-lapse sequence showing the Chilean observatories in the foreground, the Magellanic Clouds were revolving around the south celestial pole (SCP). From the LMC, I could faintly see the "light bridge" going towards the Milky Way in Triangulum Australe / Norma. This was apparently shot with a b/w CCD-camera and a very wide field or a fish-eye lens.*

Editor: The time-lapse video Karhula cites was apparently extracted from the Las Campanas "Parking Lot" webcam. This was an all-sky video camera installed so anyone with the web link could see what was in the Chilean night sky at the moment. The camera operated only at night. On page 7 above, Brian Skiff mentions to the same image Karhula describes.

Report by Timo Karhula posted on amastro 5 Feb 2016:

I observed at two sites east of Geraldton, W.A. One site is about 50 km due east; the sky darkness on different nights were \pm SQM-L 21.8, with one night at 21.9. The second site is another 50 further eastward, where the skies were SQM-L >22.0. The solar counter-glow of the Gegenschein was located between M44 in Cancer and Leo. It was easily seen, somewhat elliptical in shape, and about 15–20 degrees in height. I could discern the zodiacal band stretching out in both directions from the Gegenschein. The zodiacal band to the right (east) was harder to follow because the bright planets Jupiter, Mars, and Saturn dominated the view.

The LMC 'bridge of light' [called 'Magellan's Ghost' in this paper =ed.] stretches from the SE quadrant of the LMC all the way to Triangulum Australe. Since I already knew from prior observations what the feature looks like, it was not that difficult to spot. It was a 40-degree long band of faint light that was best seen when LMC was at the same altitude as or above the south celestial pole.

The contributions to the background light due south were: Upward to the left is the black sky. Below/to the right is the bright Milky Way, black sky, "LMC-bridge", black sky and below it the airglow. The best contrast is the black sky between the LMC band of light and the Milky Way and then it gets darker again on the other side.

Report by Robin Hegenbarth 9/10 March 2016

My observation occurred at Elandsberg Cottage, Tankwa Karoo National Park ($32^{\circ}10'25''$ S, $19^{\circ}58'31''$ E, 594 m amsl) on March 9/10, 2016, 8:40 pm to 12:30 am local time, unaided eyes only. The naked eye limiting magnitude of 7.6 was confirmed with a selection of non-variable stars in the constellation of Volans near zenith and the Tycho-2 star catalogue. I observed a band as wide as the Large Magellanic Cloud that started at the SE base of the Large Magellanic Cloud, initially leading towards the constellation of Musca. Before reaching Musca it curved downwards towards Alpha Trianguli Australis. The region at which it curved downwards was approximately where the star Alpha Chameontis is located. The band that I saw was approximately as faint as the faintest parts of the zodiacal band (which was visible almost across the sky except for the parts that crossed the Milky Way and the brightest parts of the natural airglow). I can definitely say that this band was brighter than the patches of night sky between the Magellanic clouds and between the LMC and Canopus. The feature rotated clockwise around the celestial pole during the night. I could not see this feature when limiting magnitudes were 6.8 – 7.1.

As of April 2018 the complete list of sightings is as follows:

- Antonie Pannekoek (uncertain), 1926–28 Java, Indonesia
- Sergey Gaposchkin, (uncertain), 1956 Mt Stromlo, Australia
- Brian Skiff, 1989 & 1993 Las Campanas Observatory, Chile
- David Riddle, 2005 Sossusvlei, Namibia
- Timo Karhula, 2009 Nangerwalla, Western Australia
- Iiro Sairanen, 2009 Nangerwalla, Western Australia
- Esko Luukkonen, 2009 Nangerwalla, Western Australia
- Chris Beere, 2011 Tivoli Farm, Namibia
- Dana de Zoysa, 2013–2018 Weltevreden Farm, South Africa
- Robin Hegenbarth, 2016, Tankwa Karoo & 2018 Weltevrede Farm, South Africa

Observations by Dana De Zoysa at Weltevreden Farm, Nieu Bethesda, Karoo region of the East Cape province:

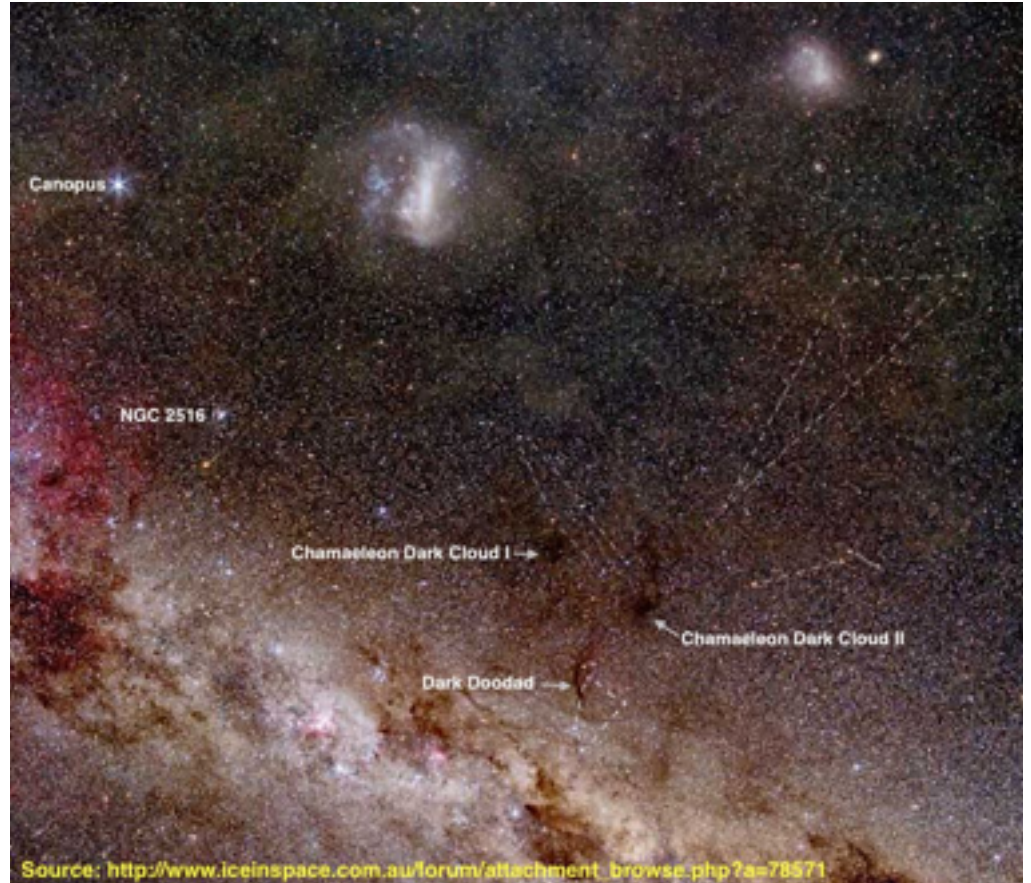
My first sighting of this feature in December 2012 was a brief glimpse of an ephemeral overbrightening that resembled a cometary tail emanating downward from the LMC toward the S quadrant of Chameleon. It was about half the brightness of the Gegenschein at the time. The brightening gave the impression of a bow wake trailing behind the LMC rather like the streamer behind the nucleus of a faint comet.

I didn't notice the emission again till January the next year, on a clearer-than-average night (average is \pm mag 7.5 visually). Again I initially detected it serendipitously about 11:00 pm. It was bright enough in averted vision to trace as a comet-like streamer from the E side of the LMC all the way over to Apus, where it dissolved into the Galactic glow. At the time I hadn't read any of the amateur forum posts about it, so I mentioned it on *Cloudy Nights*. Timo Karhula responded immediately describing his own observations. This brought me to scan the area more frequently and log the results. Like many observations, having once seen it, it became easier, given relatively similar conditions. I have observed the emission several times every year thereafter.

Over time the feature became familiar as a faint comet-tail patch streaming away from the LMC through Mensa all the way to Apus. It is slightly brighter and longer on the S side and is about the same width as the leading edge of the LMC. The northerly 'wing' fades quickly, which suggests that is part of the LMC's spiral disc/ halo.

The emission fades briefly below the vee of Mensa's brightest stars. It reappears as two slightly luminous overdensities about 2° SE of the α and θ Chameleontis star pair. These two patches are the most luminous of the lot — a term used advisedly because the visual impact is something faint on top of something fainter. These two emission blobs are $\sim 3^\circ$ in on their longest axes and have a flat luminosity distribution. They appear to fade into star-poor fields in the SW and NE quadrants.

These emissions are so ephemeral that they cannot be seen when the limiting visible magnitude falls below 7.0. Two criteria that can be used to corroborate the emission visibility are (a) the Chameleon Dark Clouds I and II are visible in roughly their shapes as seen in photographs; and (b) the Dark Doodad is visible in averted about 40% of the time.



Source: http://www.iceinspace.com.au/forum/attachment.php?attachment_id=78571

Fig. 3: This image shows the subtleties of the emission patches as described by Dana De Zoysa in S. Africa 2012–2016. They appear to be a large continuous band of emission (as drawn in the image above) overlain by an optically thin extinction patch running approx. normal to the emission. In the field they are less distinct than in this image.

Source: [2010 image by Hisayoshi Kato](#) using an apo-EL-Nikkor 21mm at F5.6N and EOS 5Dmk2-sp2 by Seo san on EM-200 temma 2 Jr. autoguided with FSQ-106ED, hiro-design off-axis guider. Exposure: 3 times x 26 minutes, 1 x 15 min, 4 x 4min, 4 x 1 minute at ISO 1,600.

Brian Skiff on imaging the Magellanic feature

In a [9 April 2011 post on amastro](#), the [Amateur Astronomy Mailing List](#), Brian Skiff of the Lowell Observatory suggested the following tips for astrophotographers interested in imaging the then-unnamed Magellan's Ghost:

A couple of points to mention in regard to picking it up both visually and photographically. The best time for viewing is at around sidereal time 12h, when the LMC is over in the west and the galactic center is rising in the east. Look along the line between the two, which goes beneath the Milky Way.

For imagers:

- 1) It is worth emphasizing that the feature is very large, and of low (but not especially low) surface brightness, about like that of the zodiacal band on either side of the Gegenschein. Thus the camera lens should be stopped down to avoid vignetting.
- 2) In addition, imagers are fond of processing their results to "flatten out" such large scale features --- obviously you will miss it if you apply any cosmetic processing of this sort: turn off that button in your software!
- 3) Another point is to use a filter or do whatever is necessary to avoid picking up the night-airglow pattern; if the detector is sensitive in the far-red, this could swamp the "light bridge". The goal would be to record only in the visual (or blue/green/yellow) range of wavelengths, excluding H-alpha and redder.

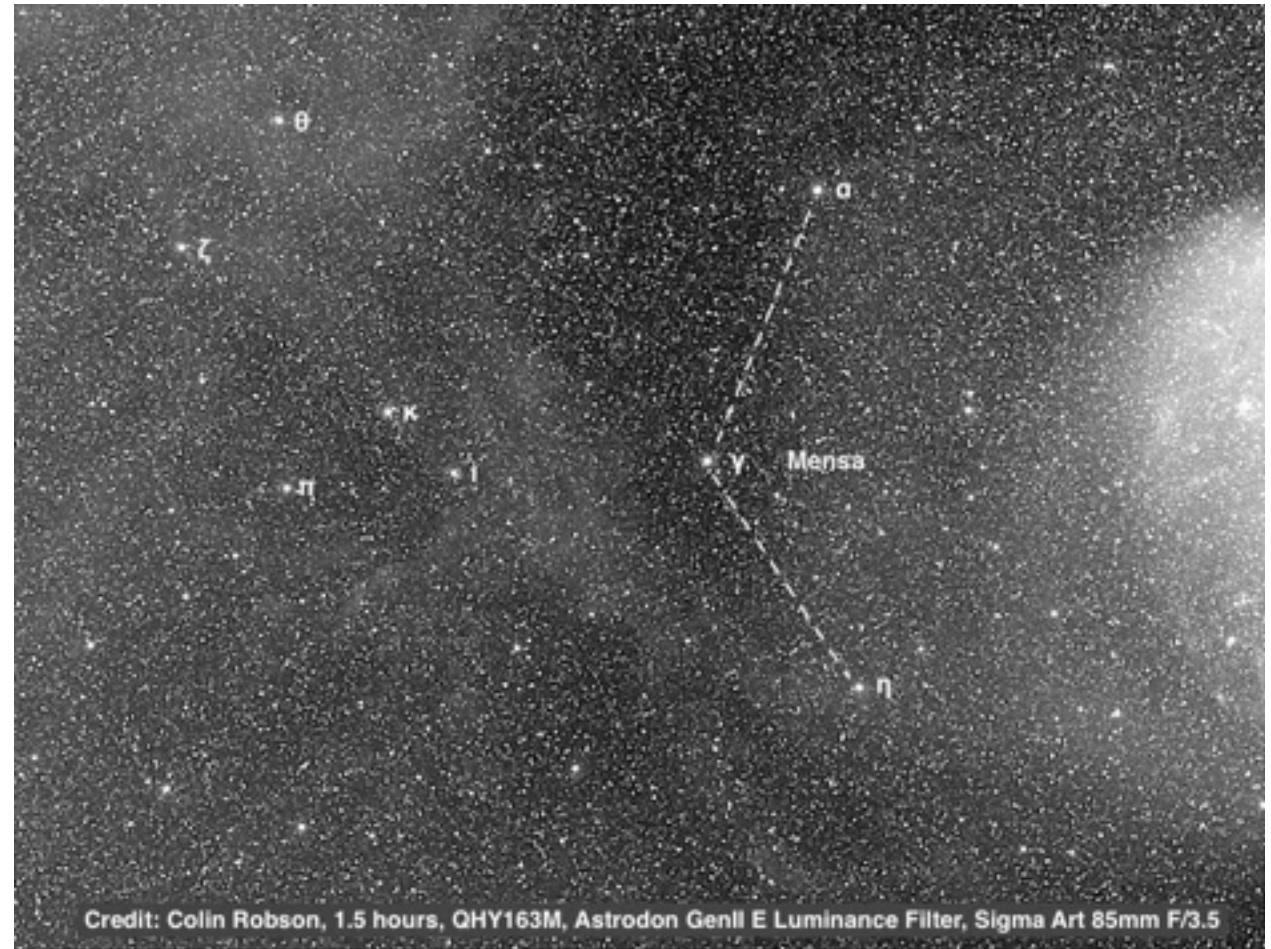


Fig. 4: Magellan's Ghost spreads out in a shallow arc from η Mensae, thickens as it crosses over π & ν Mensae; then widens to the broad patch starting at θ & ζ Mensae. This image was acquired and minimally processed in 2018 specifically for this report by the Australian astrophotographer Colin Robson.

Dust Bunnies in the Sky

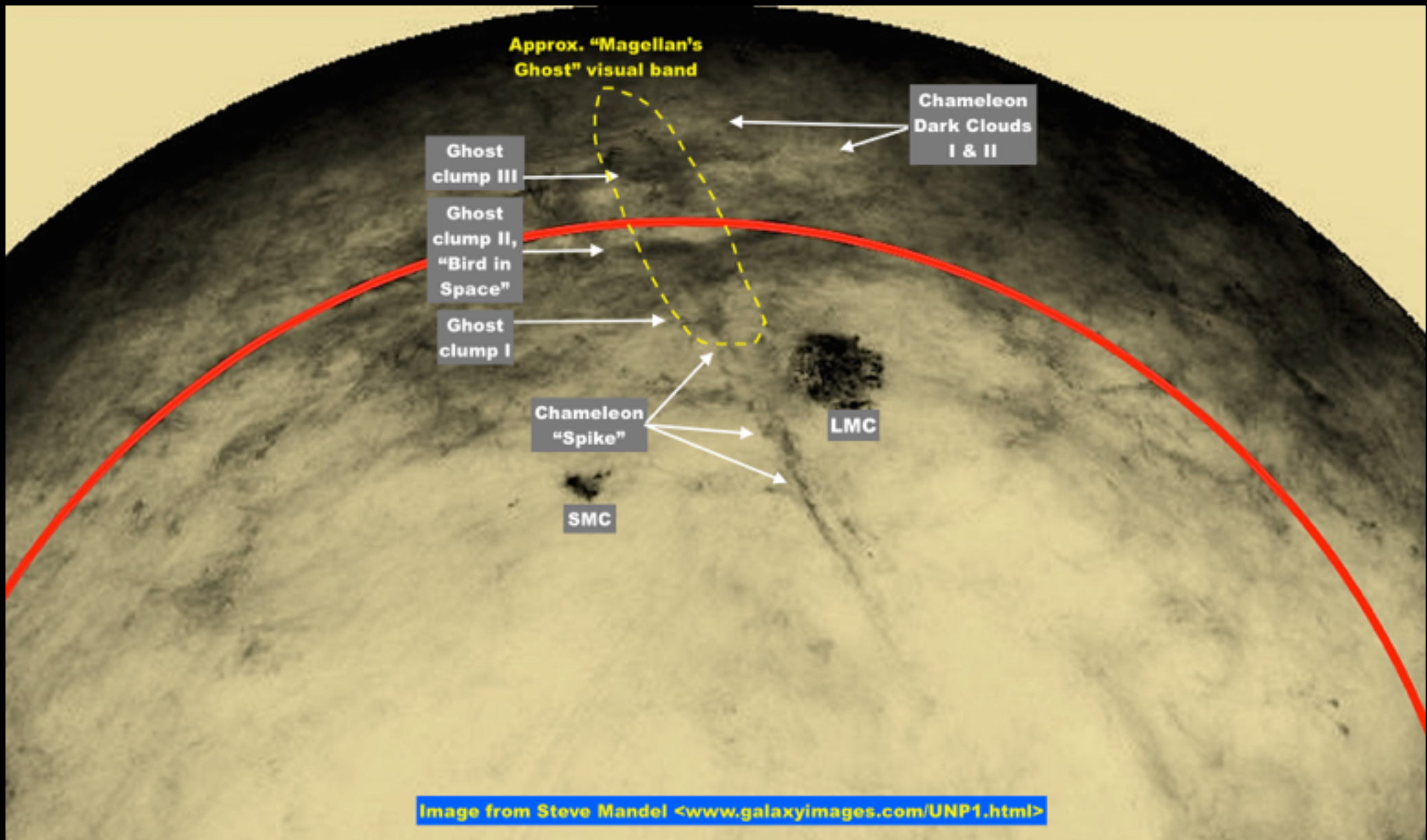


Fig. 5: Extinction map of the Magellanic quadrant of the south celestial hemisphere in [Schlegel & Finkbeiner 2011](#) and presented in negative image form by Steve Mandel in his *Unexplored Nebulae Project*. It has been annotated for this report to highlight the features referred to in the text. The "Magellan's Ghost" feature is indicated with dashed lines. Where this image shows three emission overdensities with broken and sometimes perpendicular features, the visual reports all state that the emission was seen as a faint, continuous band about 4° to 5° wide throughout its length. The "Bird in Space" and "Chameleon Spike" features are not directly relevant to the discussion here, but taken together they represent another mysterious feature which merits as much investigation as went into this report.

Figment or fragment?

The Churchillian riddle in this study is why the “Ghost” which seems so obvious to a handful of amateurs and one professional astronomer has been seen by so few others and imaged so rarely. One explanation is that this faint, possibly spurious emission lies in a region of the sky that is visually not very enticing. It lacks the physics diversity desired by professionals, and the visual drama that attracts amateurs. Only a handful of amateurs have imaged the Ghost, most notably the work of [Hisayochi Kato](#) in 2010 and 2016. The German artist-astronomer Robin Hegenbarth was [the first to make an accurate drawing of it](#), which was reproduced in the introductory image of this study.

We saw in the first section that the sparse number of observations of the Ghost is ameliorated by their long records of accurate observing. The question most of them whistled at their first glimpse was a variation of, “What’s THAT?” Dave Riddle, Timo Karhula, and Brian Skiff all answered “Galactic cirrus” almost as soon as they had finished the question. Were they right?

The typical morphology of Galactic cirrus (GC), aka Integrated Flux Nebulae (IFN), comprises linear striations, chaotic filaments, and amorphous clumps with a density gradient. The clumps are usually chance superpositions of gravitationally bound molecular clouds associated with star-forming regions. The dark nebulae Chameleon I, II, and III are clouds of this type. Only Chameleon I is actively forming stars.

GC/IFN were first distinguished from Galactic extinction (amorphous dust) in 1984 by astronomers analysing WISE satellite data. In 2005 the American Pro-Am astronomer Steve Mandel serendipitously noticed an unusual abundance of faint, dusky emission patches as he was experimenting with various [photographic filters](#) whilst imaging the M81–M82 galaxy group in Ursa Major. He noticed that some of his images hinted at extended networks of very faint emission patches well above the plane of the [Milky Way](#). Mr. Mandel had the good sense not to process these odd features out of the images as noise. Instead, he explored them further. Even better, he created

a 46-page image atlas of various GC clouds titled [The Unexplored Nebulae Project](#). Many of them had been imaged for the first time.

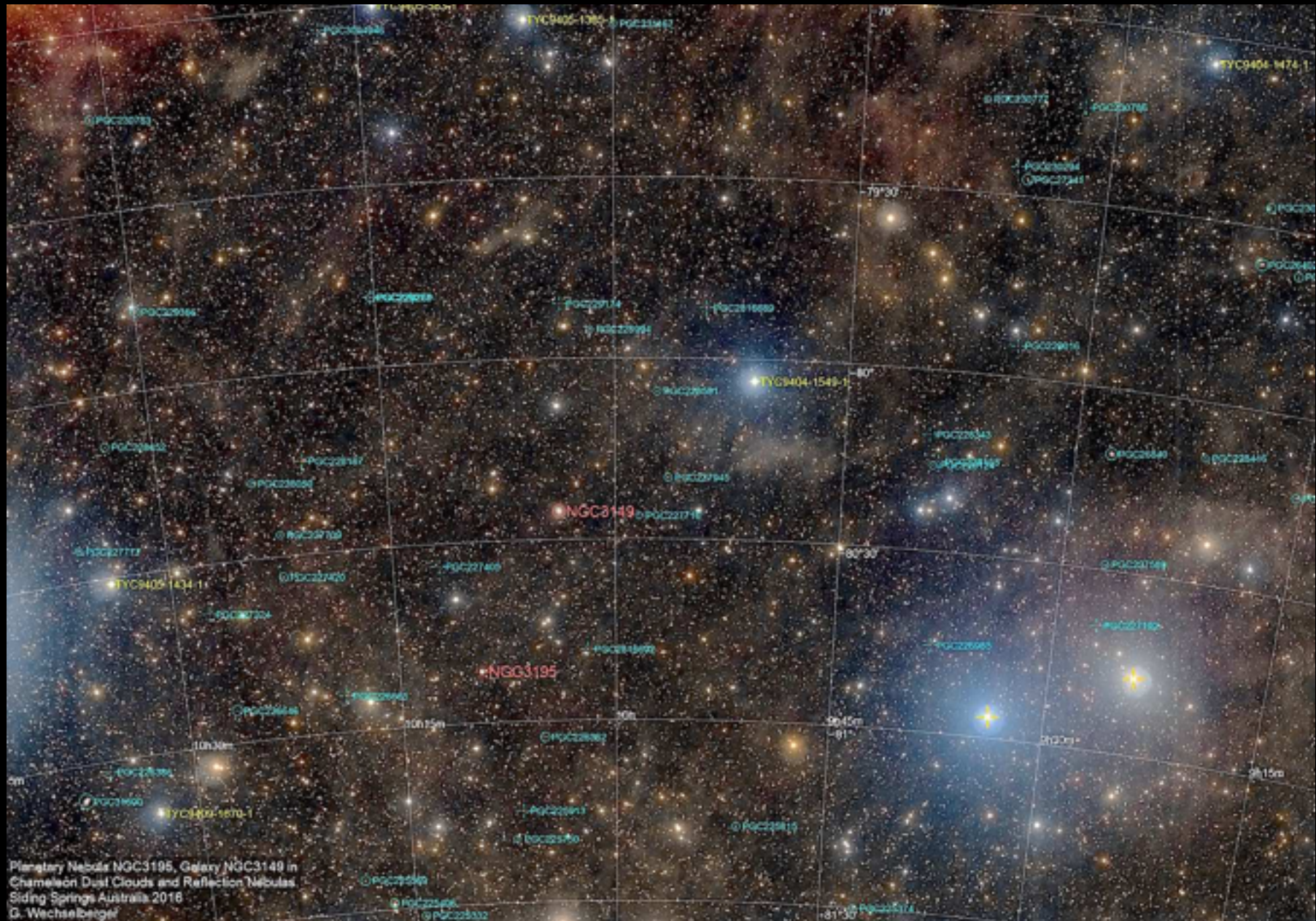
Mr. Mandel’s images were investigated by the astronomer [Adolf Witt](#), who found significant [carbon](#) signatures in them. This suggested that the nebulae were Galactic dust coated with carbon-based molecules bound by electrostatic bonds. Dust particles act as a weak electron donor. This in turn implied that the nebulae were very cold, since temperatures of 100 K volatise CO, CN, HII, H₂O, and PAHs. By 300 K galactic dust has lost its surface accretions. The lab where Galactic dust is made is colder than liquid nitrogen.

Mr. Mandel’s *Unexplored Nebula Project* was an eye-pleasing image atlas which, to its credit, introduced amateurs and professionals alike to the abundance and visual complexity of objects which were hitherto considered nuisance extinction. Mr. Mandel’s efforts turned nuisance into virtue by introducing a brand new object class to be imaged and investigated. He proposed that these difficult to photograph interstellar structures be named [Integrated Flux Nebulae](#) due to their being illuminated by the aggregate light from the entire [galaxy](#) disc. He devised this term to distinguish IFN from the more easily observed [reflection nebulae](#) illuminated by nearby [stars](#). The visual analogy to meteorological cirrus clouds became evident somewhat later.

One of Mandel’s images (**Fig. 5** on the previous page) is important to our search for Magellan’s Ghost. It was an extinction map apparently reproduced with modifications from [Schlegel & Finkbeiner 2011](#). Mandel’s image has been annotated by this writer to highlight features useful to our search.

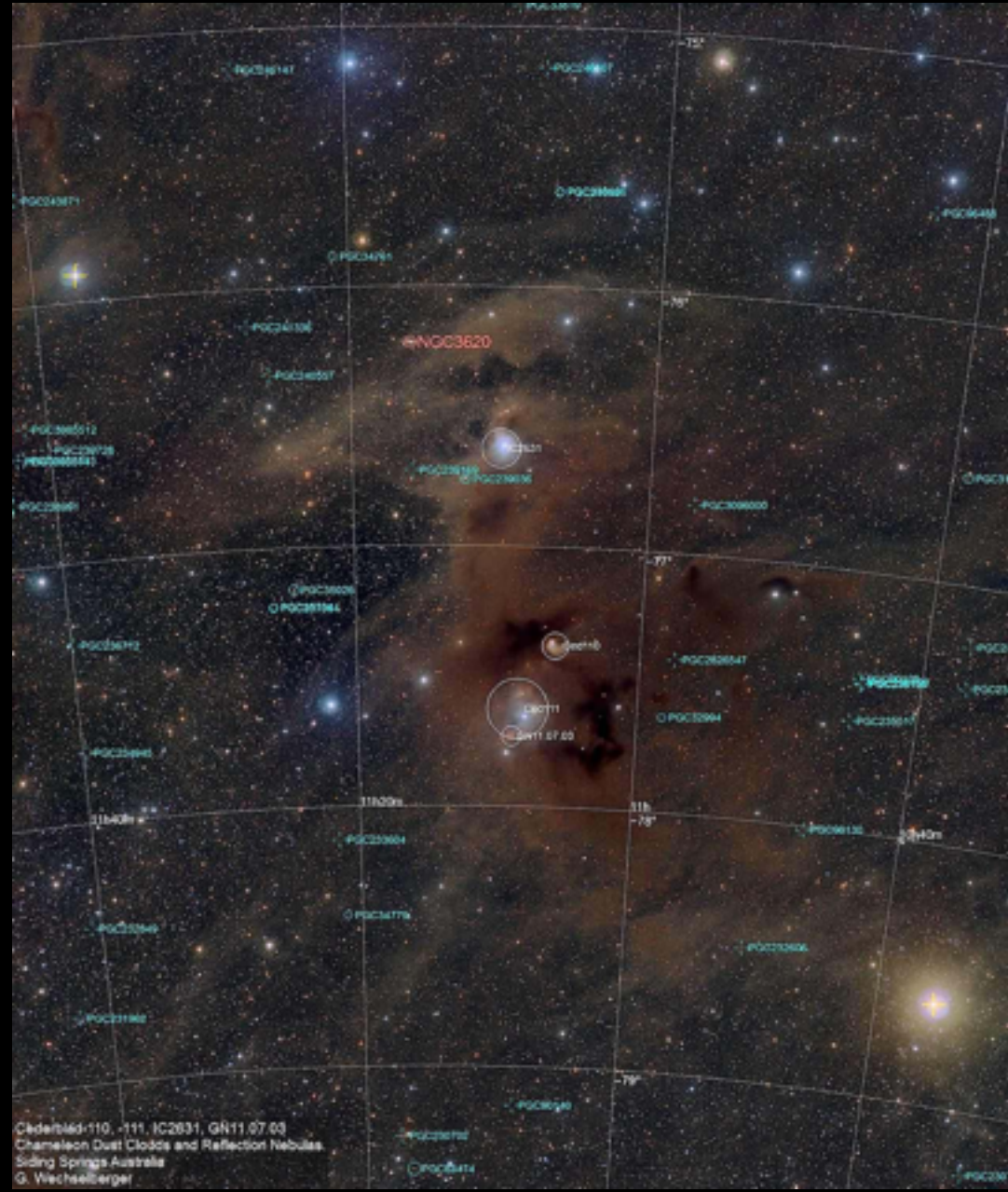
Most of Mr. Mandel’s images lacked source attribution, which limited their scientific value. The image on the previous page is not attributed. It does not state the filters used to acquire the images. It does not chart of the different contrast densities suggested by the images. It does not identify any features, although the LMC, SMC, and Galactic disc on the horizon are obvious. On the plus side, Mr. Mandel redirected the attentions of astrophotographers away from the long-familiar commonplaces and focused professional attention on a hitherto snoozy quarter of astronomical research.

PORTRAITS OF GALACTIC CIRRUS BY GERALD WECHSELBERGER



Figs. 6–7: While dark molecular clouds are present nearly everywhere in a dusty spiral, they are most easily spotted in the celestial polar regions around Ursa Minor and Octans. Typically they present as a blend of a dusky mauve-red (caused by the UV–dust–HII reaction fluorescing in the 540 nm to 950 nm bands; and blue luminescence (BL) from low-angle forescatter reflection off dust grains between the light source and the observer. If an IFN dust patch is thermally excited by nearby stars it is called Extended Red Emission (ERE), or simply warm dust. ERE spectra typically exhibit absorption lines from carbon-rich compounds and polycyclic aromatic hydrocarbons (PAHs).





Figs. 8–9: Galactic cirrus or IFN is difficult to image and is seldom noticed by visual observers. While IFN often gets labelled under the rubric ‘Galactic cirrus’ a more apt term would be ‘Galactic noctilucent’. These images show IFN patches near the South Chameleon star-forming dark clouds I and II (r), and high in the Octans polar region (l). Cirrus in the polar regions tends to be chaotic, multiply layered, comprising numerous individual particle aggregates only weakly bound gravitationally (if at all), but which show evidence of internal electrostatic coagulation. They lie 80 to 300 ly vertically above the disc plane. How they got there is discussed starting p. 44 below). Their striated morphology suggests multiple turbulent thermal, acoustic, and electromagnetic shocks.

The Importance of Being Dust

The universe has blown dust on its furniture since the first generation of stars (confusingly called “Population III”). While most accounts dwell on the mammoth $>100 M_{\odot}$ character of those first-borns, at least some of them may have weighed in at less than $8 M_{\odot}$ and therefore would evolve non-explosively. Certainly by the second generation, $<8 M_{\odot}$ stars would have formed as part of normal [initial mass function](#) (IMF) power-law distribution of any star-forming region. Their extremely low metals content affected stellar evolution, the effects of opacity, and molecule production. The early stars’ evolutionary tracks differed somewhat from today’s red giant to white dwarf tracks. The slope of the red giant branch (RGB), for example, was much steeper than RGBs today, detected by brighter luminosities at a given colour. The $<8 M_{\odot}$ evolutionary track produced either horizontal-branch (HB) helium dwarfs or asymptotic giant branch (AGB) carbon-oxygen dwarfs just as today. In both cases stars ejected enhanced metals content in doing so. Stars $<2.3 M_{\odot}$ followed the HB track; those $>2.3 M_{\odot}$ followed the AGB track. Stars over $>8 M_{\odot}$ most likely detonated as supernovae.

Near the end of their lives, those 1st and 2nd generation stars would have undergone a brief late-stage convective cycle picturesquely called “third dredge-up”. In this phase the hydrogen and helium burning shells burn so close to one another that deep, unstable convection bubbles upwell bringing large quantities of inert carbon and oxygen ash from their cores. Massive amounts of C and O (plus a bit of He and Li) spew into space.

Eventually the locally enriched interstellar medium cooled enough that H-C, H-O, C-O, and C-N electron bonding occurred. Over many stellar generations electrostatically mediated astrochemical reactions aggregated more and more simple molecules into complex cosmic dust bunnies in which particles of carbonaceous soot predominated. By the end of the reionisation era at $z=6$, the universe was increasingly abundant with minute organic solids

made of aromatic ring and aliphatic chain structures continuously enriched by stars. Two effects resulted from metals formation. (Astronomers label all atoms heavier than helium as “metals”, which tut-tuts chemists no end.) The most readily detectable effect was opacity $Z \rightarrow 1$, where $Z=1$ is the solar benchmark. All this made for increasingly complex enriched dust.

Dust at once vexes and thrills astronomers. Deep-sky astronomers grumble at the perfidies introduced by extinction. Planetary astronomers swoon over dust because it had very much to do with how we got here, how we evolved brains and eyes, and built neural networks with which to behold all this. In astrophysics, the “dust to dust” cycle means “dust to more dust”.

A second property of dust proved equally important to the evolution of the universe: magnetic fields. Magnetohydrodynamics (MHD) is an ongoing buzzphrase amid the ranks of those who check the daily [astro-ph](#) (aka [arXiv](#)) entries before they read the newspaper headlines (a custom known among [astrobites](#) devotees as “pearls before swine”). The buzziness derives from the role magnetic fields play in star formation, the distribution of matter and energy in galaxy discs, and the fiendishly complex algorithms required to model its effects. ([1](#) [2](#) [3](#) [4](#) [5](#))

The metals production of the universe’s earliest generations of stars recycled stellar ejecta into the pristine primordial H/He mix. A gas abundant with metals cools more efficiently owing to opacity, the increased radiation emissivity and ability to resist stellar radiative feedback. A cold environment favours gravitational collapse and fragmentation of star-forming clouds. First and second generation stars were the dominant radiation sources for cosmic reionization $z=12$ to $z=6$.

Until the 2000s most studies star formation did not include magnetic fields because they assumed only weak fields were present in the early universe. Those fields were then amplified by the astrophysical dynamo, including stellar rotation and galactic differential rotation, to the present μG level in the local ISM.

In the primordial universe the very feeble magnetic fields of $10^{-9} \mu\text{G}$ were amplified by [dynamo turbulence](#). On Earth dynamos are popularly associated with electrical generators in which a wire moving through a magnetic field produces a flow of electrons called a current. In space, the long, thin compression zones of shock fronts acts somewhat like a wire. The motion of the warm compressed turbulent shock front (wires) in the surrounding ambient magnetic field creates an electromotive force that redirects randomly moving electrons in a shock wave into a single direction (see the discussion of Simeis 188, [Fig. 30](#), p.35).

On Earth the wire creates an electric current. In space the shock front does the same. The overall effect is electron transfer on a large, unidirectional scale. Those electrons are then available if they encounter a zone of ionised hydrogen (i.e., free protons). An ionised hydrogen cloud is made when its hydrogen atoms are boosted to a thermal energy level of $\pm 8000 \text{ K}$ by nearby hot stars radiating energy into space and by the passage of turbulent compression waves. The atom's electrons acquire enough energy to nip off into space. The result is an ionised hydrogen H^+ cloud. Such clouds cool very slowly because in the extremely low densities of space (1 particle per 10^{-3} to 10^{-4} cm^{-3}) there is simply no way to readily transfer energy into or out of the system. Once energised they tend to stay that way.

Here dust plays its decisive trump card: the surfaces of dust particles are cold (e.g., 10 K to 100 K) because passing electrons and photons do not thermalise their relatively large masses. Dust is also weakly ionised by the presence of a certain proportion of atoms with an odd number of electrons in the outer valence shell and are therefore positively charged. Negatively charged electrons are attracted to dust, where they re-atomise with protons in the surrounding bath of free particles.

The end result is the production of HII molecular hydrogen on the surfaces of dust particles. Indeed, HII does not form anywhere else. There is very good reason why star formation is associated with HII rich dust clouds. Simply put: no dust = no us.

When the first generation Pop. III stars formed, magnetic fields amplified within the stars and also in their circumstellar disks. The first supernova explosions dispersed those fields far into the local interstellar and large scale intergalactic medium. The primordial magnetic fields, as feeble as they were ($B=10^{-9} \text{ G}$), are now known to be as decisive in the evolution of the universe as photon pressure and temperature. Today magnetic fields are comparable in energy density to thermal and turbulence energies.

For more detailed information on the composition of cosmic dust and its intricate relation with turbulence and electromagnetic fields, see the [Wikipedia entry](#) for an appetiser and [Susa 2014](#) for the five-course banquet.

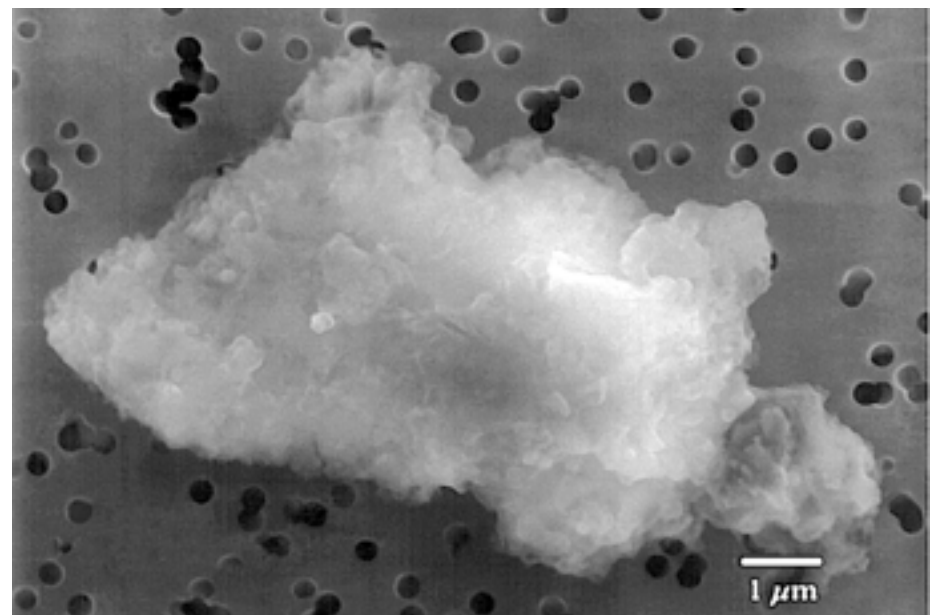


Fig. 10: [Cosmic dust particles](#) are between a few molecules to $0.1 \mu\text{m}$ in size. [This is a granule or grain](#) (distinct from a particle) conglomerate of a great many individual particles and is the approx. size of typical dust grain which makes it through the atmosphere to fall onto the Earth. This grain was captured in the [Stardust Mission aerogel trap](#). The dust density falling to Earth is approximately 10^{-6} g m^{-3} with individual particles having a mass between 10^{-16} kg (0.1 pg.) and 10^{-4} kg (100 mg).

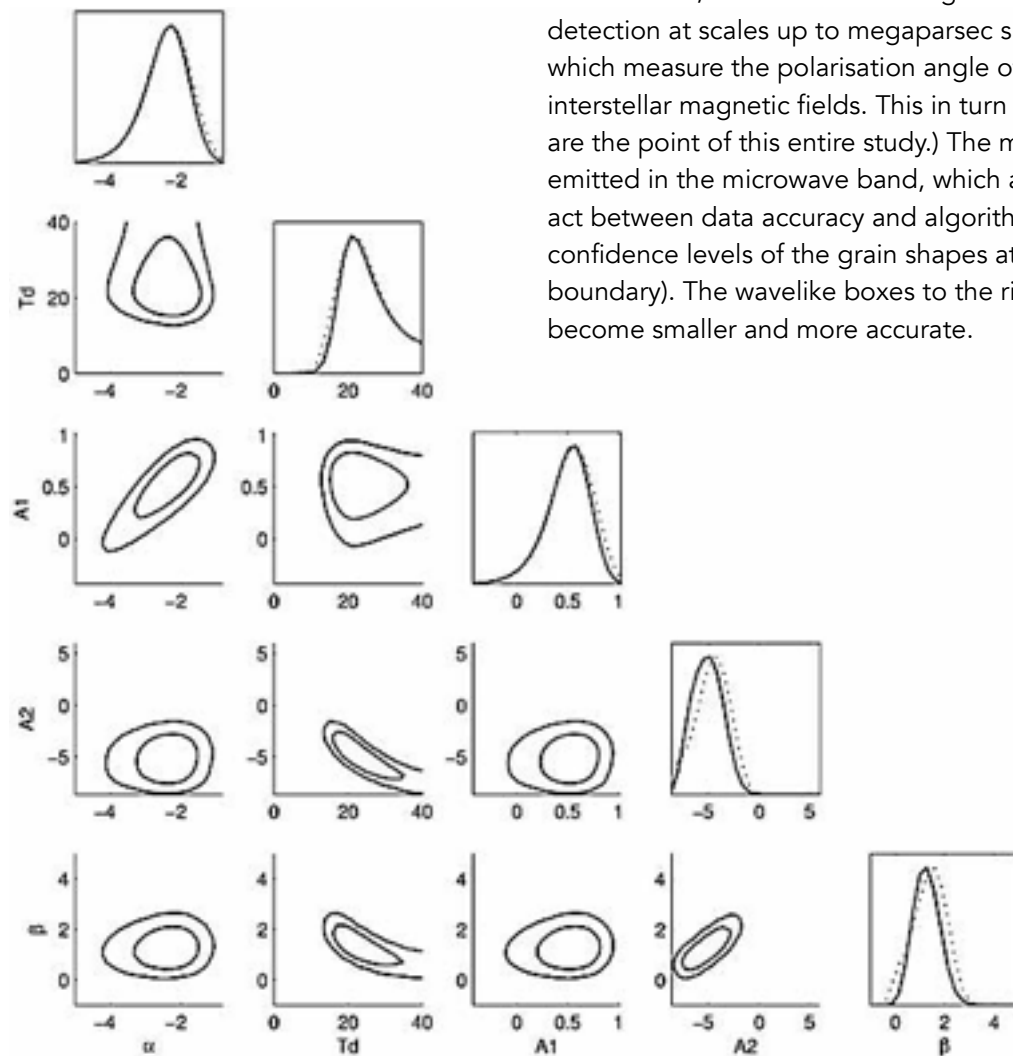


Fig. 11: How do we determine dust particle sizes, shapes, and numerical densities? A number of scientifically useful dust samples have been collected mechanically using special traps on stratosphere-flying aircraft and numerous space missions. One of them was Stardust, which used an aerogel to capture particles (**Fig. 10** above) impacting it at velocities upward of 30 km s^{-1} . Large-scale detection at scales up to megaparsec sizes is accomplished with detectors in the 3 to $180 \mu\text{m}$ band, plus polarimetry detectors which measure the polarisation angle of dust emission. Dust grains are generally elongated along one axis and tend to align to interstellar magnetic fields. This in turn polarises the starlight that passes through dust clouds. (The visible consequences of this are the point of this entire study.) The minute temperature variations of radiation absorbed from space by dust particles are re-emitted in the microwave band, which are converted from detector signal strength into a particle shape by a delicate balancing act between data accuracy and algorithm model. In this plot from [Veneziani 2010, Fig. 7](#)), the rounded shapes on the left are confidence levels of the grain shapes at the sigma 1 level (68% for the outer boundary) and sigma 2 level (95%, for the inner boundary). The wavelike boxes to the right are emission strengths from the surface of the particle as detector bandwidths become smaller and more accurate.

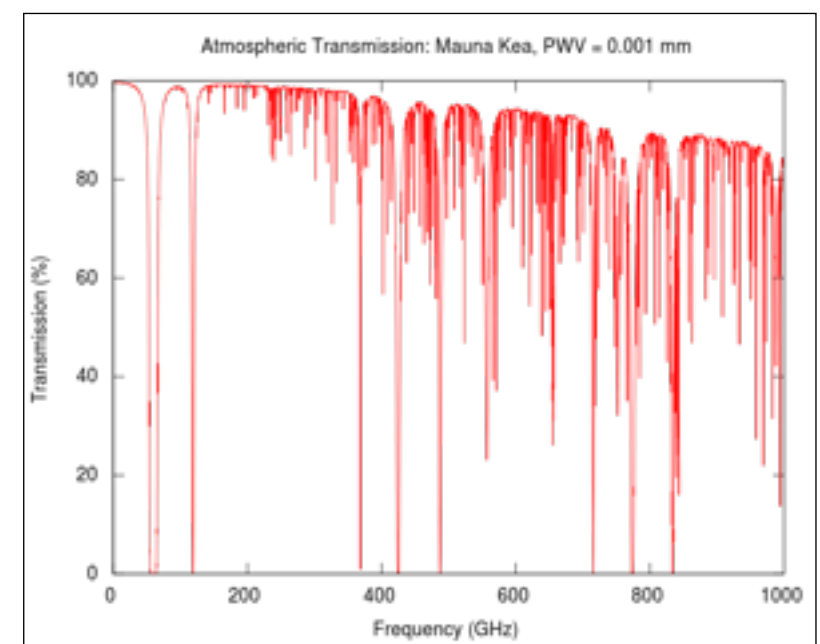


Fig. 12: The atmospheric absorption of microwaves and far infrared radiation in dry air. The absorption lines are frequencies at which microwaves are absorbed more strongly. In this 0 to 1 THz graph the microwave band range lies between 0.3 and 300 gigahertz.

The Astrochemistry of 18.6 K

The Magellanic Ghost region emits energy at a level consistent with a dust temperature of 18.6 K. With only minor variations, this is true for nearly all the studied Galactic cirrus in the south polar region comprising Chameleon, Apus, and Octans. Four distinct emission/absorption categories can produce the various streaky or blotchy patches we visual observers can see:

Reddish HII emission (e.g., California Nebula)

Bluish reflection nebulae (e.g., Pleiades ghosts)

Extended red emission (ERE), discovered in 1975 by Cohen et al is ultraviolet-excited photoluminescence of an as yet unidentified component of interstellar dust; it is often associated with the spectral signatures of polycyclic aromatic hydrocarbons (PAHs). ([1](#), [2](#), [3](#).)

Galactic cirrus is cold dust which reflects the combined emission of the Galaxy in the 26.5–28 MPSAS and is rarely observed visually due to the canonical 25 MPSAS limit of human eye.

There is a major difference between *IFN*, which is dust which originated in the atmospheres of asymptotic giant branch (AGB) stars, and *ISM*, interstellar matter made of atoms, molecules, and PAHs or polycyclic aromatic hydrocarbon compounds.

While ISM molecular clouds are present nearly everywhere in a dusty spiral, they are seen in quite different forms of emission, *red fluorescence and blue luminescence*.

Red ISM is mainly caused by the UV-dust-HII reaction fluorescing in the 540 nm to 950 nm bands. A secondary source is **Extended Red Emission (ERE)** in Galactic dust clouds. ERE is produced by fluorescing carbonaceous molecules comprising 18 to 30 carbon atoms which originates as far-ultraviolet light from hot stars. The UV converts into the red and near-IR bands by inverse Thompson scattering. The origin of these particular molecules are outflows from carbon-rich post-AGB stars. IFN extended red emission can be imaged using very long exposures (12–30 hours) near the Galactic poles.

Blue luminescence (BL) is low-angle reflection off dust grains between the light source and the observer. The blue glow around the Pleiades is an example.

ERE, HII, H α , BL differ from IFN differ in several regards:

Composition. *IFN* is composed of dust particles made up of hydrogen, CO, and trace elements and is seen most commonly in shadow as it absorbs light from afar. It emits in the millimetre and micron bands. We see it only indirectly by reflected light, if we see it at all. **ISM** is electromagnetic emission from warm atoms. which bear spectral signatures of their source(s); most of it is H α emission associated with star-forming regions or HII clouds.

Structure. Typically *IFN* appears presents as streaky elongated linear filaments which criss-cross each randomly without a noticeable pattern. *ISM* usually presents a distinctly gaseous appearance with billowy rounded and soft edges, amorphous structure, and are often layered one atop another. Multiple layers of extinction are much more common than we suspect when we detect them visually. *Here is a good example*. The thready or filamentary structures are ubiquitous due to the dust's having been shocked by repeated ionisation fronts, protostellar jets, and magnetic field lines that align dust particles along the magnetic field lines normal to the particles' long axes. They become slightly charged like any dipolar structure within a magnetic field. The "Lagoon river" in M8 is actually one side a magnetic flux stream which originates in the Herschel 36 very young star-forming complex. The "river" on the opposite side is visible in amateur telescopes but is much broader and is easily overlooked.

The aggregate luminosity of the entire Milky Way raises IFN dust grains to ±15 K. At that temperature the grains can act as a catalyst for two hydrogen atoms to bind into HII. This process occurs almost exclusively on dust grains, and is fundamental to the very existence of the universe as we know it.

Stars cannot form out of H_I atomic hydrogen because neutrally charged particles must overcome their repulsive electrostatic Coulomb force before they can bind. The extreme pressure of the interior of a star is one way to overcome Coulomb repulsion — squash it harder than it can repel. Molecular H_{II} is slightly dipolar and responds to electromagnetic field forces. It readily combines with other atoms with an electrical charge. Put succinctly: no H_{II} = no stars.

Emissivity. IFN is rarely visible to the unaided eye. It is a specialty of experienced observers using large-aperture, low-magnification, extra-wide-field 150 mm to 200mm diameter reflectors of very short f/2.7 to f/3.5 focal ratios. Mel Bartels is well regarded in the professional community as a pioneer in this kind of original observation using equipment specifically designed for the purpose. The ready availability of ultra-wide 82° and 100° eyepieces with focal lengths chosen to produce exit pupils matching those of the specific observer has inspired a small band of serious Pro-Ams who research the physics producing the phenomenon they record. Their standards are strict: the observing locations must be remote from any light pollution, humidity below 20%, ground elevations above 1500 m (4700 ft), and away from jet stream winds. The now-common minimum acceptable standard is 21.5 MPSAS visually or a reading of >21.5 on a Sky Quality Meter.

Location. Most IFN are well above the Galactic Plane; indeed, the most commonly photographed IFNs are in Ursa Major/Minor and Apus/Chameleon/Octans.

Absorption. IFN can be seen as shadow bands if it lies in front of a bright extended background object. The “skid marks” across the disc of M81 were attributed as the relic of an ancient interaction until their true nature as Milky Way galactic cirrus became known.

What is the "flux" in Integrated Flux Nebulae?

The term *flux* is a measure of the density of charged particles passing a specific area such as a detector plane, measured in units per second. The flux in IFN is electromagnetic emission from dust and / or gas usually (but not always) found at high galactic latitudes. IFN is not illuminated by nearby stars but rather by the cumulative glow of the galaxy itself. Long-exposure images by [Rogelio Bernal Andreo](#), [Tony Hallas](#), and numerous others reveal the IFN's full extent around a typical dusty spiral.

There is a distinction between flux made visible by *backscatter* IFN, meaning the combined emission of the Galaxy reflecting off dust more distant than the stars in the disc (e.g., the Galactic polar regions); and *forescatter* IFN, which is dust illuminated by forward grazing reflection from bright disc stars:

Backscatter is analogous to atmospheric cirrus clouds near sunset reflecting the reddened light from the Sun. The well known IFN originally identified as M81 "Arp's Loop" is an example of backscatter.

Forescatter is analogous to atmospheric haloes, solar pillars, and other atmospheric effects from ice particles in the stratosphere. The well-known blueish reflection nebulae around the Pleiades are an example of forescatter.

Cosmic dust

Most cosmic dust particles are between a few molecules to 0.1 μm in size. A small amount of dust consists of refractory (able to withstand high heat) minerals that condensed from matter left over after star forming episodes. The density of “stardust” falling to Earth is approximately 10^{-6} per m^3 of air at sea level per day, with each grain having a mass between 10^{-16} kg (0.1 pg) and 10^{-4} kg (100 mg).



Fig. 14: For an IFN cloud to become visible on deep photographic plates such as the POSS plates or Rogelio Bernal Andreo's image above, the illumination source at the cloud must be about -5.5 magnitude. The Milky Way's estimated brightness as seen at the radius of polar IFN has been estimated at approx. -7 magnitude. The very low spread is one reason why IFN contrast levels are so tricky to image. Allan Sandage measured the surface brightness of the brightest part of the cirrus near M81 (#32 in Herschel's list of nebulous regions) at $\sim 24.5 \text{ mag/arcsec}^2$, which is barely above the commonly accepted limit of 25 MPSAS for visual detection.

Fig. 13: Galactic IFN haloes such as this 31-hour exposure of M31 are notoriously difficult to process without inadvertently losing or inflating science data. The signal-to-noise ratios are so close to each other that considerable experience and a touch for the subtle make the difference between the informative and the ordinary.



Dust and the mass/luminosity relationship

Dust at high galactic latitudes effects observational accuracy in different ways depending on the waveband used in a given study. The most critical is dust's effect on the cosmic microwave background (CMB). The CMB reaches us in exceptionally minute signal strengths which translate after processing into thermal temperature variations in the 10^{-4} K range. (That's about how much a grain of sugar adds to your waistline — a handy number to ignore the next time you make that donut order a big one.)

In the early days of CMB mapping, the *Wilkinson Microwave Anisotropy Probe* (WMAP) was tuned to the frequency range 23–3000 GHz in the 13 mm–100 μm bands. At frequencies above 100 GHz the emission of dust in thermal equilibrium with its surroundings is dominated by large grains in the interstellar radiation field. Large grains sponge up microwave emission while affecting optical bands rather little (they're dark, aren't they?).

WMAP found a temperature variation of 7 K to 20 K, but the CMB itself is only 2.73 K. Such a large gap limited the accuracy of mapping the CMB at finer scales. This in turn placed poor constraints on the values of the Universe's density and temperature during the critical phase when the Universe cooled through the free-free proton/electron barrier, allowing free particle to bind into hydrogen atoms, thus bequeathing the Universe its photons.

It was impossible to tell from WMAP data how dense and warm a dark matter core had to be to attract enough gas to form stellar objects. A good example of stymied CMB mapping was the [mass-to-luminosity \(M/L\) relationship](#) of dwarf galaxies. Astronomers discovered that the fewer luminous stars a dwarf galaxy has, the larger its dark matter mass. The dwarf irregular IC 1613, for example, has a M/L ratio of 2.3, while extremely faint dwarfs like [Segue I](#) and the nine ultra-dim dwarfs found in Southern skies in 2015 by [Koposov et al.](#) have M/L ratios in the 2000 and up range. The upside-down conclusion, "The heavier it is the fainter it is" ran counter to everything known about the mass/density rules of star formation.

Why was there an apparent inverse ratio between a dwarf's mass and its luminosity? If there were no dark matter the opposite could be expected:

more mass = more stars. The answer loomed out of the gradually improving accuracy from COBE, [DIRBE](#), and [BOOMERanG03](#) missions. The larger the diameter of a primordial collapsing dark matter cloud at the time it reached the critical density at which its gas infall would form the first stars, the lower the mass of gas with which it could do so. The early birds at $z = >7$ got the worm while the latecomers got the gas. The mass was there all right, but it was too thin.

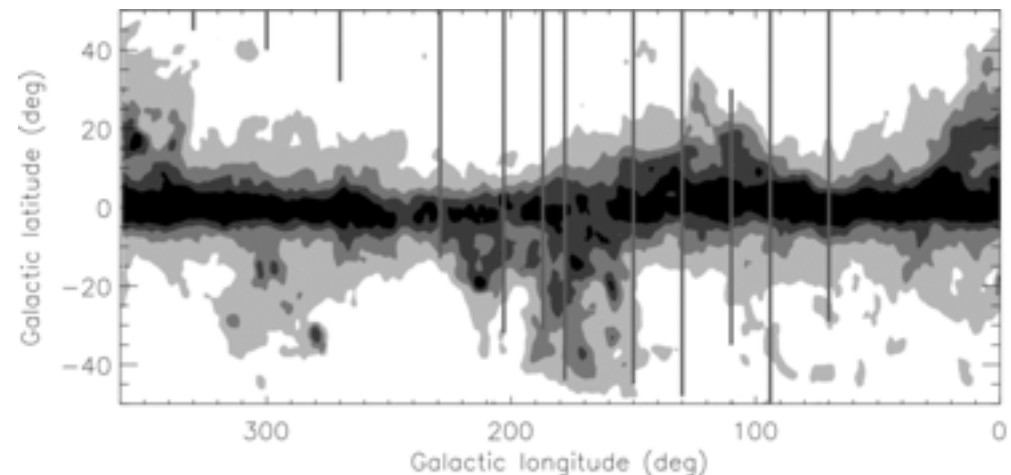


Fig 15: Dust extinction map of the Milky Way from [de Jong 2010](#) Fig 1. The darkest band in mid-plane are approx. the same as measurements presented in Schlegel 1998. The vertical bars are related to CMD measurements and are not relevant here.

Early reports in the literature

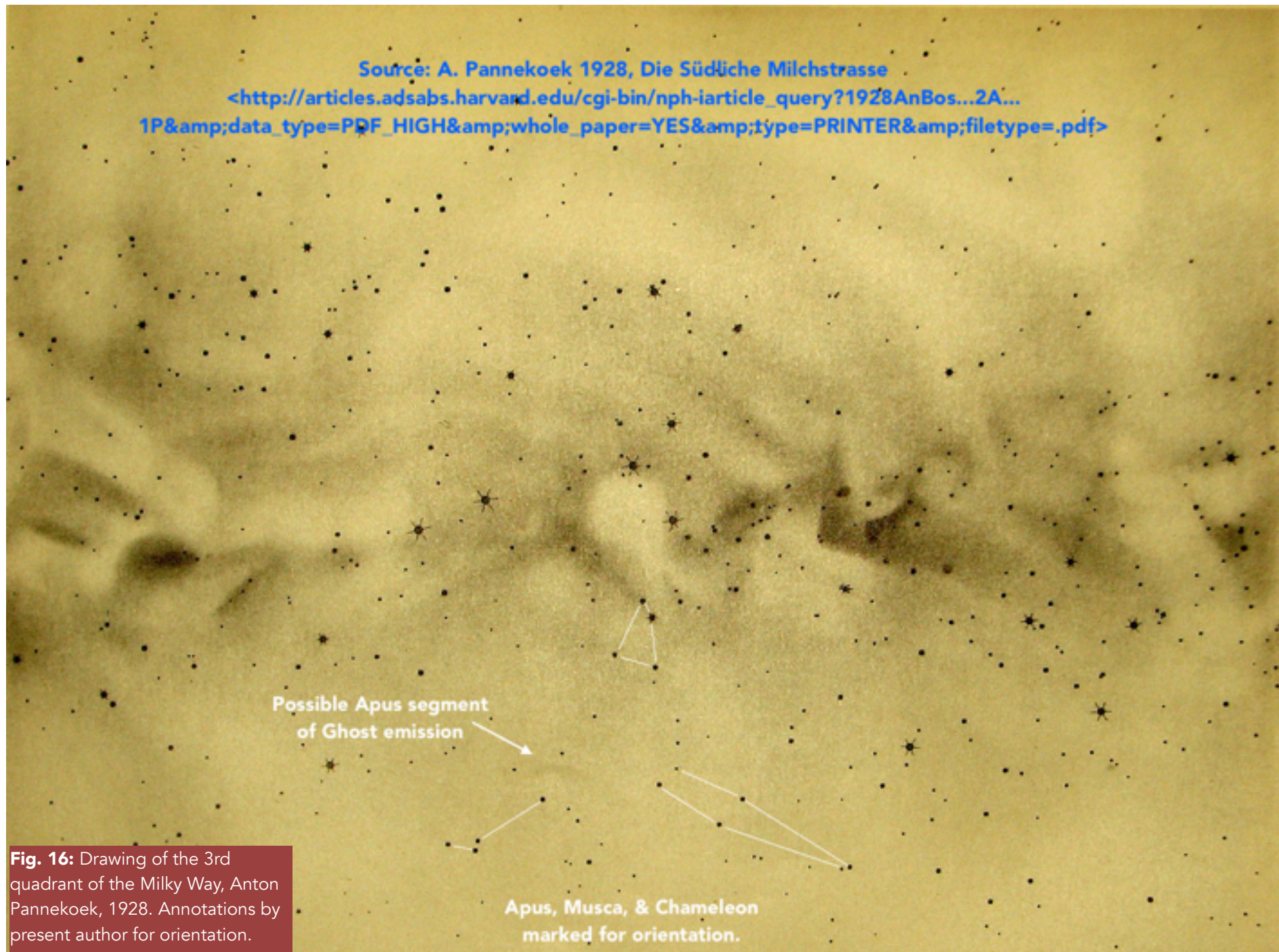


Fig. 16: Drawing of the 3rd quadrant of the Milky Way, Anton Pannekoek, 1928. Annotations by present author for orientation.

Pannekoek 1928

The first person to record an emission feature near the LMC may have been Anton Pannekoek in *Annalen v/d Bosscha Sterrenwacht* 1928, observing from Lambang, Java (Indonesia). At only -7.7° S, the Chameleon–Apus region rises to only about 27° at meridian. Given what we know about the observability of the Magellanic Ghost today, Pannekoek is unlikely to have seen it. He did make some notes of the region, though. German Ghost observer Robin Hegenbarth (Fig. 1) translated the two paragraphs of the Pannekoek 1928 study which may refer to visual observations shown the blue boxes in the reproduction of his page (r):

Fig. 17, §22: "A wide, diffuse light flux emerges between nu and theta Car, from I-q Car, with a triangular tip towards omega Car. From there, it continues toward alpha-lambda Mus. A very faint light band extends towards alpha-gamma - delta Cha, which is separated from the glow in Volans by a band that runs from beta Car downwards. The light band nu-omega Car - alpha-lambda Mus surrounds a darker patch that includes the dark bay lambda Cen - z Car. A faint light band between lambda Cen and theta Car dissects this patch. Above this, there is a dark lane from theta 1/2 [?] z Car towards delta, epsilon Cru towards lambda Cen, which merges into lambda 1/4 [?] 65 Cen and sends a branch via z Car upwards. Below this light stream there is a dark band or a bunch of dark patches below lambda Cen towards lambda Mus, 1/3 [?] theta Car and south east of theta Car. There is a dark space between gamma TrA 1/2 [?] delta Mus. Below this dark space, there is a faint, wide band from gamma-alpha TrA towards beta-gamma-alpha Aps that can perhaps be traced to gamma-delta Cha."

Fig. 18, §U.A. 22: "The lower boundary of this light stream runs along G Car, gamma Cha, beta and alpha Aps and 3 degrees South of alpha TrA. Around gamma, delta Mus this light is slightly brighter. Between gamma, delta, alpha, and beta Mus there is a faint and dark band that merges into this boundary light and ends above delta Mus. A faint, semi-circular, convex light arc runs towards South from gamma to alpha TrA. Between these stars it is darker."

A 39

ausläuft, nach u. nach $\zeta - \xi$ Vol abnimmt, und sich nach r. bis B Car ausdehnt. Von dem Licht χ Car – α Pic wird er durch eine Dunkelheit zwischen B Car und α Pic getrennt. Auch zwischen ϵ Car und β Vol, etwas nach α Vol hin, ist es vielleicht ein wenig dunkler.

22. Zwischen ν und θ Car entsteht dem Lichtband $I - q$ Car ein breiter, schwacher Lichtstrom, mit einer Dreiecksspitze nach ω Car; von dort geht er weiter nach l. nach $\alpha - \lambda$ Mus. Nach unten zu breitet sich von ihm ein ganz schwaches Licht nach $\gamma - \tau - \delta$ Cha aus, das von dem Schein in Volans durch einen Streifen getrennt wird, der l. an β Car entlang nach unten geht. Das Lichtband $\nu - \omega$ Car – $\alpha - \lambda$ Mus umschließt einen dunkleren Raum, von dem die dunkle Bucht λ Cen – z Car einen Teil bildet. Ein schwacher Lichtstreifen λ Cen – θ Car zerteilt ihn; über diesem liegt ein dunkler Streifen, von θ $\frac{1}{2}$ α Car in der Richtung nach β ϵ Cru, der oberhalb von λ Cen mündet, dort λ $\frac{1}{4}$ 65 Cen in das Licht eindringt und einen Seitenast l. an z Car entlang nach o. schickt. Unterhalb des Lichtstreifens liegt ein dunkles Band oder eine Reihe dunkler Stellen, die unterhalb λ Cen, auf λ Mus $\frac{1}{2}$ θ Car und s.o. von θ Car angegeben wurden.

Zwischen α β und $\gamma - \delta$ Mus liegt ein dunkler Fleck; nach r. u. verläuft er als Streifen, der halbwegs K Car nach s. umbiegt; l. o. setzt er sich schwach fort und bildet einen dunklen Flecken η Mus $\frac{1}{2}$ α Cir, der das helle F Licht begrenzt. Ein schwacher Lichtstreifen geht über $\gamma - \delta$ Mus, der sich verbreitert die Richtung α Cir einschlägt und darauf noch breiter werdend sich nach γ TrA hin ausdehnt. Von γ δ Mus geht ein sehr schwacher Schein streifenförmig nach α Aps; r. davon liegt ein dunkler Raum nach $\gamma - \delta$ Cha hin. Ein dunkler Raum befindet sich γ TrA $\frac{1}{2}$ δ Mus; u. ihm zeigt sich ein sehr schwaches, beeites Band von $\gamma - \alpha$ TrA nach r. u. nach $\beta - \gamma - \alpha$ Aps, vielleicht noch bis $\gamma - \delta$ Cha erkennbar.

23. Von dem hellen Lichtfleckchen F geht der Lichtstrom, zuerst abnehmend, östlich nach α Cen und α Cir. Ein ununterbrochener Lichtstreifen geht von F gerade nach α Cir und unten an ihm entlang, und setzt sich schwächer fort nach β TrA. Nach u. breitet das Licht sich schwächer aus nach α und γ TrA; hier wird es vielleicht wieder etwas heller. In der Mitte schließt sich das schwache von δ Mus kommende Lichtband an (22).

Der Lichtstreifen m Cen – α Cir wird von den höherliegenden Teilen des Lichtstroms durch eine Reihe dunkler Flecken getrennt, die zusammen oft wie ein dunkler Streifen α Cir – J Cen aussehen; der deutlichste liegt β $\frac{1}{2}$ m Cen, unregelmäßig gebogen, in verschiedener Form beschrieben; andere sind angegeben J $\frac{1}{2}$ m Cen, α Cir $\frac{1}{2}$ β Cen, und ein Streifen auf der Linie J Cen – α Cir. Ihre Fortsetzung finden sie in einer Gruppe viel auffälliger.

- U.A. 22. In der U.A. geht die untere Grenze des Lichtes über G Car, γ Cha, β und α Aps, und 3° s. an α TrA entlang. Um γ δ Mus herum ist das Licht etwas heller; zwischen γ δ und β Mus ist ein schwach dunkler Streifen, der nach r. in das Randlicht mündet, nach l. oberhalb von δ Mus aufhört. Ein schwacher halbkreisförmiger Lichtbogen konvex nach s. geht von γ nach α TrA; zwischen diesen Sternen ist es dunkler.

- U.A. 23. In der U.A. wird das Licht I. vom Kohlensack im weiteren Verlauf nach l. nach Circinus und β Cen, allmählich schwächer. Die u. Grenze des hellen Lichtes ist ein Bogen γ Mus, η Mus $\frac{1}{2}$ α Cir, γ TrA. In dem gleichmäßigen Serom liegt ein hellerer Streifen u. an β und α Cen entlang, der über γ δ Cir weitergeht und sich dann bis ι Nor $\frac{1}{2}$ η Aps und ι Nor $\frac{1}{2}$ ζ Lup verbreitert. Ein abgerundet-dreieckiger schwarzer Fleck befindet sich zwischen $\theta - \epsilon - \delta$ Cir. Nach u. liegt ein gleichmäßiges Licht bis γ und β TrA; ein dünner Lichtstreifen geht über γ TrA nach δ und ist noch bis η Aps zu verfolgen. Der schwache Bogen $\gamma - \alpha$ TrA ist noch weiter bis β TrA zu erkennen.

A. Pannekoek 1928, Die Südliche Milchstrasse, Annalen v/d Bosscha Sterrenwacht
<http://adsabs.harvard.edu/abs/1928AnBos...2A...1P>

de Vaucouleurs 1955

The Ghost feature was first imaged in May 1955 when Gérard de Vaucouleurs produced a large-scale mosaic of the Magellanic Clouds. He erroneously concluded that a filament of Galactic cirrus was part of the LMC's spiral arm structure. He interpreted a slender emission (labeled "Galactic cirrus filament" on the annotated version of his chart to the right) as a spiral arm of the LMC:

The most interesting formation revealed by the long exposures is the anomalous spiral arm or filament stretching north-eastwards from near $4h\ 45m, -73^\circ$, where it emerges from the main spiral pattern [of the LMC], to about $3h\ 25m, -55^\circ$, where it reaches the edge of field 3. Apart from some irregularities (e.g., near $4h, -70^\circ$), perhaps due to foreground obscuration, its course is regular and its width decreases continuously from about 2° near its origin to less than 1° near its tip. It presents on the Ektar plates a smooth, nebulous appearance and is not marked in the star counts to $m = 14$; its luminosity estimated at about 25 to 26 mag/sec² in its middle section, tangent to k Reticuli, must therefore be due to stars fainter than $M = -4.7$. The lack of bright supergiants contrasts with their abundance in the inner regular arms. The projected length of not less than $20^\circ = 15$ kpc indicates the gigantic scale of this formation which is tentatively interpreted as the antigalactic arm or counter-tidal filament in the gravitational interaction between the Large Cloud." (de Vaucouleurs 1954b)

The erroneous interpretation of the filament as a spiral arm of the LMC is understandable given the knowledge of the time. The LMC was suspected to be a perturbed barred spiral. Galactic cirrus as we know it would not be identified for another seven years, by Beverly Lynds (see below). Not until Nidever 2008 would it become clear that a large amount of gas and dust is being ejected from the SE quadrant of the LMC, which presently streams across the SW arc towards the LMC to form a second stellar bridge between the LMC and SMC.

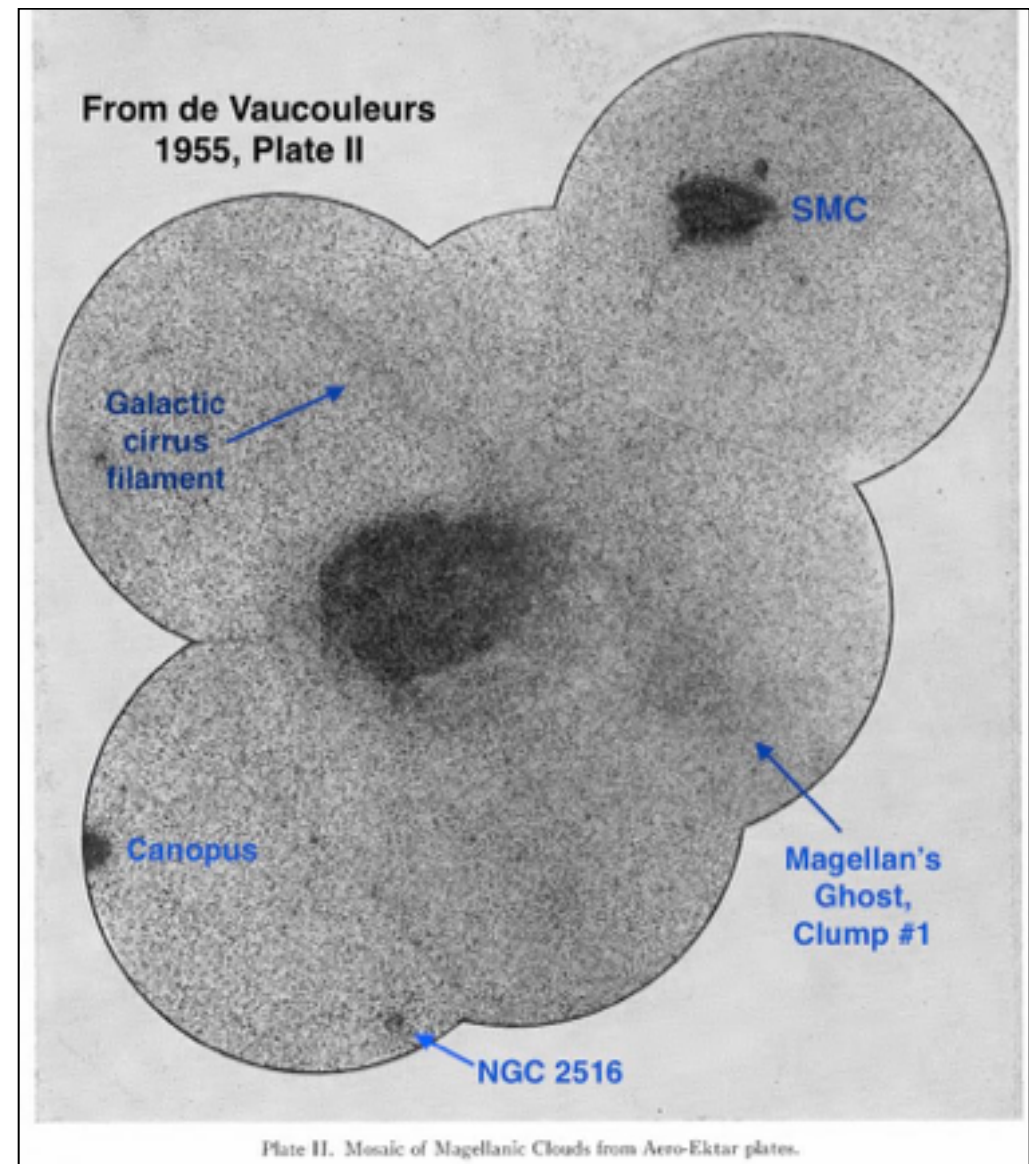


Fig 19: Annotated image from de Vaucouleurs, *Studies of the Magellanic Clouds*, Astronomical Journal, 60 #1227, May 1955.

1955 May

THE ASTRONOMICAL JOURNAL

133

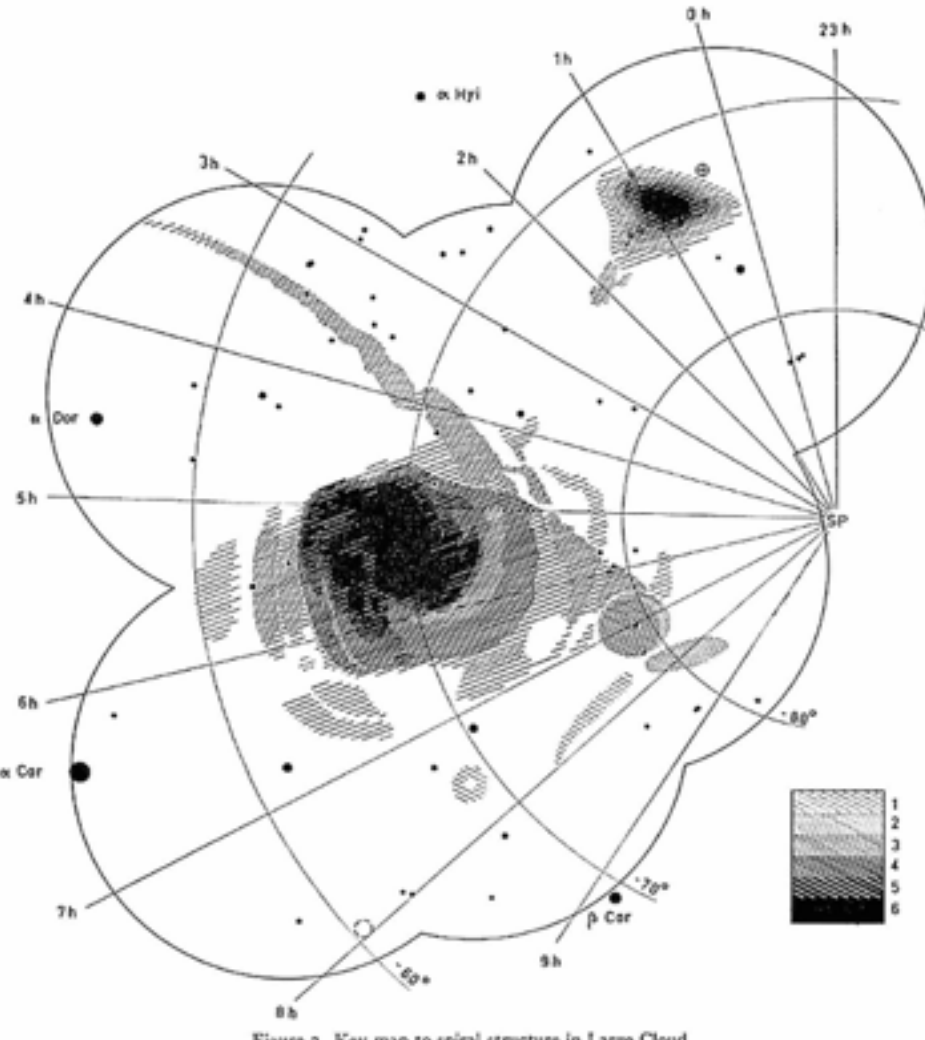
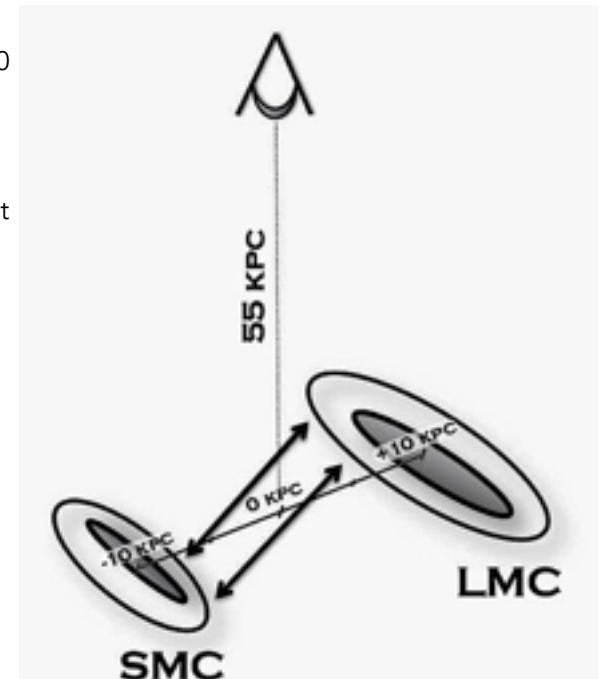


Fig. 20: de Vaucouleurs prepared this map based on his examination of the Aero Ektar plates he made, supplemented with the early POSS plates taken in the early 1950s. The bulbous structure SW of the LMC disc may correspond with the emission overdensity labelled as Clump 1 in this study.

Hodge 1967

In the mid 1960s the indefatigable Paul Hodge wrote a number of papers related to the LMC and the Magellanic System in general. One of them, *The Large Magellanic Cloud* by Hodge and Frances W. Wright, was a formidable image-rich text intended to aggregate all the known information about the LMC. Published by the Smithsonian Press (Washington DC) in 1967 it comprised 108 pages and 166 plates, 82 in yellow (to mag 17.0) and 84 in blue (to mag 17.5) at a plate scale of 16 arcsec/mm. It was reviewed by Sydney van den Bergh in [RASC Vol. 61 No. 5](#), who admired it so much he took a copy on his next visit to Cerro Tololo. Finding a physical copy may be difficult: it is [not available even in the Smithsonian ADS database](#).

Fig. 21: The SMC and LMC are at a heliocentric distances of ~ 60 kpc and ~ 50 kpc, respectively, and are separated by ~ 18.9 kpc. The tilt of the two galaxies with respect to each other means that the opposite sides of their disks illuminate each other. Source: [Barger et al 2013 Fig 15](#).

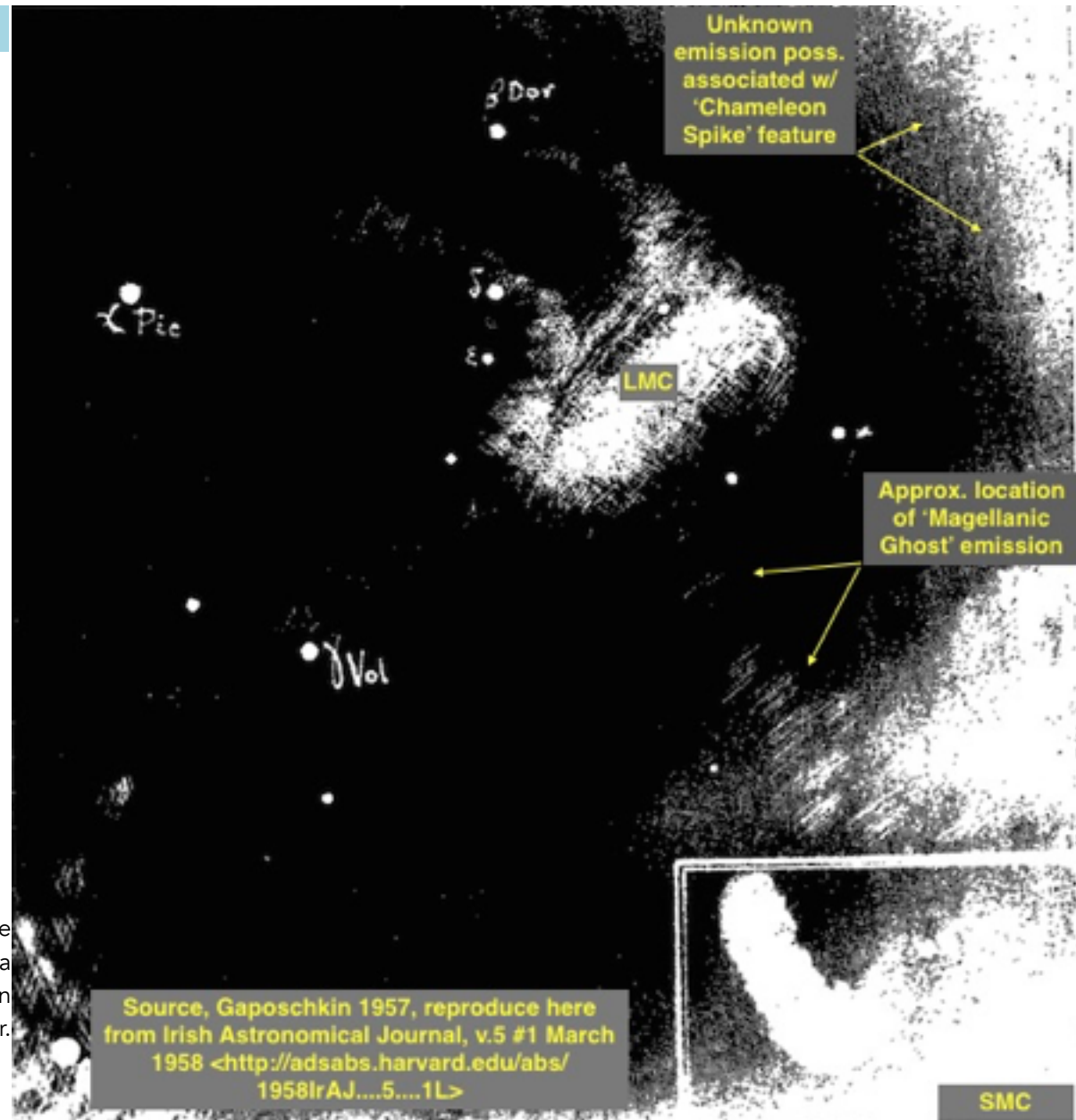


Gaposchkin 1958

It appears that the first person to mention a previously undetected emission feature near the LMC was the Russian born astronomer Sergey Gaposchkin in his article *Visual Brightness and Form of the Magellanic Clouds* in *The Irish Astronomical Journal*, 1958 p.4–6. His sketch can be found [here](#), but it is inconclusive what exactly his image reveals, and whether it coincides with the observations reported here. Gaposchkin wrote:

The L.M.C. resembles visually an S-shape pattern in which the upper end is less curved than the lower. The bar, or the main trunk of the Cloud, is directed practically straight towards gamma Volantis which is the apex of the Kite constellation above Beta Carinae. The very faintly delineated shades on the periphery of our pattern around gamma Volantis may well be of spurious nature. In the projection the Milky Way is not far from the LMC; the gaseous smoke of the Galaxy rising along a broad lane from the sun towards Carina can protrude high up and surreptitiously link the Galaxy with the Cloud. Another such visual linkage may be perceived starting from Gamma Velorum, irregularly sprawling under Canopus and joining the Cloud about Beta and Delta Doradus; and a third begins under the Cloud and reaches the Milky Way at Corona Australis [sic*] after passing the South Pole.

Fig 22: Sergey Gaposchkin's drawing of the LMC is available online only in this rather crude reproduction taken from a microfiche image in the library of the [Armagh Observatory](#) in Northern Ireland. The annotations are by this author.



Source, Gaposchkin 1957, reproduce here
from Irish Astronomical Journal, v.5 #1 March
1958 <<http://adsabs.harvard.edu/abs/1958IrAJ....5....1L>>

* Gaposchkin meant Triangulum Australis.

Lynds 1965, Sandage 1976

In 1975–76 Allan Sandage of the Palomar Observatory [undertook a deep-sky survey of the N galactic polar circle](#) using the 1.2 m (48") Schmidt camera. His goal was to find distant galaxy clusters that would extend the Hubble diagram. But unexpected faint diffuse emissions turned up in high equatorial latitudes near the M81 – M82 galaxy group. Sandage traced them to Dark Nebula No. 1778 in Beverly Lynds' [Catalogue of Dark Nebulae](#) (NRAO / ApJ 1962) which was located at $l = 359^\circ$ $b = +37^\circ$. Lynds catalogued and described 1,806 obscuration zones in her 1965 [Observations of High-Latitude Dark Nebulae](#) (*PASP Abstracts* 1965, p.134).

Over time Lynds' 1965 "dark nebulae" came to be more narrowly defined as Galactic Cirrus or Integrated Flux Nebulae since many of them exhibited extended red emission at very low energy levels. Her original 1962 entry for Nebula #1778 cited " $l = 358.85$, $b = 36.92$, RA = 15 37.2, Dec = -7 0, AREA = 0.86, OPACITY = 3." She went on to analyse #1778 more thoroughly:

The dark nebula No.1778 in the *Catalogue of Dark Nebulae* is located at $l = 359^\circ$ and lies 37° above the galactic plane. On the Palomar Sky Survey prints the nebulosity appears to be faintly luminous. A low-dispersion spectrum of this nebulosity was obtained by W. Livingston and C. R. Lynds using an image intensifier tube and the Kitt Peak 36-inch reflector. It covered the wavelength range of 4000–7000 Å. No emission lines were detected other than those of the night sky, but a 10-minute exposure of the nebula showed a stronger continuum than a 20-minute spectrum of a nonluminous comparison field. Therefore it is concluded that the nebula is of the reflection type.

In order to get a quantitative measure of the brightness of the nebula, photoelectric observations were made with the Kitt Peak 36-inch telescope, U, B_f, V filters, and a diaphragm 13 mm in diameter, which corresponds to 3.7 minutes of arc. Seven runs across the nebula were made by turning off the drive and allowing the nebula to drift across the field of view. The nebula appears to be of relatively uniform surface brightness; $V = 11.9$ in the 3'7 diaphragm, or 23.3 mag./arcsec². The $B-V$ color index of the nebula is about +1.5, and it was essentially undetectable through the ultraviolet filter.

An estimate of the absorption in the nebula was obtained by making star counts on the blue Palomar print. Very rough magnitudes were found by using the Lick Observatory 20-inch astrograph photograph of the region.

This photograph has a limiting magnitude of 19, as compared to 21 for the Palomar print. In addition, the short exposure on the Lick photograph defines stars of 15th magnitude, and first order spectra show up for stars of 11th magnitude. It was then necessary to interpolate between these magnitudes. The Wolf diagram of counts in a neighboring clear area and the nebula indicate an absorption of about 2.5 to 3 magnitudes and a distance of not more than about 100 parsecs.

The nebula subtends an angle of about $1/3^\circ$ which corresponds to a linear diameter of 0.6 parsec at a distance of 100 parsecs. The radius of 60,000 a.u. would make the object similar to Bok's "Larger Globules" with a particle density of about 2×10^{22} gm/cm⁻³ and mass of about $0.2 M_\odot$.

From its situation, the nebula appears to be an extension of the Scorpius-Ophiuchus complex of dark nebulae. However there appears to be no star so located as to account for the measured surface brightness of the nebula.

In another of astronomy's many belated "ahead of their time" predictions, Sandage anticipated the need for an all-sky extinction survey, which had to wait two decades before [Schlegel & Finkbeiner 1998](#) took the baton:

Two of the new high-latitude nebulosities (at $b = +40^\circ$ and $b = -50^\circ$) are reflection nebulae. This requires the presence of high-latitude dust, and a source of illumination. Calculations of surface brightness set out in Sec. III suggest that the illuminating source is the integrated light from the galactic plane. The argument is carried if the galactic plane is, in fact, the source of illumination, then the presence of dust in any high-latitude field must produce reflection nebulosities, and further that the value of the surface brightness permits calculation of the optical extinction through the halo in that direction.

Sandage estimated the surface brightness of the dust clumps in his images at ± 27 MPSAS based on their approx. distance as 100 parsec and particle density of 10^{-3} cm^{-3} . He had insufficient information to project the total numbers of Cirrus patches but he suspect them to be considerable because of their numbers in his very limited sample. In Section V, “*Consequences*” of his paper, he suggested that magnetic fields could produce the clouds’ striated shapes:

Special plates taken in continuum radiation show the regions to be reflection nebulae. *Calculations suggest that the source of the illumination at these high latitudes is the flux of the total galactic plane.* [Italics added for emphasis.]

This flux at any height h above the plane is equivalent to $M_V = 6.73$ visual magnitudes, independent of h . If the same grains that scatter the galactic light also cause the extinction Δm of the background objects in the line of sight, then a relation exists between observed surface brightness and Δm .

The question where the dust comes from is of interest. There is much prior evidence for matter in high galactic latitudes, principally from the polarization map of Mathewson and Ford (1970) and from the work by Heiles and collaborators of the HI column densities for $|b| > 10^\circ$ (Heiles 1974 [[1](#) (*PDF is 555 pages*), [2](#), [3](#), [4](#)]. From their correlations of galaxy counts, HI column densities, polarization vectors, and the well-known nonthermal radio loops, it is clear that dust must be present in the same region as the neutral hydrogen, the magnetic fields, and the relativistic electrons of the synchrotron loops.

Heiles (1976b) has also presented evidence that the HI loops are expanding, and he suggests supernovae explosions for their origin. Hence, there may be a natural way via these events for dust to reach the high latitudes from the plane. The heights are probably modest. We suppose that the order of distance to the reflection nebulae studied here is ~ 100 pc. If the proportionality between dust density and HI column density is the same at high latitudes as in the plane, then regions of high N_{HI} should be regions of strong reflection nebulosities. Our two areas discussed here are consistent with this view because for both directions ($\ell = 187^\circ$, $b = -50^\circ$; $\ell = 140^\circ$, $b = +40^\circ$) the neutral hydrogen maps show great HI density.

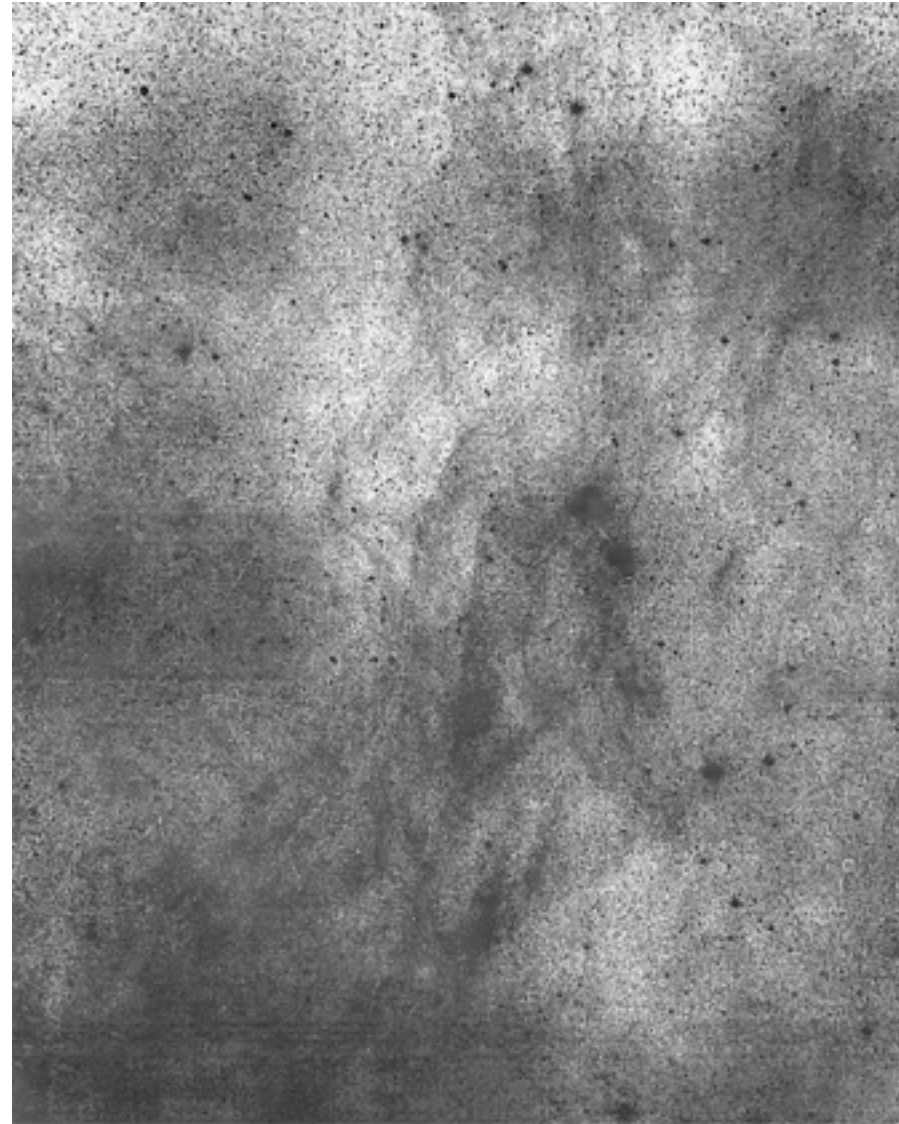


Fig. 23: Sandage 1976 high-contrast print from the original Palomar Sky Survey showing field centred on Eridanus $3^{\text{h}} 1^{\text{m}}$, $-6^\circ 00' \text{ m}$ ($\ell = 187^\circ$, $b = -50^\circ$), field size $3^\circ 12' \times 4^\circ 4'$. [Astronomical Journal v.81 #11, Nov. 1976.](#)

Sandage correctly surmised that the size of the observed nebulae in his report meant they could not be illuminated by a single or a few stars:

In this section we ask whether the integrated light of the galactic plane is sufficient to produce the observed surface brightness of the nebulosities, as previously suggested by van den Bergh (1966).

By this account, Sydney van den Bergh was therefore the first to relate the idea that the aggregate luminosity of the Galactic plane itself could illuminate an object placed at a shallow angle between an earthly observer and the object.

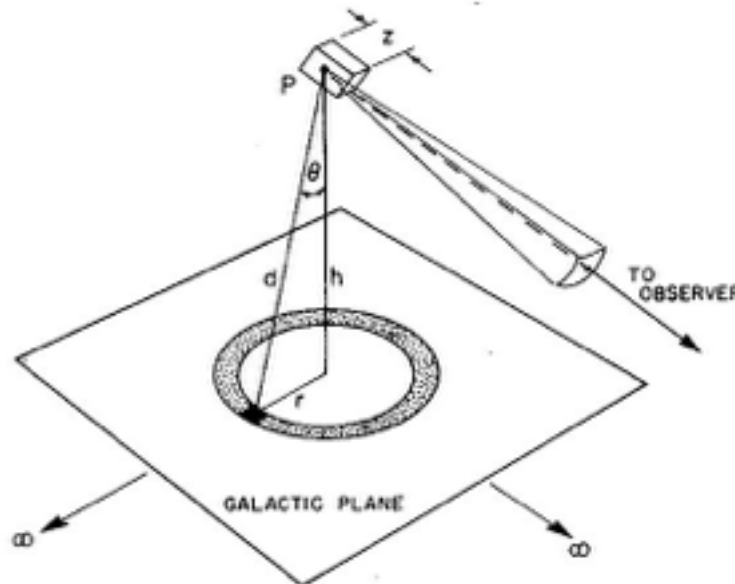


FIG. 1 Geometry of the illumination of point *P* by the galactic plane, and the subsequent scattering of the incident flux toward the observer.

Fig. 24: Geometry of the illumination point *P* by the galactic plane and the subsequent scattering of the incident flux toward the observer off-scale to the right. Source, Sandage, *Astronomical Journal* v.81 #11, Nov. 1976.

Do we call it Cirrus or Integrated Flux?

Why do we call Galactic polar-region dust "cirrus"? The professional community conveys mixed messages. Some papers refer to "Galactic cirrus"; others employ the more accurate term "integrated light of the Galactic plane" originally coined by Sydney van den Bergh. "Integrated flux" is the more accurate description because it defines dust clouds in terms of photons originating in the stellar activity of the disc plane, not in the dust itself.

Depending on the size and location of the dust cloud, the orientation of its constituent particles, their albedo, and the incoming incidence angle of the arriving light, photons from anywhere in the Galactic disc might reflect off a filamentary strand of cirrus in the celestial polar regions. Few incoming photons actually qualify on all counts, but those are numerous enough to raise an extended cloud of them to unaided-eye visibility.

The specific term "Integrated Flux Nebula" was coined by the American amateur astronomer Steve Mandel in the mid 2000s. He was unaware that Allan Sandage had explained that term 1976, but Mr. Mandel's phrase is now commonly used.

Prof. Adolf Witt of the Univ. of Toledo (OH) USA has clarified how the "Galactic cirrus" term entered the picture:

Alan Sandage (1976) already discussed and explained such nebulosities, and their extent became fully known to the astronomical community from the infrared all-sky maps produced by the IRAS satellite in the mid-1980s. It was then that the term "infrared cirrus" was coined, which was not a good choice because the cirrus can be observed at optical wavelengths as well, as Sandage and [Steve] Mandel, among others, had shown." (pvt. communication Apr 2018)

Mr. Mandel may not have originated the terminology of the emission, but he certainly did discover that Galactic cirrus has a reddish or "mauve" hue that would not be the case if their surface brightness was strictly the result of reflection. Mr. Mandel used various filters to determine that their faint red glow was not from H α singly ionised hydrogen emission.

Riddle in a mystery wrapped in an enigma

Magellan's "Ghost" is not the first time the Magellanics have been steeped in mystery. To paraphrase Churchill, for three centuries these bright nocturnal clouds were a riddle in a mystery wrapped in an enigma. They were a mariner's apparition sometimes seen, sometimes not, depending on the state of the sea and the air (to say nothing of the mariner). The darker the surroundings the more certain they seemed. They were variously described as a trace, a wraith, a ghost, a chiaroscuro, a half-existing thing. Sometimes they were in plain sight, like the smoking gun on a table spotted by the ever-alert Sherlock Holmes. Other times they were as fleeting as the transfer of large amounts of cash from an offshore island to an investment account in Macau.

As smoking guns go, the late 15th century Italian historian Peter Martyr d'Anghiera, found a good one, though he didn't know it at the time. In a series of letters and reports that were published from 1511 to 1530 in his chronicle of Spain's explorations in the Americas titled *De orbe novo* ("On the New World") he made a passing reference to two glowing objects which appeared from May through July in the Southern night sky from the island that Columbus named La Española (Hispaniola today). He called them *nubes*, or "clouds".

Three decades later, Antonio Pigafetta sailed with Ferdinand Magellan on his circumnavigation of the world in 1519–1522. He logged the objects as "*nuvem*". The rather more credulous deck hands thought the Clouds were the spirits of Jesus and the Good Thief winging their way heavenward. At the clouds' present rate of motion around the Galactic disc, there will be plenty of time for the Good Thief to repent before he gets there.

A century and a half later Johann Bayer's 1603 *Uranometria* showed them without labels in the 49th and 51st chart of his *Synopsis coeli inferioris austrina* ("Overview of the southern hemisphere"). A later 1661 re-edition of his *Uranometria* labeled them *nubecula major* and *nubecula minor*. Nicolas-Louis de Lacaille's 1756 star map referred to them as *le Grand Nuage* and *le Petit Nuage*. Eventually the clouds came to be indelibly associated with Magellan, even though he was not the discoverer.

The rise of image-based dark cloud cataloging

One night in 1784 the usually reserved William Herschel exclaimed to his sister Caroline recording his observations on the ground below, '*Hier ist wahrhaftig ein Loch im Himmel!*', or 'Here is truly a hole in the heavens!'. She dutifully recorded it, even including the exclamation mark.

Herschel had glimpsed one of the dark nebulae in the Ophiuchus Nebular Complex. He reported the discovery the following year in *Philosophical Transactions Series I* 75:2135, 1785. For the next century until astrophotography arrived following the work of E. E. Barnard, astronomers were undecided whether these dark objects were true voids or simply regions that had few stars. Hardly anyone suspected they might be bright nebulae that didn't shine. Astronomers didn't know why stars shone in the first place. It was a little like stamp collectors buying pricey little pieces of paper to dote lovingly on the glue side.

Systematic surveys of the distribution of dark nebulae were undertaken by relatively few early astronomers. The most extensive was Lundmark and Melotte (1926), based on the 1903–04 [Franklin-Adams charts](#). Their map listed 1500 objects, most of which were in the higher galactic latitudes. Barnard's [Catalogue of 349 Dark Objects in the Sky](#) (Univ. of Chicago Press, 1927) listed objects that he identified using his own photographs. His is still considered one of the landmark photo atlases and is highly desired in the antiquarian collector's world. The physical data of Barnard's 349 objects are accessible [here](#).

In 1960 J. Sh. Khavtassi of the [Ambastumani Astrophysical Observatory](#) in Georgia, USSR published an atlas of galactic dark nebulae based on the 1934 photo atlases of Ross and Calvert and Heyden's 1952 plates. This was listed as a supplement to Khavtassi's 1955 catalogue of dark nebulae 20° above and below the galactic equator. In 1962 Beverly Lynds updated these earlier catalogs with her own [Catalogue of Dark Nebulae](#). She produced an 1,806-entry compilation by meticulously examining POSS-1 plates acquired with the Palomar 48-inch Schmidt camera and entering the data — on IBM computer punch cards!

The work owes its origin to a suggestion by Sir David Gill, pointing out the desirability of a photographic research into the structure of the Milky Way. Mr. Franklin-Adams subsequently extended the scheme to the photographic charting of the whole sky.

With this end in view he obtained from Messrs. Cooke & Sons in 1898 a 6-inch lens of the three-piece type working at $f\ 4.5$, designed by Mr. Dennis Taylor to give good definition over a large field. This lens was so successful that a larger one of similar type was ordered; it was delivered in 1903 and was of 10 inches aperture and 45 inches focal length, giving very good images over a field $15^\circ \times 15^\circ$ on a scale of 20 mm. to the degree.

Mr. Franklin-Adams and his assistant, Mr. Kennedy, used this lens at the Cape Observatory in the years 1903–4, and the Southern sky was photographed with exposures of 2 hours for each plate. After his return to

Fig. 26: Extract from an account of the landmark [1903–1911 Franklin-Adams photographic research of the structure of the Milky Way](#).

The need for image plates covering $15^\circ \times 15^\circ$ fields corrected for the blue end of the optical range went beyond the capabilities of equipment at the time. That shortcoming inspired the development of both new equipment and new ways to use it. In response, serendipity waved its magic wand over Yorke, England in 1870 and gave the world Dennis R. Taylor. This young man in his early twenties was blocked from higher education because of his working-class origins. In 1892 he went to work for Thos. Cooke & Sons as a trainee barely out of school. He found that he had a gift for optical design. He was equally skilled at business sense. In five years he was chairman of the company.

The parameters for the Franklin-Adams survey were formidable given the limitations of optical design at the time. The long-focus $f/15$ traditional achromat doublet obliged long, ponderous optical tubes, which in turn demanded massive mounts. They were wholly inadequate for the $15^\circ \times 15^\circ$ plates demanded by the *Franklin-Adams Atlas*. Dennis Taylor pushed his creativity to its limits and came up with a 6-inch design with the unheard-of speed of $f/4.5$. The design took a totally original approach: three separate glass elements separated by wide air gaps. The success of the design evolved into the landmark Cooke Triplet lens design which set the standard for astronomical (and personal snapshot camera) imaging until after World War II. Some Nikon macro lenses still used the design as recently as the 1990s.

Where does cosmic dust come from?

With the 1927 publication of E. E. Barnard's *Catalogue of 349 Dark Objects* astronomers began to classify distinct cloud types. Amorphous lumpy blobs with sharp density gradients were visually distinct from linear streaks, but when examined spectroscopically they often seemed to be composed of much the same atomic and molecular hydrogen, plus varying ratios of elements heavier than helium. Over the years spectroscopists discovered the signatures of carbon monoxide (CO), hydroxyl (OH), cyanogen (CN), ammonia (NH₃), formaldehyde (CH₂O), and other carbon-based molecules. Collectively they are termed *polycyclic aromatic hydrocarbons* or PAHs. Molecular spectroscopy became more sophisticated until by the 1960s it was a significant science.

A major step forward came from outside astronomy when Hannes Alfvén developed the principles of magnetohydrodynamics (MHD) in the 1960s. Alfvén first coined the word in 1942 and received the Nobel Prize for his work in 1970. The basic concept was straightforward — fluid dynamics and electromagnetism interact reciprocally in an electrically conductive medium.

About that same time metal-oxide semiconductor (MOS) technology devised ingenious new ways to compress millions of slide rules, compasses, protractors, and drafting tables onto a wafer the size of a match head. Then a pinhead. Today a pinpoint.

MHD lofted into space along with gravimeters and particle counters as soon as politicians got over gloating over how big their bleeping spheres were. The electromagnetic spectrum dramatically broadened across the 1970s and 1980s as space-based platforms ventured into the realm of x-ray and gamma energies on one end, and the millimetre to sub-micron realms on the other. Because interstellar dust is readily detected in the micron band, astronomers realised these tiny smoke-sized molecular aggregates were too complex and important to be dismissed as a mere nuisance. One of the most far-reaching properties was that an aggregate of molecules with electric dipoles (the sequence of an atom's positive and negative charges within a molecule's structure) would act as the magnetic dipole moment of the entire particle. The particle would orient itself perpendicular to magnetic field lines.

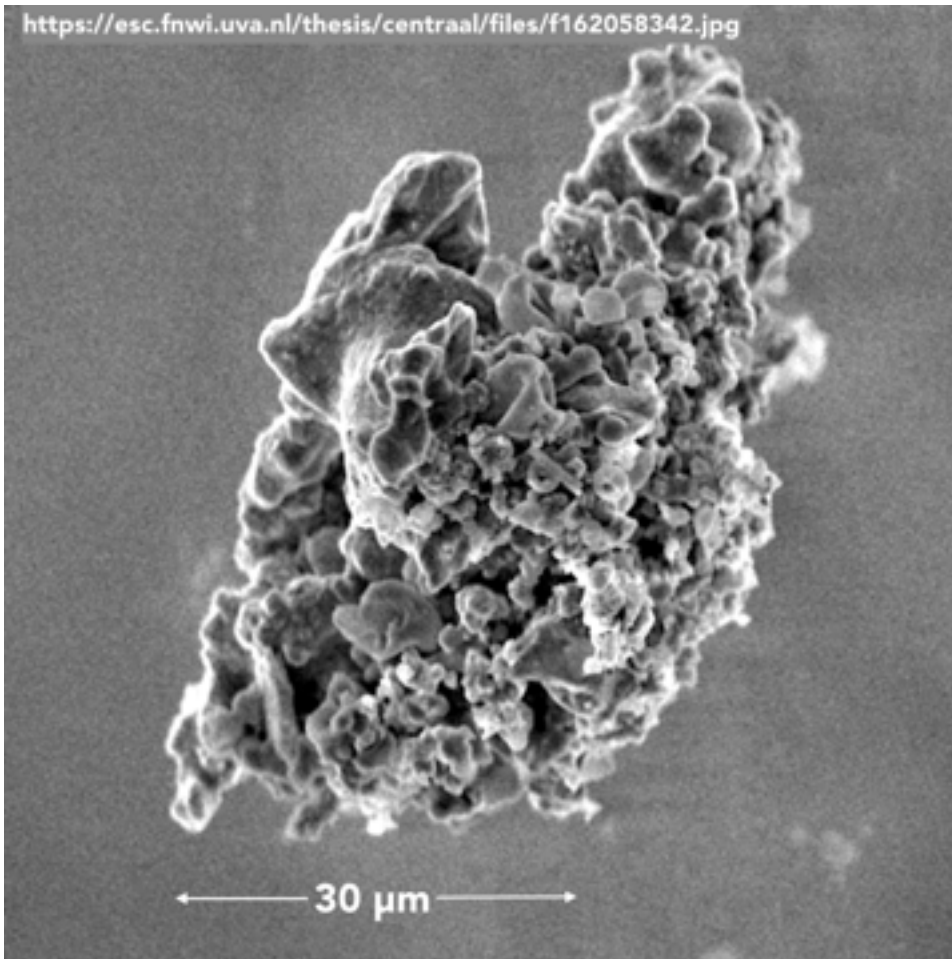


Fig. 26: Most cosmic dust particles are between a few molecules to 0.1 μm in size. Larger marticles such as this one are conglomerates of many small ones. Most dust originates in the cool atmospheres of asymptotic giant branch stars (AGB) during a brief evolutionary swan song called Third Dredge-Up. The star is highly unstable at this point. Deep convection to bring vast quantities of carbon and oxygen up from the hot but inert core. In the cool stellar atmosphere it coagulates into tiny particles and is expelled into space as cosmic soot. Grains observed in IR and UV include graphite, polycyclic aromatic hydrocarbons (PAHs), silicates, carbonates, and sulfides. Some grains are needle-shaped; some are dense cores covered with ice mantles; still others are fractal fluff balls. Above is one of the particles gathered during the [Stardust satellite mission](#) to trap dust in silica gel for return to Earth.

Fig. 27: Nearly all interstellar dust particles acquire a magnetic dipole moment as simple molecules accrete onto their surfaces over time. A magnetic moment (μ) measures the tendency of a molecule or atom to align itself with any magnetic field around it. The magnetic dipole resembles a tiny bar magnet with north and south poles (hence "dipoles"). Its potential or susceptibility to align with an external magnetic field depends on the aggregate dipole moment of all the molecules adhering to it. Examples of the dipole moments of molecules commonly found frozen onto dust grains are:

Hydroxyl HO $\mu=1.66$ Debye

Water H₂O $\mu=1.8546$ D

Nitrosyl hydride HNO $\mu=1.62$ D

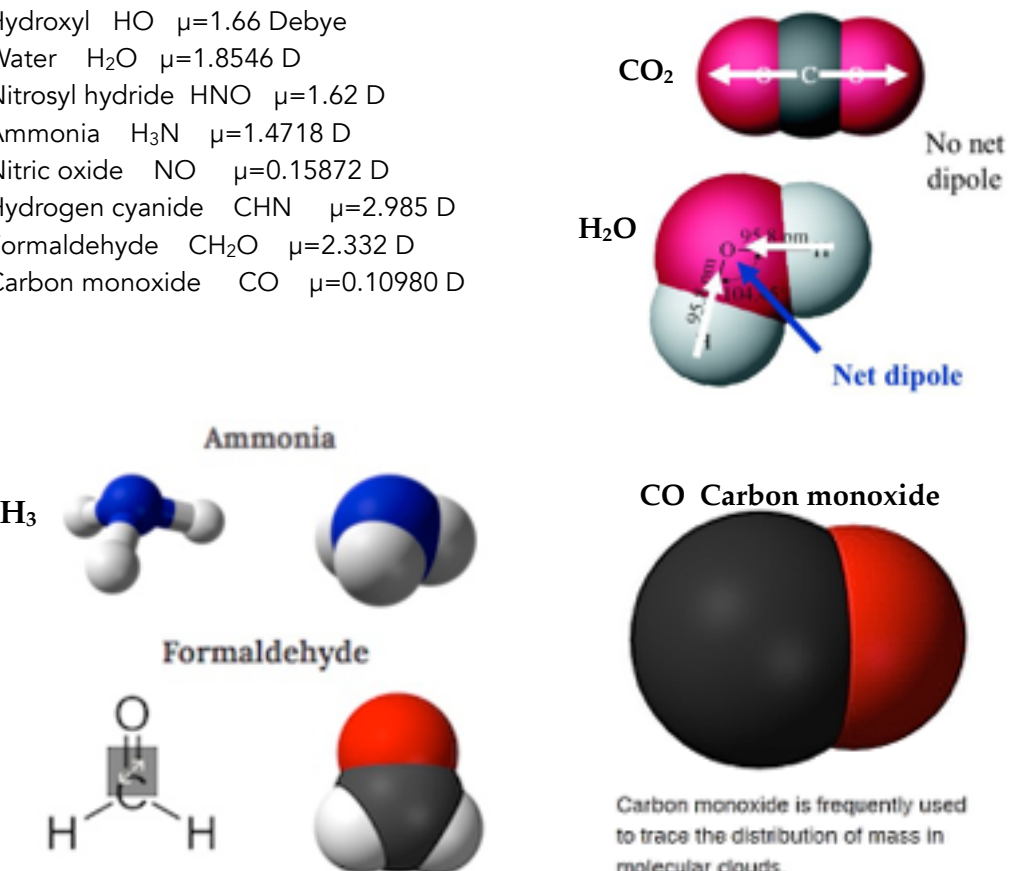
Ammonia H₃N $\mu=1.4718$ D

Nitric oxide NO $\mu=0.15872$ D

Hydrogen cyanide CHN $\mu=2.985$ D

Formaldehyde CH₂O $\mu=2.332$ D

Carbon monoxide CO $\mu=0.10980$ D



Parting the Curtains

As digital acquisition and processing techniques improved between the 1980s through the 2010s, dense dust clouds became seen as a critical catalyst in the gas/stellar magnetohydrodynamics of galaxy, and not just in the spiral arms where most of it lies. The typical gas-to-dust mass fraction in a disc galaxy is less than 1%. Gas clouds whose scale lengths varied from several parsecs to several hundred parsecs were found to have higher metallicities the closer they were to the disc. Galactic cirrus contain relatively little HI and HII gas because their remote location so high above the disc plane, and because much of it has frozen out as molecular species on the grains. Even today we have an incomplete picture of the 3D tomography of Galactic dust clouds in the polar regions.

Source crowding is a significant constraint when studying dust clouds near the disc plane. Astronomers rely on column density counts as the easiest tracer of molecular cloud mass — typically $N_H = 10^{19} \text{ cm}^{-2}$ for volumes of 1 H atom per 10^{-4} cm^{-3} , i.e., the average density of the Milky Way halo. However, while the Herschel satellite made it possible to precisely determine column densities from dust emission, the data was unclear how distant any given parcel might be. While it is straightforward to calculate total atomic hydrogen column density via the relation $NHI/E(B-V)$ using the 21 cm band, there is no easy way to calculate a specific segment of that column. Line-of-sight (LOS) source blending diminishes above 35° Galactic latitude, which happens to be about the same angle the celestial poles are above the disc plane.

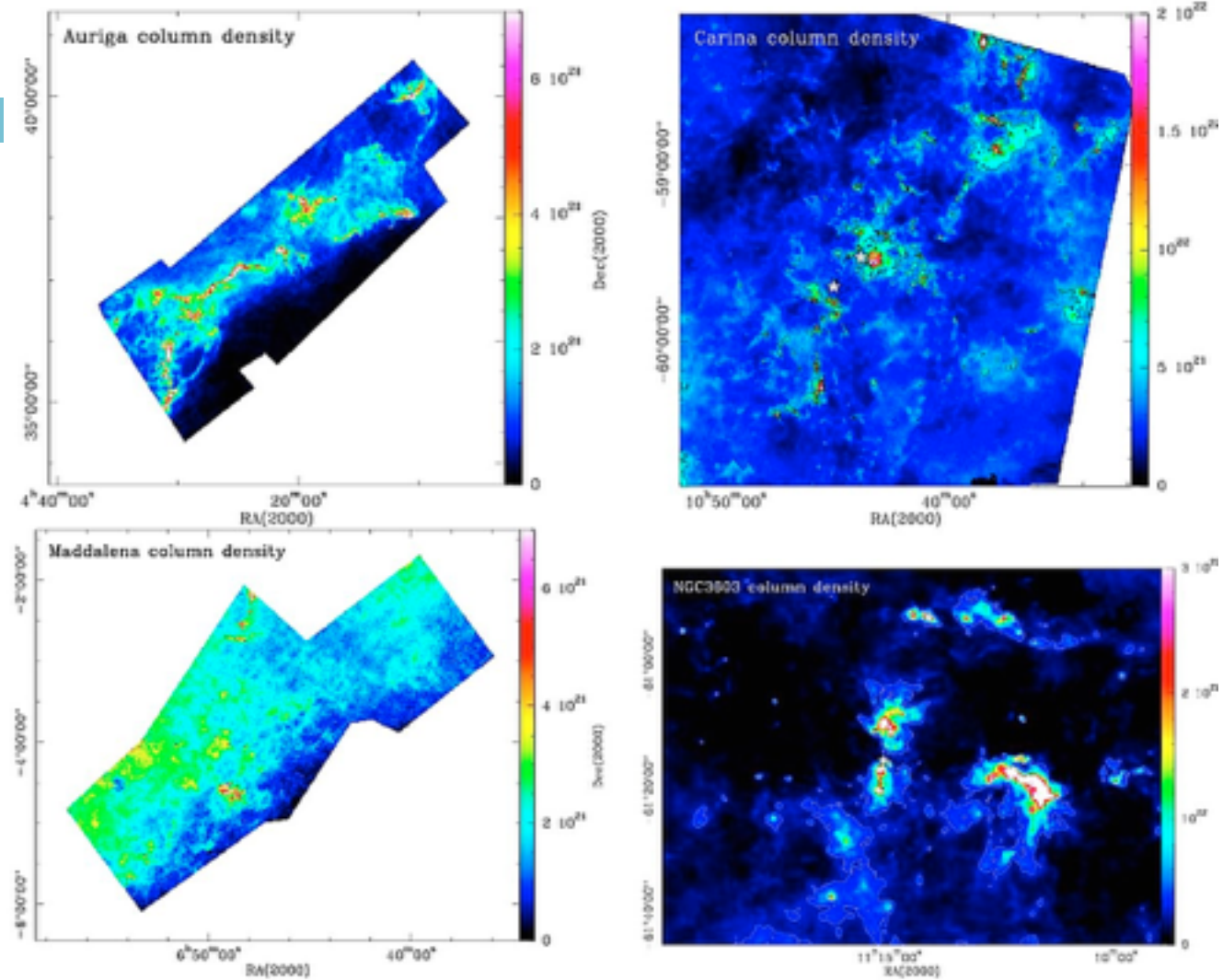


Fig. 28: It is difficult to distinguish the emission of a specific cloud when there is significant cross-talk from foreground/background clouds. [Here four high-latitude dust regimes are compared](#). Low-mass and high-mass star-forming clouds tend to have similar column densities. The critical factor driving cloud collapse is internal supersonic turbulence. (1, 2, 3.) At higher column densities, shock fronts prevail according to the power law $\rho = r^{-\alpha}$ where α is the power-law tail. At gas densities (ρ) above $N_H > 10^4 \text{ cm}^{-3}$ gravitational energy surpasses the gas's internal energy density. The cloud free-falls rapidly into protostar clumps. Leftover dust is ejected back into space, forming linear threads. The threads acquire their skinny elongated shapes from turbulent shock fronts after clouds go subsonic and collapse into protostars.

Interstellar Dust and Magnetic Fields in the M8 Lagoon Star Forming Region

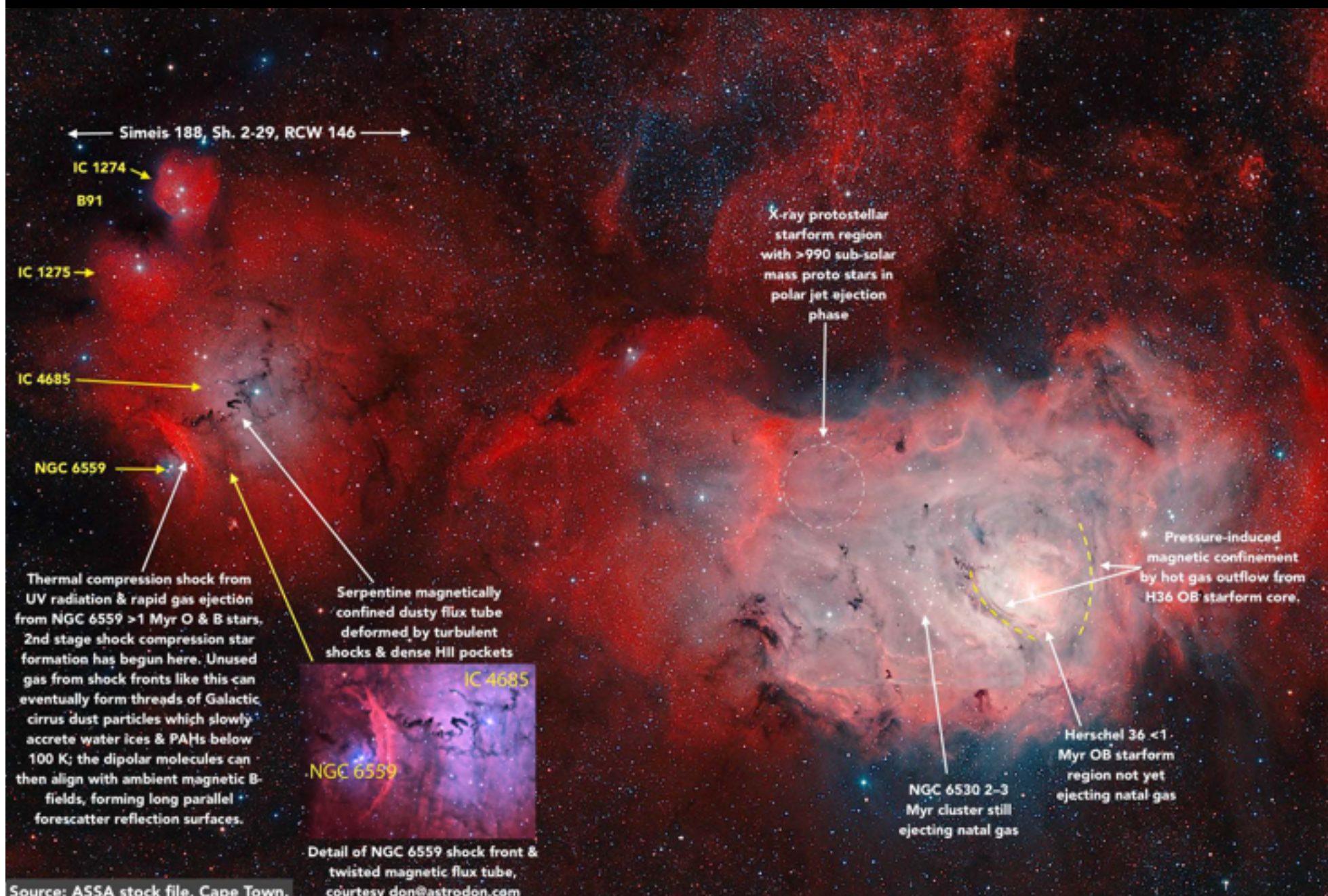
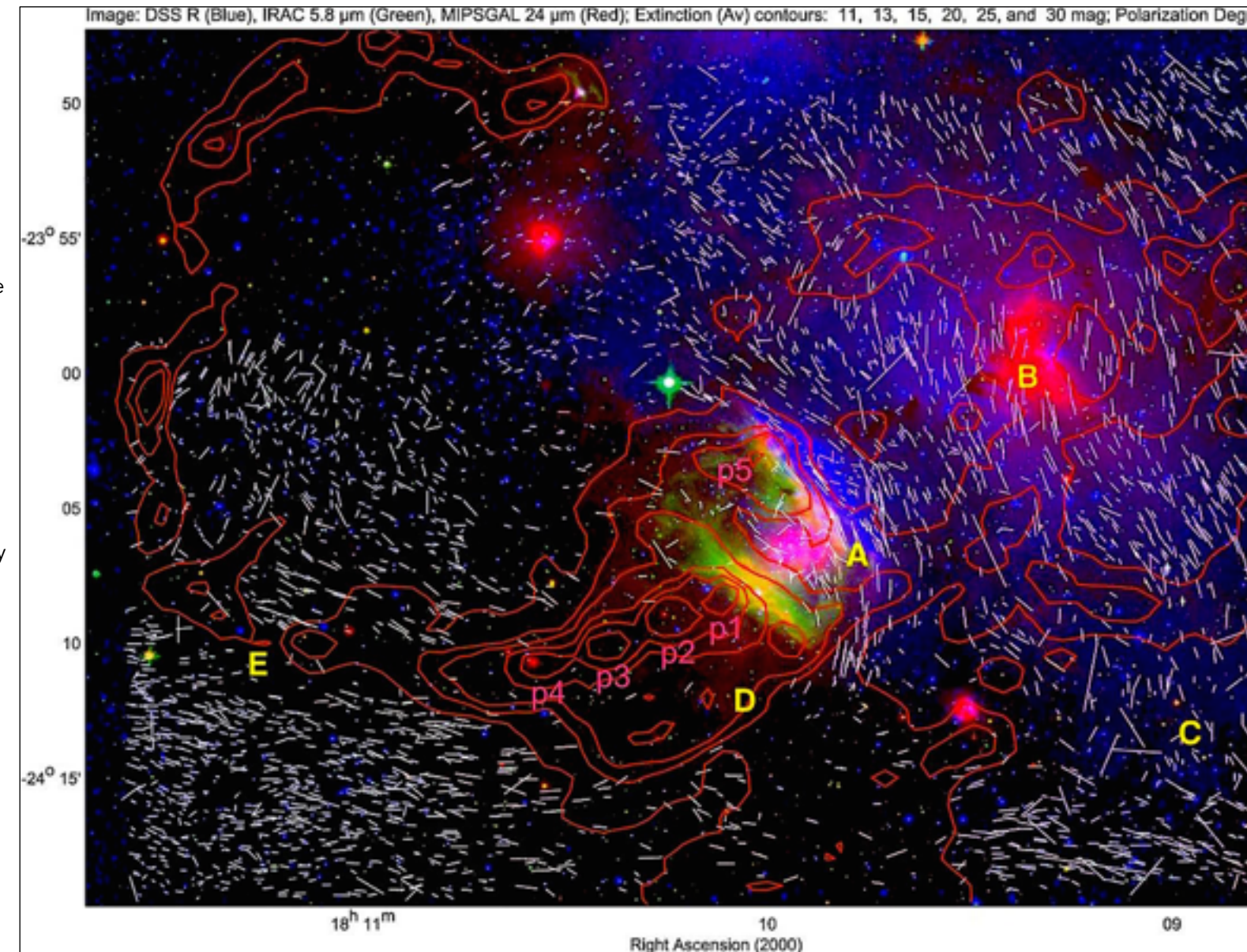


Fig. 29: The M8 star-forming complex is an example of the intricate relationship between cold gas/dust clouds; collect-and-collapse gravitational free-fall into star clusters; subsequent natal gas ejection starting ± 0.5 million years after star formation; magnetic field confinement that quenches turbulence shock; and gas dispersion by shock fronts. The small inset image shows HII's pressure-heated reddish shock morphology when an ionised gas bubble is compressed by high-Mach ($M \approx 20$ to >100) shock front. The trapped gas in the lens-like bubble is redirected along its long axis by magnetic confinement. Inset detail courtesy of Astro Don.

Fig. 30: In this FIR image of Simeis 188 we see the intricate relation between magnetic fields and the distribution of interstellar dust. Simeis 188 (aka SH 2-29) is on the easternmost edge of the giant Lagoon Nebula complex lying 4000–6000 ly from the Sun. Thermal and turbulence shock fronts act as transition cushions between intra-cloud regimes with different physical properties. (In oceanography they call these thermoclines and isohaline contours.) The shock fronts serve as [a particle transport interface](#) redirecting gas and dust away from the collision front and out toward the edges. Shock waves have high proportions of electrically conductive ions in them, hence the particle velocity out of the system is more sensitive to magnetic pressure than thermal pressure. The velocity of the gas flow is determined by the sound speed (Mach unit) and the [Alfvén speed](#) (oscillation between the electric field and the [magnetic field](#)).

In this image the contours are visual extinction A_V ; the colours are red=Spitzer MIPS 24 μm ; green=Spitzer IRAC 5.8 μm ; blue=DSS R-band. The clumps p1–p2–p3 are subsonic cores collapsing in free-fall into star-forming cores. The opaque void in the upper left is a dense gas reservoir losing mass via transport along the white stripes which stand in for magnetic field lines in this overlay. The length of the lines



indicates the relative travel distance compared with others in the image. Magnetic field lines pile up along dense gas interfaces. The Simeis 188 magnetic strength value is $\approx 400 \mu\text{G}$ and aligns in patterns shaped by HII compression. Studies of the extinction patterns reveal two distinct populations of grain particle size. The contrarian effects of grain coagulation and grain fragmentation contribute to local heat gradients associated with UV-emitting stars. The polarisation vector is parallel to the sky-projected component of the magnetic β -field lines. Source: [Santos et al 2014](#).

Do filamentary molecular clouds make filamentary dust clouds?

Until the mid 2010s the standard picture of star cluster evolution was that ambient magnetic fields present in nearly every galaxy act as the primary stabilising pressure against thermal and ionisation turbulence shocks that gas and stars bequeath to galactic discs. Magnetic pressure shields gas bodies against dispersion while it simultaneously constrains the tendency of those gas bodies to collapse. Over time, magnetic resistance and turbulence insistence wear each other down until gas clouds can free-fall into cores dense enough for stars to light up. The stars then proceed to live dismaying messy lives. Gas makes stars, stars make dust. Magnetic fields obligingly feed them all.

For many years astronomers thought that magnetic forces inhibited thermal and ionic turbulence on time scales of about 10 Myr through [ambipolar diffusion](#) (1, 2, 3) in which neutral particles slowly bleed out of an ionised cloud. This picture shifted focus when certain properties predicted to occur in real clouds could not be detected in them. For example, star formation regulated by ambipolar diffusion predicted a higher mass-to-flux ratio in a cloud's molecular hydrogen core than in the cloud's atomic hydrogen envelopes.

When this was not observed in real clouds despite many careful screenings, an alternative theory proposed that huge molecular clouds collapsed globally — all over and all at once. Stars would form very quickly (100,000 to – 500,000 years) until the hottest of the stars produced enough UV ionising radiation to quench further star formation by blowing the unused gas away. UV is the most powerful of several forces at work in the overall process of [stellar feedback](#). Another feedback component is high-velocity gas ejection from hot stars, such as Wolf-Rayet bubbles (see [Fig 42](#)). Still another was cosmic rays.

The catastrophic collapse theory had its problems. It predicted a small number of very hot and massive star clusters but fewer low-mass clusters. The sky begged to differ — many more small clusters than large clusters are produced during the typical molecular cloud's 50-million-year star-making cycle. (1, 2, 3.)

Another theory was then proposed that [the sound speed \(Mach number\)](#) in a gas cloud regulates star formation. In this view, turbulence plays a crucial dual role. On large scales, turbulent kinetic energy stabilises clouds and inhibits rapid collapse. On local scales the size of a cluster, supersonic shock

waves regulate the pace and mass of star formation. This results in a [multi-free-fall scenario](#) in which [many shock waves infall from many directions](#). These self-dampen to subsonic velocity over a system-wide crossing time.

An inverse effect occurs in the interacting expansion shocks of a Wolf-Rayet nebula. Multiple sequential eruptions erupt in a reverse multi-free-fall expansion. A series of supersonic ejection threads merge into a shock field that resembles a thick bubble (see [Fig. 42](#) on p.48).

While we usually think of shock waves as coming one at a time from supersonic jet airplanes or the blast wave from a terrestrial detonation, stellar ejecta clouds merge large numbers of shocks over time into an expansion bubble. [This simulation](#) shows multiple ejection from a model galaxy disc.

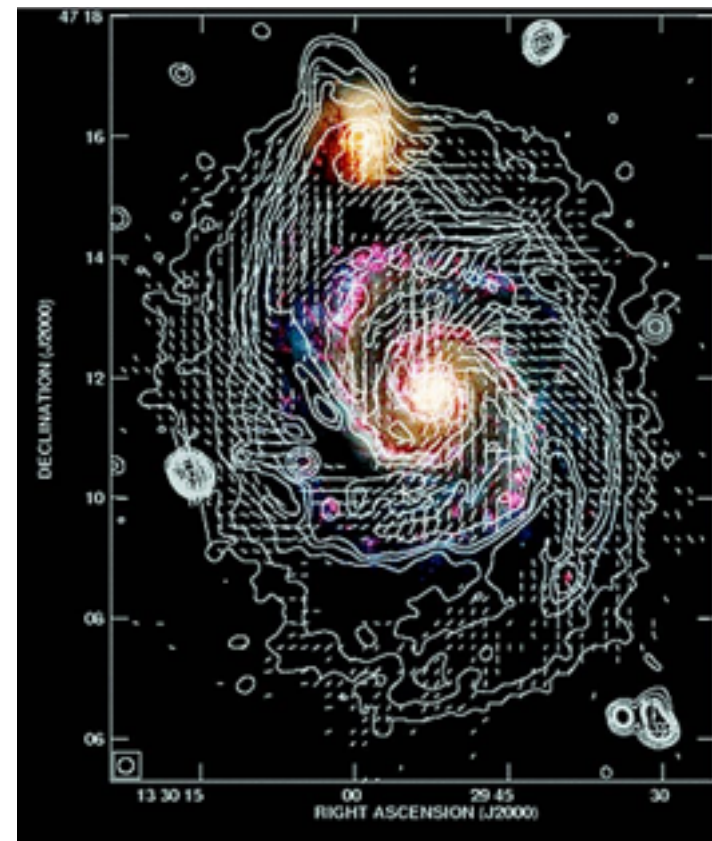


Fig. 31: The M51 Whirlpool Galaxy is often studied to compare its system-wide magnetic field with the local-scale arm and interarm gas dynamics. Star formation in the disc violently disturbs the spiral arm's overall β -field. The magnetic field of the arms is disturbed by thermal and sonic shock fronts. Conversely, the large-scale field is little disturbed because it is coupled to the overall disc's weakly compressed diffuse, warm gas. These effects are termed [bimodal magnetic field structure](#).

Magnetic attraction

Most Galactic cirrus is characterised by filaments and threads produced by magneto-acoustic star formation processes as molecular clouds infall toward star clusters. But what produces the structure of ejected natal gas? Why do we see so many filamentary dust clouds so high in the Galactic disc yet so many amorphous clouds near the disc?

There is a veritable cottage industry of astrophysical studies of star cluster formation, but few indeed are the astronomers devoting their careers to what happens to the leftovers. Astronomy is hardly alone in its paeans to the chandeliers of glitter to the neglect of the dust on the furniture. What upscale fashion magazine lavishes full-page features on a couturier's crumpled remnants? The swatches are no less beauteous, they're just in the wrong place. The same can be said for filaments in Galactic cirrus.

There are commonalities between pre-collapse molecular clouds and post-cluster molecular debris. For one, both pre- and post-cluster natal gas lies within a large spiral arm with an ambient β -field circling with the disc's rotation. For another, pre- and post-cluster filaments do not move very far laterally or longitudinally within the spiral arm. Hence dust clouds endure similar torque stresses throughout the entire gas-to-cluster, cluster-to-gas cycle.

During a cluster's formation epoch, supercritical forces of magnetic confinement and supersonic shocks weaken each other until their parent gas cloud becomes critical enough that gravitational collapse can initiate a star cluster. In most cases a number of

clusters form sequentially within a filament of molecular gas — a process aptly-named "beads-on-a-string formation". ([1](#), [2](#), [3](#), [4](#), [5](#), [6](#), [7](#), [8](#)) However, our interest here is what processes are at work on the other end of the cycle. What converts a star cluster's expelled gas and dust down in the Galactic disc into the cirrus-like filaments that we see ± 100 pc above the disc?

The magnetic, kinetic, and chemical properties at work during the supercritical-to-subcritical transition are generalised forces that exist in the spiral arms of any disc galaxy. They interact with each other to transform gas clouds into star clusters. But do those forces — magnetic fields, turbulence, and in particular protostellar jets — work the other way?

Protostellar jets have recently come to be seen as the lead actor who enters the stage once a star cluster has formed. (Watch [video version of the lower right quadrant](#) in the video still of **Fig. 48** on p.51.)

Given the ubiquity of poloidal and toroidal magnetic fields associated with stars embedded in a Galactic β -field being subjected to spiral disc torques, is there a common thread, so to speak, that operates analogously to the gas expansion when magnetic and turbulent forces interacted during compression?

Several models have been advanced to explain the various features of Galactic cirrus. An early model was based on shock compression from stellar feedback, supernovae, and turbulence ([1](#), [2](#), [3](#), [4](#)). However, the model did not explain a common property in molecular clouds: filament size, shape, density, and distribution.

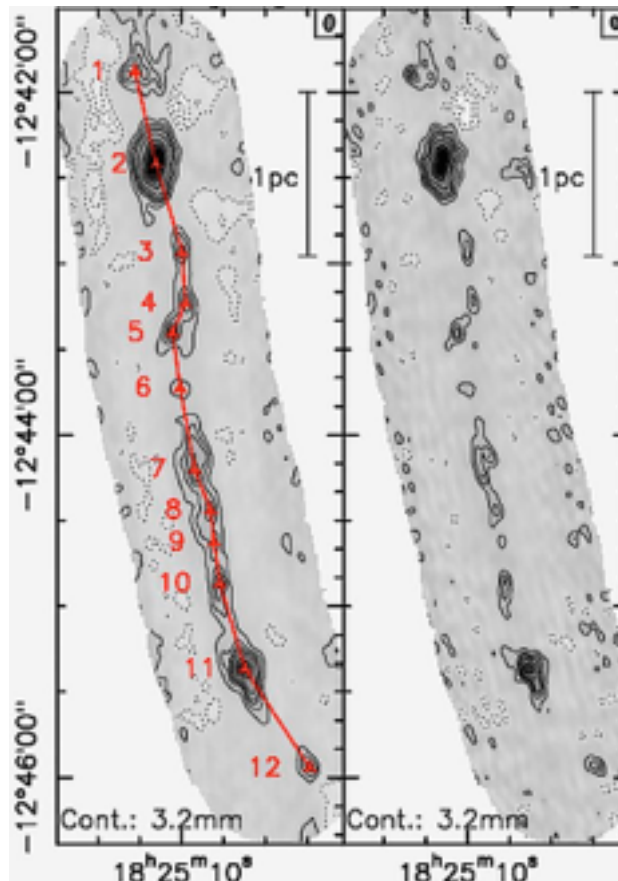


Fig. 32: Beads-on-a-string star formation in magnetically confined gaseous filaments.
Source: [Beuther et al. 2015](#).

Herschel springs a surprise

Astronomers had known from the 1960s that the large-scale gravitational force of galactic spiral arms can form filaments in gravitationally unbound complexes. A well-studied example is the Polaris Flare cloud in the N Polar Region. (The most flagrantly understudied example is the home of Magellan's Ghost, the Chameleon-Musca-Apus-Octans complex in the S Polar Region.)

In 2001 Padoan et al. held that dusty filaments were stagnant dense, post-shock gas from young star clusters. At first the filaments were thought to be shaped by supersonic flows, but astronomers suspected that magnetic fields also had a role in channeling mass onto the filaments.

In 2011 the Herschel telescope provided data that surprised everyone: filaments, no matter where they were, were a uniform ± 0.1 pc wide. At first, astronomers thought this pointed to the primacy of turbulence over magnetic confinement. The reasoning was that in a plane-parallel shock front the thickness (designated λ_{sonic}) of the post-shock gas layer is related to the thickness L of the preshock gas by $\lambda \approx L/M(L)^2$, where $M(L)$ is the Mach number and $M(L)^2$ is the compression provided by the hydrodynamic shock.

That, however, could not explain why dust filaments had . . . of all things . . . a thermal gradient. How could they? They lie in the coldest crannies of the galaxy. What possibly could warm their little bones so far out there in the brutal dumping ground of unwanted stellar wastes?

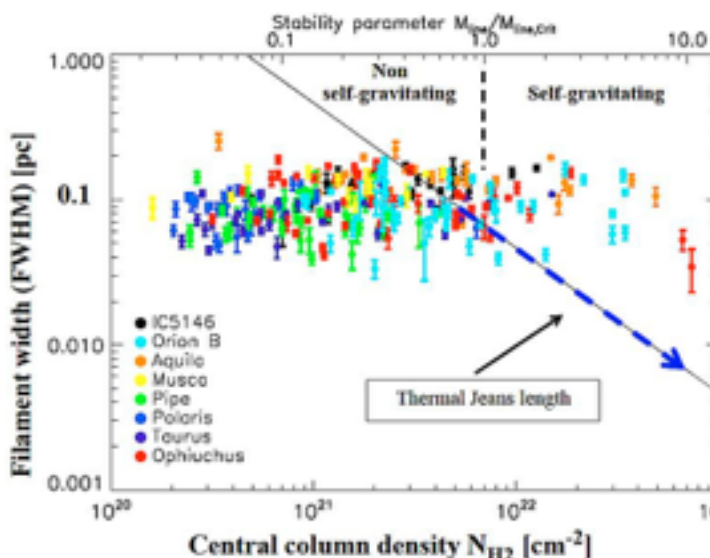


Fig. 33: If large-scale turbulence provides a plausible mechanism for forming the filaments, the fact that prestellar cores tend to form in gravitationally unstable filaments (André et al. 2010) suggests that gravity is a major driver in the subsequent evolution of the filaments. Source: [Arzoumanian 2011](#).

Temperature/density readings across IC 5146 (aka the Cocoon Nebula in Cygnus) showed that the nebula's filaments' internal temperature dropped from ± 14.5 K along the outer edges to ± 11.8 K in the middle. At the same time, the filament density gradients went from $N_H = \pm 4.5 \times 10^{19}$ at the edges to $N_{HII} = \pm 1.5 \times 10^{22}$ in their centres. Moreover, the filaments were inexplicably uniform in their length-to-width ratios, at 0.1 pc wide and roughly 40 times that long.

The Cocoon Nebula was chosen partly because its location was in Herschel's ambit, but also because it is a stellar nursery replete with young stellar objects (YSOs) amid a bumptious crowd of main sequence stars up to the mass of B1 at $14 M_\odot$ which would be emitting UV powerful enough to clear the nebula of its gas. As star-forming models go, it was a poster child.

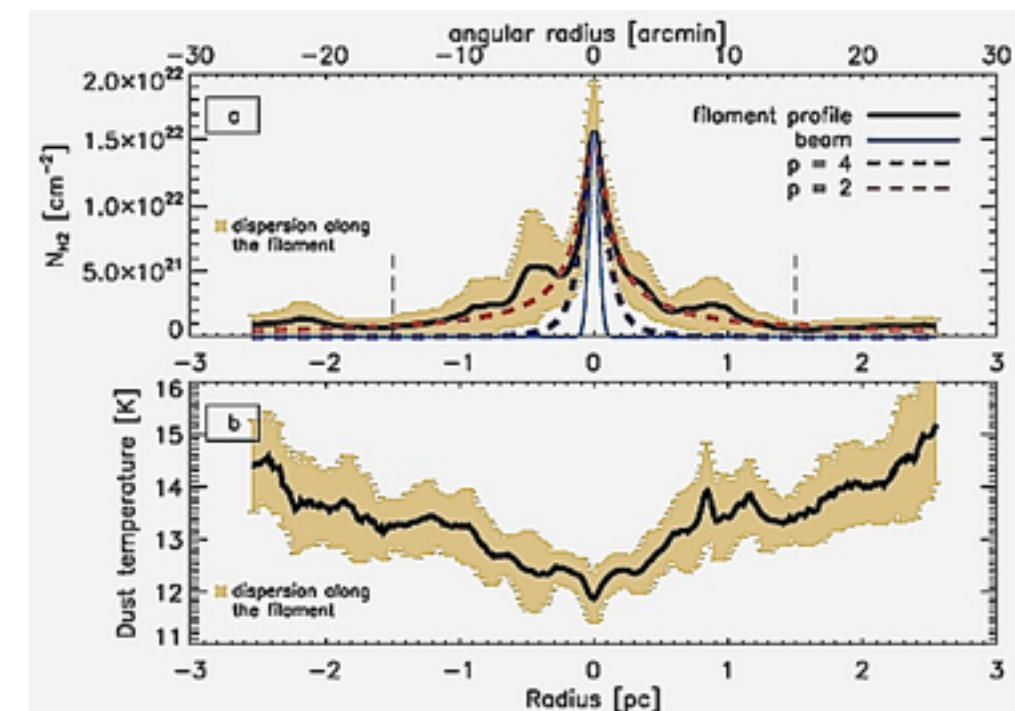


Fig. 34: While gas/dust filaments in star-forming nebulae were not especially surprising, that the translucent, non-stellar Polaris Flare cloud exhibited the same temperature and density gradients was difficult to explain.

The wealth of data provided by the Herschel telescope suggested two other mechanisms that might operate in the formation of filamentary cirrus. Both presumed that magnetic β -fields were dynamically important:

- The first was *gravitational contraction controlled by the β -field* (1, 2, 3.). This interpretation derived from observations of the Taurus molecular cloud complex and the Pipe Nebula which revealed an ordered large-scale magnetic field characterised by elongated condensations perpendicular to the large-scale field. Star formation was initiated when gas gravitationally ordered along the field lines. If the gas mass-to-magnetic-flux ratio approach the critical density for the conditions of a particular filament, star formation would begin in that filament. This mechanism was comparatively slow because the gas condensations in the filaments were only moderately supersonic. Star formation rate was moderated by by magnetic field pressure rather than turbulence pressure. The clusters were characterised (and therefore could be identified) by the small average masses of their stars and that only about 1% or less of the magnetically critical gas actually turned into stars during the limited free-fall time.

- The second was *Anisotropic sub-Alfvénic turbulence* (SAT). This view held that turbulent pressure tends to channel gas distribution along the field lines, hence produces filaments aligned with the β -field. The competition between gravitational and turbulent pressures in a medium dominated by β -fields will elongate the cloud either parallel or perpendicular to the β -fields while reaching equilibrium.

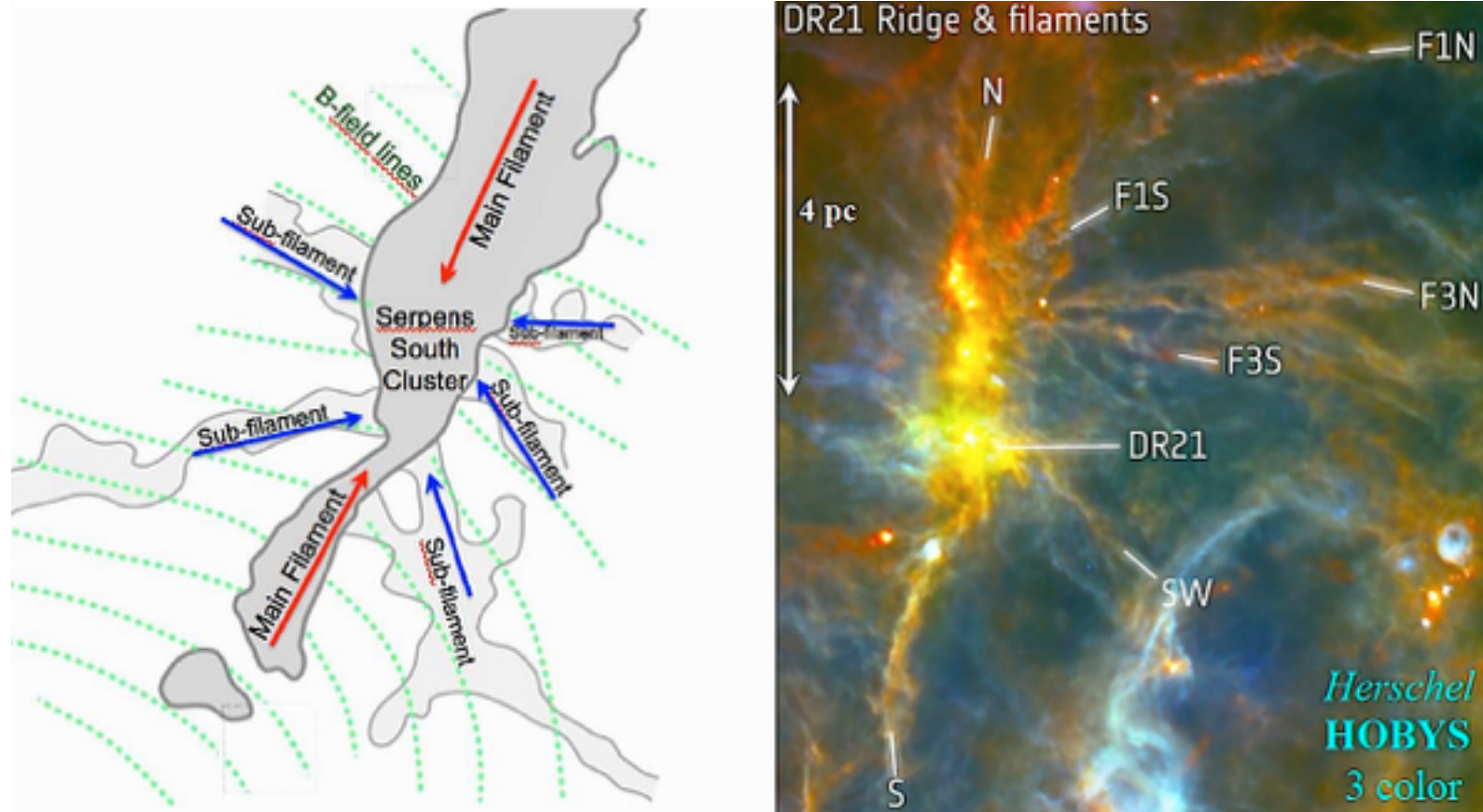
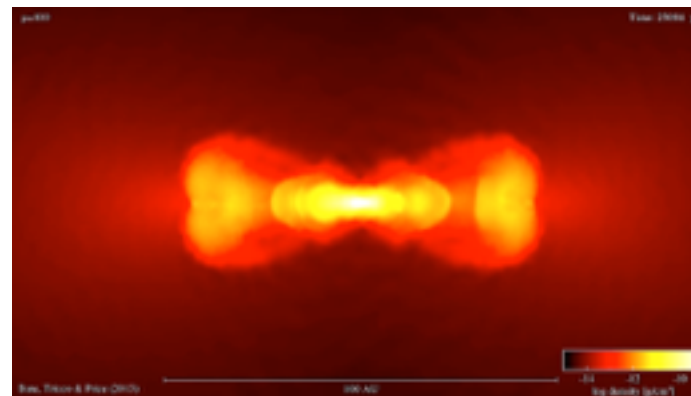


Fig. 35: Accretion flows from sub-filaments onto main filament, a common pattern comprising a typical ridge structure dominating a network of infalling sub-filaments. Source: (l) [Sugitani 2011](#) & [Kirk 2013](#); (r) [Herschel HOBYS 3-color](#) image from [Hennemann, Motte et al. 2012](#).

How filamentary striations arise — an example from protostellar jets

Observations of similar-looking striated filaments in widely different conditions suggest a waveform or vortex aetiology. Toroidal vortices are responsible for conglomerating dust into rings in protoplanetary discs, for example. Toroidal instability arises from variations in dust-to-gas ratio, which concentrates dust grains in a disc. Instabilities during dust settling introduce a vertical entropy gradient. An entropy gradient drives a pressure inequality, which in turn can create toroidal gas vortices which in turn channel dust into

Fig. 36: Collapse of a molecular cloud core to stellar densities in simulations of stellar core and outflow in radiation magnetohydrodynamic simulations (from Bate & Price 2013).



The sim on the right is #4 of a sim set which reveals how protostellar jets form in pre-main sequence star-forming clouds up to $8 M_{\odot}$. Magnetic and thermal forces contribute to the launching of a stellar outflow. The four simulations trace (a) the formation and evolution of the first hydrostatic core, (b) the collapse to form a stellar core, (c) the launching of outflows from both the first hydrostatic core and stellar cores, and (in the above image) (d) the breakout of the stellar outflow from the remnant of the first core.

The four sims illustrate the roles of magnetic fields and thermal feedback on the outflow launching process. The structure of the stellar core is insensitive to variations in the initial magnetic field strength. With strong initial magnetic fields, accretion on to the stellar cores occurs via inspiralling magnetised pseudo-discs with negligible radiative losses. Magnetic field strengths of >10 kG can be implanted in stellar cores at birth. (View each sim [here](#): 1, 2, 3, 4.)

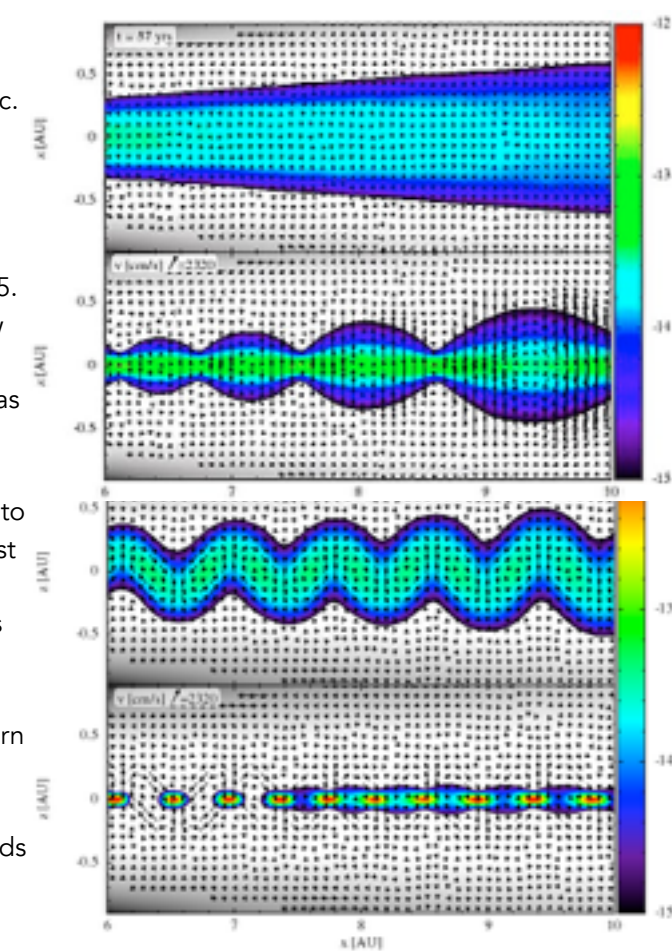
rings. Dust rings are typically observed in continuum emission of the dust's scattered light. Entropy instability may also foster dust agglomeration — yet another mechanism for transporting angular momentum within a galaxy disc.

[See this example](#) of the chaotic energy exchange in the disc plane.

Source: [Loren-Aguilar et al 2015](#), Toroidal vortices and the conglomeration of dust into rings in protoplanetary discs.

Fig. 37: These four animations illustrate the development of instabilities in a protoplanetary disc. Millimetre radii dust particles are initially distributed throughout the gas with a uniform dust-to-gas density ratio of 0.01. The gas disc has a vertical scale height $H/r=0.05$. The [online animations 1, 2, 3](#) show vertical slices through the disc, giving the azimuthally-averaged gas and dust densities.

The dust settles towards mid-plane, but slows as it does so due to drag with the gas. This forms a dust layer thinner than the gas disc. A baroclinic instability then develops at small radii, which then spreads outwards through the disc, which strengthens into a sinusoidal pattern of toroidal vortices. The dust becomes corrugated. The vortices migrate larger dust particles towards the centres of the vortices.



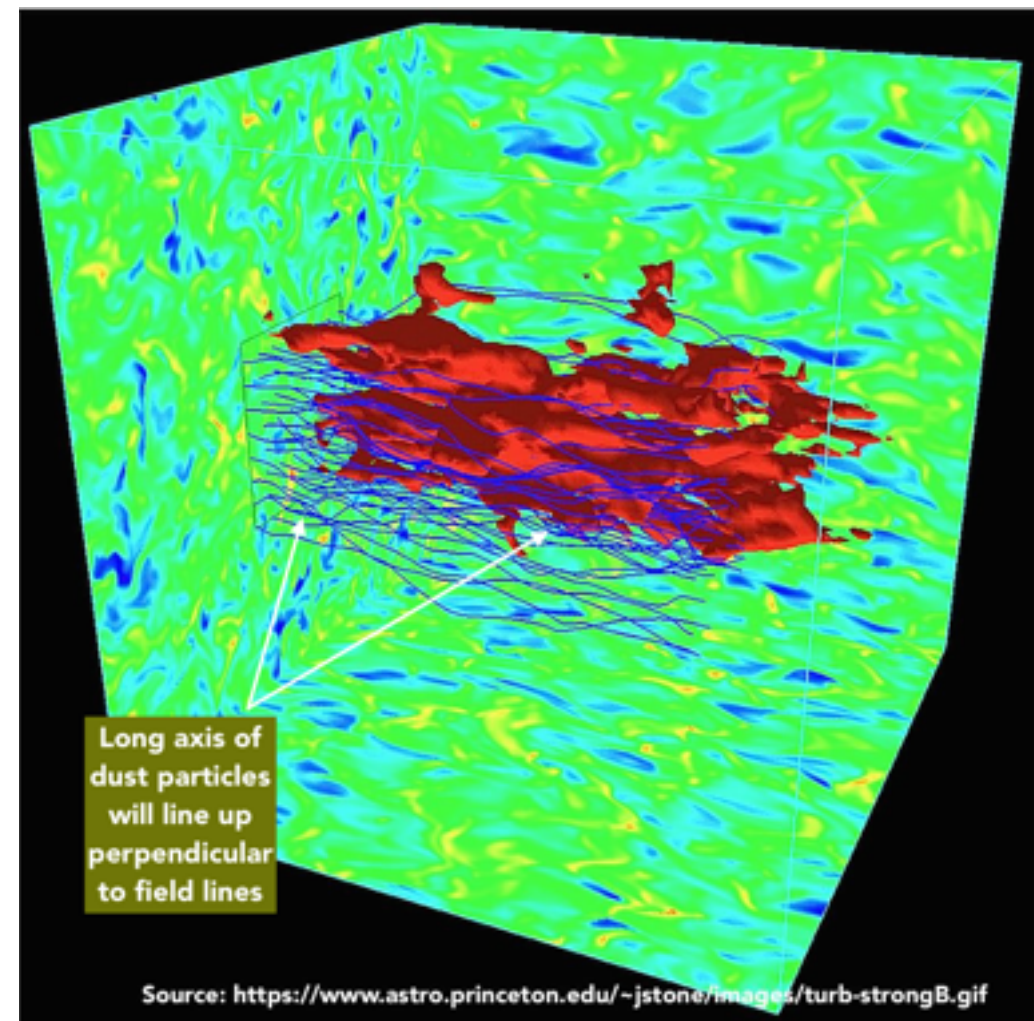
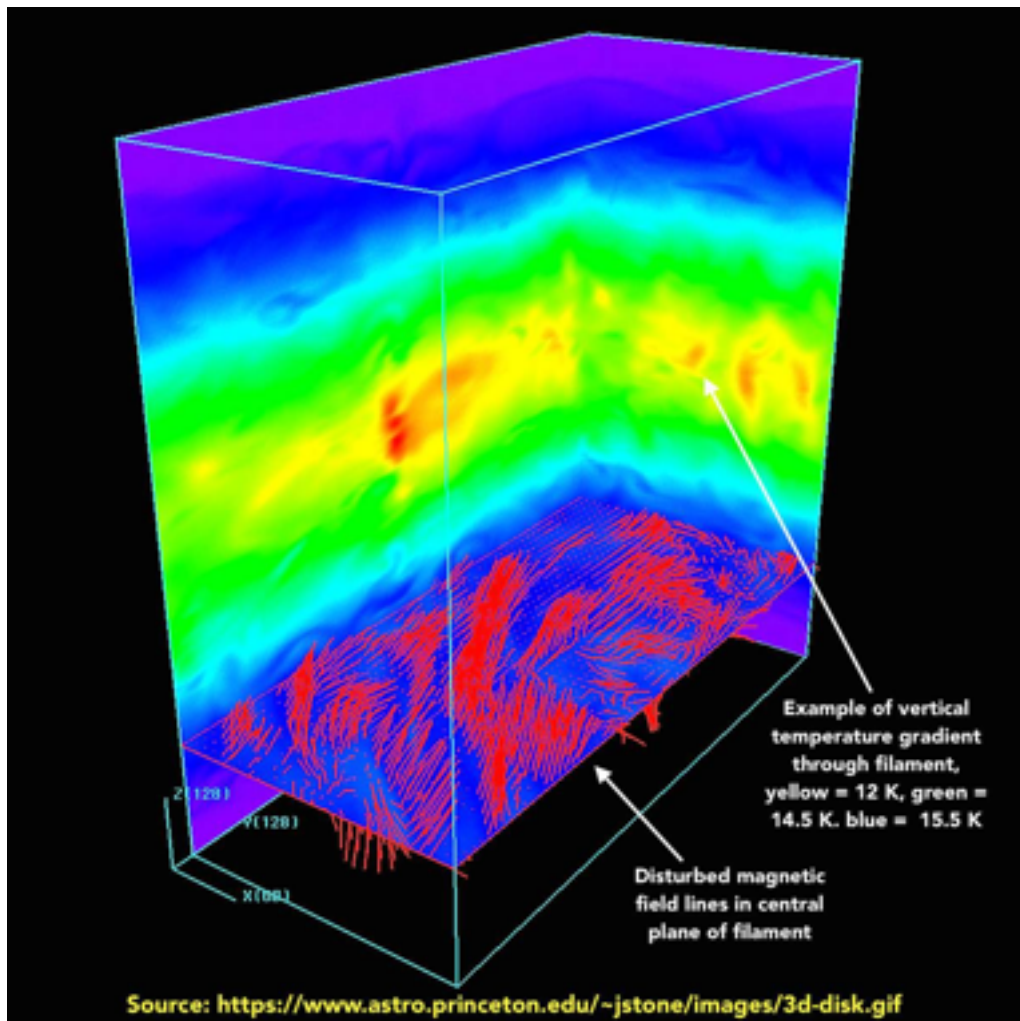


Fig. 38: Cirrus-like dust filaments might look like a plate of spaghetti, but they act like the sauce. Their surface density rises from edge to centre. They have a slight temperature gradient due to turbulent compression and super-Alfvénic magnetic field turbulence. They are slightly cooler along the centreline because the overlying gas mass has absorbed some of the incoming UV photon and cosmic ray energy. These computer-generated models depict gas/dust filaments in or near the disc plane. Galactic cirrus 82–130 pc above that plane has not been studied with the thoroughness enjoyed by disc clouds. All we can do for the moment is make reasoned guesses as to whether the filament physics displayed above replicate well in the much colder, quieter remoteness far above the fray of life in the disc plane.

The interaction of protostellar jets, Mach >1, and solenoidal fields

A statistical study of young stellar objects in the vicinity of 322 mid-infrared bubbles detected by Spitzer revealed that fast shocks of velocity v_{sh} of a few thousands km s $^{-1}$ produce hot gas with temperature well above 10 6 K, which slowly cools thus providing long lived high pressure bubbles. The shocks also efficiently produce nonthermal pressure components of highly amplified fluctuating magnetic fields and relativistic particles with partial pressure P_{nt} which may reach a sizeable fraction $\eta < \sim 0.5$ of the shock ram pressure. These nonthermal components may affect the ionization and sources of turbulence in molecular clouds. Source: [Nonthermal particles and photons in starburst regions and superbubbles](#), Bykov 2015.

During the 1970s computer technology was widely applied to astronomy for the first time. In 1965 Penzias & Wilson had detected microwave photons from an epoch when the first atoms steamed off a primordial soup of electrons and protons. In so doing they put an observational foundation under the theory of the Big Bang. The Space Race injected unheard-of funding into what amounted to a scientific windfall to adjudicate a political tug-of-war. Astronomy luxuriated in a welcoming bubble bath of telescopes, observatories on the ground and soon into space, more precise detectors, bandwidths they could never have even dreamed of before, and those hopeful wallflowers at university budgeting conferences, astronomy professors. Ph.D.s soon leapt off the campuses and even into space, delighting astronomy magazines, National Geographic, and TV with splendours of the heavens we could scarcely imagine the year the last auto with Brobdingnagian tail fins rolled off the line. It was all quite jolly, actually.

Along came desktop computers to inject unheard of calculation speed and accuracy into astronomy departments all over the world. Every advance set the scene for the next two advances. Next thing we knew they were in our cell phones. In 1973, Princeton University astronomers Jeremiah Ostriker and James Peebles devised numerical N -body simulations to study how galaxies work. N -bods as they were called in the irreverent 70s had been known and used before, but memory limits and computer processing speeds yielded unrealistically coarse-grained models. Even Ostriker & Peebles in the USA and Yakov Zel'dovich & Jaan Einasto in Moscow and Tartu had only 100 2 data

points to represent objects in a plane. Today N -sims calculate tens of billions of data points in 4D at megaparsec scales through the entire life of the Universe. By 2015 computer modeling had become so sophisticated and widespread that it was nearing parity with observation.

More germane to our quest after the reality of Magellan's Ghost, by 2014 astrophysicists were modeling the interplay of magnetic fields, gravitation, multiple free-fall scenarios, using sound speed as the sock puppet for the hard numbers behind turbulence's fluid chaos. [[1](#), [2](#), [3](#), [4](#), [5](#), [6](#), [7](#), [8](#), [9](#), [10](#), [11](#), [12](#), [13](#), [14](#), [15](#), [16](#), [17](#).]

While molecular clouds should be gravitationally unstable and collapse on their global mean freefall time-scale, in reality they take 10–100 times longer. The actual SFR per freefall time (SFR_f) is only a few percent. This is difficult to account for using traditional 3-element turbulence–magnetic fields–gravity models. Other physical mechanisms must exist that counteract the rapid global collapse in 3-element models.

One candidate for modulating molecular cloud collapse and dissipation is protostellar jets. These jets not only add to but can actually reinforce the velocity fields of normal stellar outflow. Moreover, they continue to add energy to the ISM after traditional gas ejection is completed. Models constructed by Federrath et al 2015 and 2016 showed that clouds collapse on a gravity-only mean freefall time but produce stars at an unrealistic rate. If, however, turbulence, magnetic fields, normal stellar feedback, and now protostellar jets are included, the SFR_f is 0.04.

However, 0.04 is still two to four times greater than observed rates. ([Krumholz & Thompson 2012](#), [2](#), [3](#)) [Federrath et al. 2014](#), [2](#), [3](#)). Today this problem has been addressed with good results by [Krumholz et al. 2014](#), [Tom Peters et al 2016](#), and the sims of the [SILCC Project](#). These propose that two other momentum-driving forces are at work: *Photon Bubble Instability* (PBI, [Blaes & Socrates 2003](#), [2](#)) and *Radiative Rayleigh–Taylor* (RRT) instability ([Krumholz et al. 2009](#), [2](#), [3](#)). The SILCC Project simulations vividly illustrate that momentum feedback is a powerful feedback force.

Dust grains are sub-micron refractory [able to withstand high heat] particles built up by accreting gas atoms and molecules from their surrounding medium. They are a necessary – indeed vital – component of the interstellar medium. There are of two basic types of grain: silicates and carbonaceous grains. Dust alters the physics and chemistry of its surroundings in multiple ways. One of the most important is absorbing ultraviolet (UV) radiation from hot O type stars that pepper galaxy discs and hot star-forming regions. About 30% of the stellar light at UV wavelengths is reprocessed by dust grains and re-emitted in the infrared. A small fraction of the absorbed energy is returned to the ISM via photoelectric emission, which is the dominant heating source of the extended red emission (ERE) in the diffuse ISM. Dust affects the thermal balance of the ISM by locking away cooling species such as C+ and Si+.

Grains play a dual role in astrochemistry: (a) they shield molecules from dissociating UV photons, and (b) act as an electrostatic catalyst for the formation of HII and complex organic molecules. HII is made only on the surfaces of dust grains, hence dust is the primary construction material of molecular clouds. The size distribution and chemical composition of dust determine each grain's interaction with matter and radiation. In molecular clouds dust grains are shielded from UV radiation and collision sputtering. They build mass by accreting atoms and molecules in a two-tier process of (a) binding gas atoms or molecules onto the tiny surface areas of sooty particles until they become grains, and (b) agglomerating large grains out of many small ones.

The ISM is classified as (a) the *cold neutral medium* or CNM [the realm of Galactic cirrus]; (b) a *warm neutral/warm ionised medium* (WNM/WIM) that comprises the cores of molecular clouds; and (c) a *hot ionised medium* (HIM) that pervades the ISM whether or not there is star-forming activity.

By 2000 Fiege & Pudritz (2, 3, 4, 5) used simulations to demonstrate that magnetic fields stabilise gas/dust filaments against gravitational collapse in two ways: (a) toroidal fields reinforce gravity in squeezing filaments; (b) poloidal fields along the filaments provide magnetic pressure support against gravity.

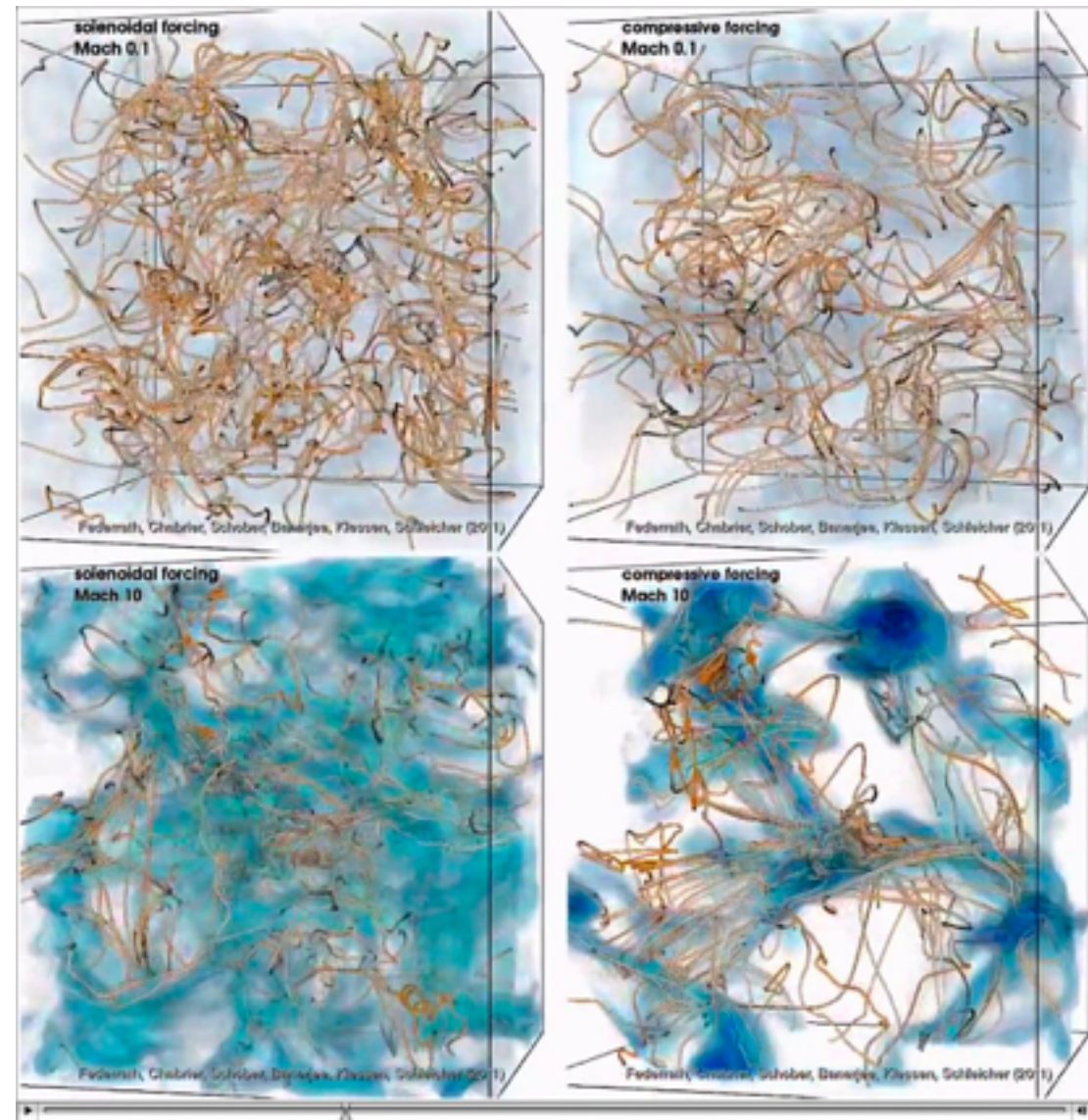


Fig. 39: Turbulent magnetic field structures in four computer models that assumed different physical properties. The effect of Mach speed is striking. Solenoidal forcing is produced by electrons moving through magnetic flux tubes (gas solenoids). Compressive forcing arises by the sharp variances in gas pressure produced by shock waves produced during star forming and stellar radiation. This suggests that the Galactic cirrus clouds of Magellan's Ghost originated as high-Mach magnetic torques which produced multiple fine filaments from originally diffuse dust produced in the Galactic disc plane. (See 1, 2, summarised with a [full-motion sim here](#).)

How do magnetic fields affect dust particles?

Magnetohydrodynamic (MHD) simulations are an experimental proving ground for studying the evolution of turbulent gas in a magnetic field. In [2016 Soler et al.](#) examined the relative orientations of density gradients and magnetic fields in 3D MHD simulations. In the sim runs which included algorithms for decaying turbulence, filaments at low densities aligned parallel with magnetic field lines, but at high densities the alignment shifted to perpendicular. The behaviour was inexplicable, but the data came from the 2013 Planck release and was robust.

In a re-look using [Planck XIX 2015](#) and [Planck XXXV 2016](#) polarisation data, the data confirmed that magnetic fields tend to align parallel with diffuse filaments. The data indicated polarisation fractions as high as 20% at low total gas column density (N_H), but decreased systematically with increasing N_H to a low baseline for $N_H > 10^{22} \text{ cm}^{-2}$ densities.

In the diffuse interstellar medium, magnetic β -field energy dominates the mix of gravity and thermal energy. The Planck results provided convincing evidence that a magnetic β -field directs infall linear with diffuse gas. This suggested that dense filaments tend to self-gravitate perpendicular to the magnetic field, an effect called solenoidal flux. (See [Fig. 39](#) on p.43 and [Soler et al 2016](#).)

The [2016 Planck Collaboration XXXII](#) analysed the relative orientation between density structures and polarisation across nearly the entire sky and concluded that most of the elongated filaments or ridges are predominantly aligned with the magnetic field as measured on the structures. Again the statistical trend became less striking as column density increased.

All this suggests that we can expect that the polarisation fraction will be on the order of 20% and possibly more in the thin gas densities at Galactic cirrus altitudes of 82 – 130 pc above the Galactic plane.

About 80% of the dust condensed from ejected oxygen-rich stars consists of [amorphous silicate precursors](#) of crystalline compounds, e.g., enstatite and forsterite, whose spectral signatures have been detected in specific Mg/Si ratio by ESO spectroscopy. ([Jaeger et al. 2003](#)).

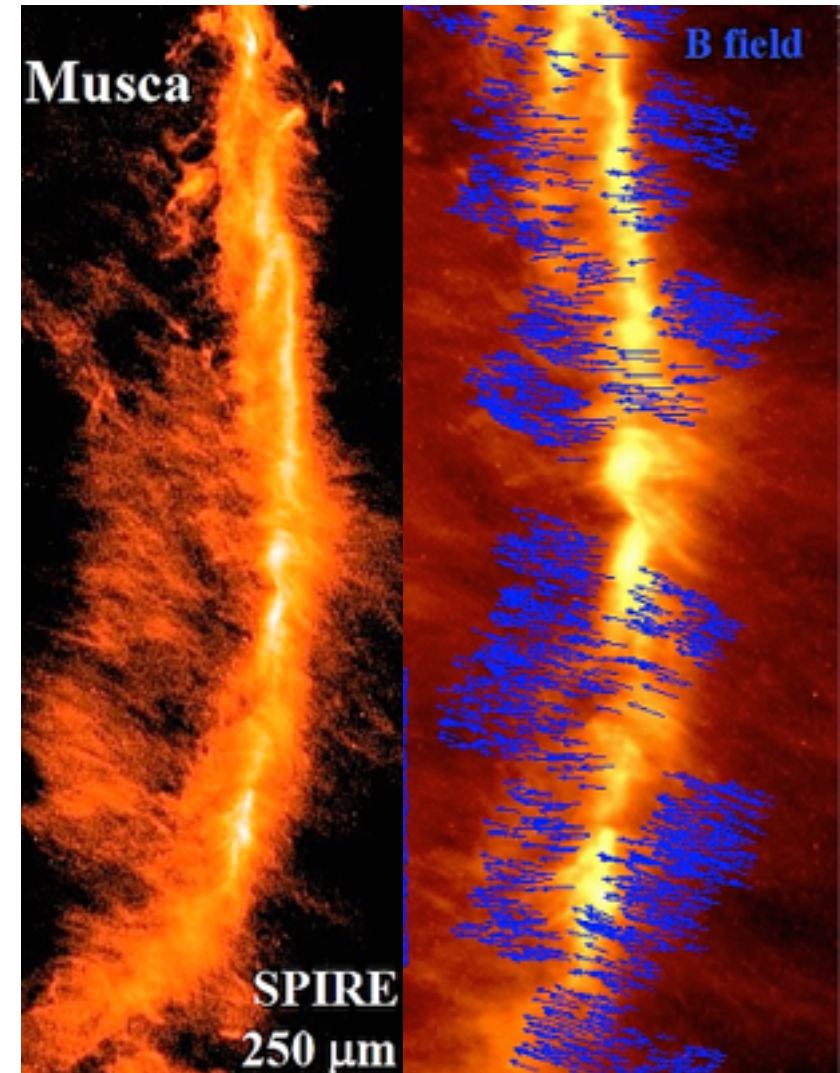


Fig. 40 a & b: The Musca filament (affectionally called “Dark Doodad” by the amateur community) is a striated filamentary structure of the “ridge-and-rivers” type seen earlier in Fig. 36. The chirality of field lines parallel with the diffuse filaments aligns Galactic cirrus dipolar particles perpendicular to the field lines. Source: [Pereyra & Magelhaes 2004](#); [Cox et al. 2016](#).



Fig. 41: Whether the mean magnetic field is parallel to cirrus filaments (suggesting formation by compression), or perpendicular (suggesting formation by gravitational contraction) the dispersion of the polarisation constrains the strength of the magnetic field. [Klessen et al 2005](#) found that progressive fragmentation tends to dissipate into braided filaments with plume-like shapes the further they rise into the halo. See this [visualisation](#) from [Kormandy 2012](#). The discovery of toroidal magnetic fields in high-latitude clouds suggested a model in which flux tubes rising out of the galactic plane become force-free and predominantly toroidal at high latitudes. Some high-latitude clouds may be gas streams that are falling back toward the galactic plane within braided ropes of magnetic flux. See the p. 52 discussion of radiation-driven [Rayleigh–Taylor instability as a driver of supersonic turbulence](#) at high Galactic latitudes.

How does the dust get so far out there?

Throughout this discussion we have noted that Galactic cirrus is often striated or filamentary. That *anything* in the universe should be predominantly filamentary seems a conundrum. All through our lives and studies of astronomy we have been conditioned to think of objects in space as a plausible approximation of a sphere. Do any of us recall a teacher informing us there is more spaghetti in the universe than meat balls?

In a manner of speaking, the analogy is germane. The Galactic medium is affected by four primary mass-energy exchanges, some of which tend to mold as others tend to shred:

- Gravitation
- Turbulence
- Magnetic fields
- High-velocity outflows along polar jets

Introducing outflow from stellar jets to the standard mix of gravity, turbulence, and magnetic fields opened a new chapter in interstellar medium dynamics: the role of Mach number. Jet velocities are measured by their \mathcal{M} function (sound speed). The velocity of a disturbance moving through gas or a magnetic field is mediated by the local \mathcal{M} function in any given region of interest, such as our Magellan's Ghost. The \mathcal{M} function is not simply a propagation velocity, it is how that velocity affects its surroundings. On Earth Mach 1 or $\mathcal{M}1$ is the time it takes for a pressure wave to propagate a distance of 1 km. In space it is the crossing time between one wavecrest and the next across a given parcel of interstellar space. A value for $\mathcal{M}1$ commonly accepted for the thin regions of galaxy haloes where the average density is $N_H = 10^{-3} \text{ cm}^{-3}$ is $\mathcal{M}1 = 200 \text{ m s}^{-1}$, or 720 km hr^{-1} . (See box on next page.) In a warm dusty disc region like that surrounding Earth, $\mathcal{M}1$ is often taken to be 10 km s^{-1} .

Particle densities and therefore sound velocities reach far higher numbers during star formation; 10^4 gm cm^{-3} is commonly accepted as the critical

density at which gravitational free-fall can no longer be resisted and star formation can begin.

Space is not a tidy place. Gas densities can vary dramatically even in the relatively low-shear corotation* zone surrounding Earth and the lofty removes of Magellan's Ghost. The most common molecular environments in a disc galaxy are:

Molecular Clouds: $\rho \sim 10^4 \text{ atom/cm}^{-3}$, $T = \pm 10 \text{ K}$

Cold Neutral Medium: $\rho \sim 20 \text{ atom/cm}^{-3}$, $T = \pm 100 \text{ K}$, scale height 150 pc

Warm Neutral Medium: $\rho \sim 0.5 \text{ atom/cm}^{-3}$, $T = \pm 10^4 \text{ K}$, scale height 400 pc

Warm Ionised Medium: $\rho \sim 0.5 \text{ atom/cm}^{-3}$ $T = \pm 8000 \text{ K}$

Nearly all young stars are formed in the Galaxy's 100-ly thick disc plane, yet its very old stars can be found several hundred light years above or below the plane. Magellan's Ghost clouds are 240 pc away from us, but their actual vertical distance above the Galactic plane varies between 82 and 130 pc. (Our Sun was born in the disc plane but now resides 60 light years above it.)

The typical turbulent pressure of disc gas at the radius of the Sun is ± 10 times the thermal pressure, much of it due to supernovae. The interplay between supernovae shocks and the local gas phase leads to feedback processes that form molecular cloud complexes and subsequent star formation.

* The Solar System lies within the Galaxy's co-rotation zone. Spiral galaxies rotate differentially because they are not rigid objects. The circular speed of the individual stars around the centre is not the same speed as the spiral waves, which rotate in the same direction but at about half the velocity, depending on distance from the centre. The zone where the stellar rotation and spiral rotation speeds are the same is called the corotation circle. Our Sun is slightly inside the Milky Way's corotation radius, which is 1.06 times further out from the Galactic centre than the Sun. The Magellan's Ghost cirrus clouds also lie in or very near the corotation circle. They are relatively little disturbed by the disc's shear torques. In a sense, Earth and Magellan's Ghost bask in a privileged zone, relatively free of the twists and turns that make spiral arms beautiful to look at but beastly to live in.

Disc heating

Disc heating affects dust particles much the same way it affects gas. Adiabatic heating expands gas and dust analogously to cosmic expansion, in which space itself expands and everything inside expands with it. Individual dust particles are so minute as to be near nullities amid the array of forces pervading galaxy discs. One quadrillion cosmic motes packed into a volume smaller than a match head requires the entire earth to move a gram scale from 0 to 1. As the disc thermalises from stellar activity it expands adiabatically in a manner analogous to the cosmic expansion of space itself. A modest supply of new particles arrives via HVAC infall and the thin wind of pristine gas along cosmic filaments. Much of the infall gas ends up in the halo; little makes it to the disc itself (1, 2, 3, 4). Cosmic infall is estimated to provide about 25% of our Galaxy's replenishment requirement at current rates.

A good example of the effects of long-term disc heating is the location of star clusters older than 6 Gyr. NGC 188, NGC 6491, and M67 lie high in the thin disc's version of the stratosphere, where there is little shear or wind to disrupt them. Only Collinder 261 in Musca lies near the plane, but its longevity is due to the good luck of having been born in the corotation circle like the Sun and our Magellan's Ghost clouds.

Galactic cirrus clouds are dipole-coherent as well as self-bound. Their dipolar moments align with the ambient $0.5 \mu\text{G}$ magnetic β -field generated by the dynamo activity in spiral arms. In a random volume large enough to contain 10 to 20 dust clouds — the approx. number of clouds that may be part of the Magellan's Ghost emission complex — the spiral arm β -field acts on the entire group of clouds to slowly align their dipole moments.

Carbonaceous dust has a very low albedo; it is nearly black at optical wavelengths; it is an absorber/emitter. Several other forces may also affect Galactic cirrus's appearance and location today:

- Radiation trapping capacity of the dust particles themselves (1, 2).
- Disc heating from spiral arm wave dynamics (1, 2, 3).
- β -field flow tangential to spiral arm rotation (1, 2, 3) variables (1, 2 (lower left), 3, 4).
- Gravitational perturbation from molecular clouds (1, 2, 3).

- High-velocity ejection bubbles from Wolf-Rayet stars and luminous blue variables
- Cosmic rays. The observed energy density of 1.5 eV cm^{-3} of relativistic particles in the vicinity of the Earth is comparable with energy densities of superbubbles from supernovae and nuclear cluster starbursts, e.g., [NGC 3603](#) (1), [Westerlund 1](#), and [Westerlund 2](#). (1, 2, 3).

The speed of sound in "empty" space

Mach 1 or $\mathcal{M}1$ in space is the time it takes for a pressure wave to propagate past a given point. It is also taken to be the crossing time of a star cluster, the time it takes to go from one side across the middle to the opposite side. Sound speed is derived through the Ideal Gas Law:

$$v_{\text{sound}} = \sqrt{\frac{\gamma k_B T}{m}}$$

Assuming that a given parcel of interstellar space is heated uniformly by the CMB, it will have a temperature of 2.73 K. The interstellar medium comprises protons and neutral hydrogen atoms at a density of about 1 atom cm^{-3} . In the equation above $\gamma=5/3$, and $m=1.66 \times 10^{-27} \text{ kg}$, hence the $\mathcal{M}1$ v_{sound} is 192 m s^{-1} .

In reality few places in space are that cold or precisely that density. The interstellar medium varies from 10 K deep in molecular clouds to 10^7 K in the intergalactic medium. The inferred values for temperatures in the nearby interplanetary medium, for example, is $>10^4$ K. The cosmic intercluster medium is 10^7 to 10^8 K. Astronomers estimate that $\mathcal{M}1$ in the gas medium of the South Polar Circle at the ≈ 400 ly altitude of Magellan Ghost to be on the order of 10 km s^{-1} .

Sound speed plays a crucial role in many astrophysical processes. For example, if the sound crossing time for a gas cloud exceeds the gravitational free fall time (time for a gravity-driven disturbance to propagate), pressure is unable to resist gravitational collapse and the cloud will infall to a denser cloud, and if conditions are right, a star.

Can low-altitude events produce high-altitude effects? Examples of high-velocity gas ejection.

The striated appearance of polar Galactic cirrus originates in the mix of solenoidal and compressive forcing that produce the 0.1 pc flux tubes shown in **Fig. 37** on p. 40. Only a small percentage of any given giant molecular cloud actually forms stars. A certain portion of excess gas is ejected back into the local medium during the time span between leaving the Hayashi Track and the end of the T Tauri stage when protostellar stars eject excess gas in thin powerful polar jets. Half a million to a few million years later, O and B stars eject the rest of the unused gas via UV forcing. See this [simulation of UV feedback](#) to gas (from [Federrath 2014](#)).

Once the gas leaves the virial radius of its cluster, it is assaulted by turbulent fronts while being contrarily constrained by magnetic fields. Magnetic fields order gas into streams that align perpendicular to field lines to form a [solenoidal field](#). Turbulent compression originates from many sources, e.g.:

- Ionised gas hurled from fast-rotating Be stars and massive binaries forms toroidal rings which stream charged particles into sinuous helicoids.
- Mismatched binaries transfer hot threads of gas across their Roche lobes, some of which escapes into the local medium as electrically and thermally charged particle streams.
- Nonbinary Wolf-Rayets (see right) and luminous blue variables [erupt clouds of complex filaments](#) ([Gendelev 2014](#)). If the stars are binaries or multiples, bilobed homunculus bubbles form, as in the famed Eta Carinae homunculus (**Fig. 47**).

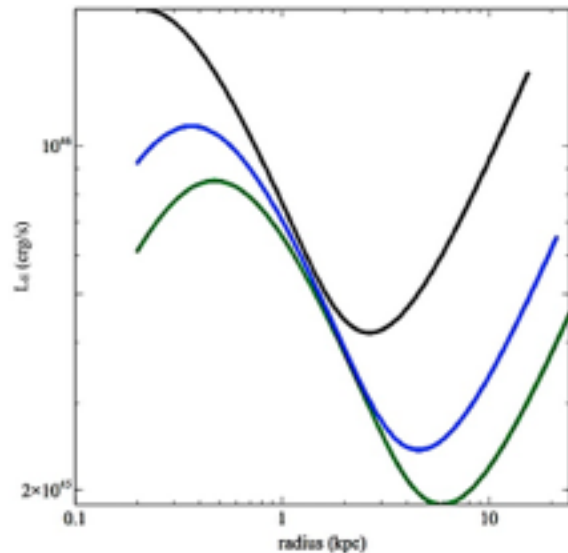
Since carbon compounds are made largely in the outer atmospheres of AGB stars (not typically found hundreds of parsecs above the disc plane) the question is how it is transported into regions so remote from stellar outflows. In the disc plane life is so traumatic that it breeds endless repetitions of chaos nurturing chaos. Yet even as galaxy discs undergo multiple generations of stellar birth/death cycles, their gas and dust is simultaneously converting energy absorbed by particles into heat. Dust acts like a thermal sponge. Bit by bit chaotic shock is converted into a thermal gradient. Over time galactic discs thermalise via adiabatic heating. Incrementally warming gas responds by incrementally expanding, carrying any massive object along with it.

via [disc heating](#) [see [1](#), [2](#), [3](#), [4](#) and a [more traditional textbook exposition here](#)].



Fig. 42: WR 23 is a Wolf-Rayet star near the Carina Nebula that has been ejecting massive bubbles of gas from its surface for approx. 10,000 years. The bubbles originate in convection zones deep in the star's envelope and rise somewhat akin to steam bubbles in boiling water. When the bubbles reach the surface they eject large pistoles ([see this sim](#)) which fragment into multiple shock fronts. The fronts flatten and slow on the leading edge as they encounter less-dense gas from earlier generations of bubbles. The gas immediately behind pushes into the decelerating leading edge, injecting energy density across a broadening front that becomes a thick bubble. See [Toalá 2015](#) for an excellent review of WR nebula.

Fig. 43: Radiation pressure which preferentially imparts kinetic energy to dust but leaves gas molecules unaffected is shown in this chart. Dusty gas is ejected when the excitation luminosity L exceeds the effective Eddington luminosity in the volume containing the particles. The E_{eff} luminosity is inversely proportional to IR and UV opacity. Eddington luminosity is a function of radius for different opacities in isothermal shells. In the fiducial example at the left, $\sigma=200 \text{ km s}^{-1}$, $M_{\text{sh}}=5\times 10^8 M_{\odot}$. Black curve: $\kappa_{IR}=5 \text{ cm}^2 \text{ g}^{-1}$, $\kappa_{UV}=10^3 \text{ cm}^2 \text{ g}^{-1}$ [$f_{dg}=1/150$, MW value]. Blue curve: $\kappa_{IR}=15 \text{ cm}^2 \text{ g}^{-1}$, $\kappa_{UV}=3\times 10^3 \text{ cm}^2 \text{ g}^{-1}$ [$f_{dg}=1/50$ MW value]. Green curve: $\kappa_{IR}=25 \text{ cm}^2 \text{ g}^{-1}$, $\kappa_{UV}=5\times 10^3 \text{ cm}^2 \text{ g}^{-1}$ [$f_{dg}=1/30$ MW value]. Source: [Ishibashi & Fabian 2016](#).



curve: $\kappa_{IR}=5 \text{ cm}^2 \text{ g}^{-1}$, $\kappa_{UV}=10^3 \text{ cm}^2 \text{ g}^{-1}$ [$f_{dg}=1/150$, MW value]. Blue curve: $\kappa_{IR}=15 \text{ cm}^2 \text{ g}^{-1}$, $\kappa_{UV}=3\times 10^3 \text{ cm}^2 \text{ g}^{-1}$ [$f_{dg}=1/50$ MW value]. Green curve: $\kappa_{IR}=25 \text{ cm}^2 \text{ g}^{-1}$, $\kappa_{UV}=5\times 10^3 \text{ cm}^2 \text{ g}^{-1}$ [$f_{dg}=1/30$ MW value]. Source: [Ishibashi & Fabian 2016](#).

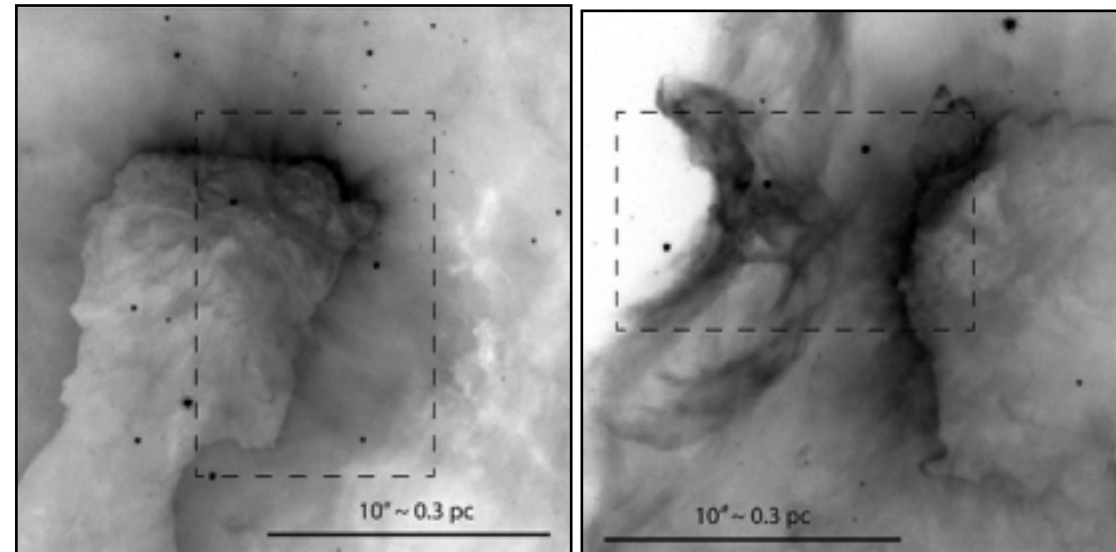
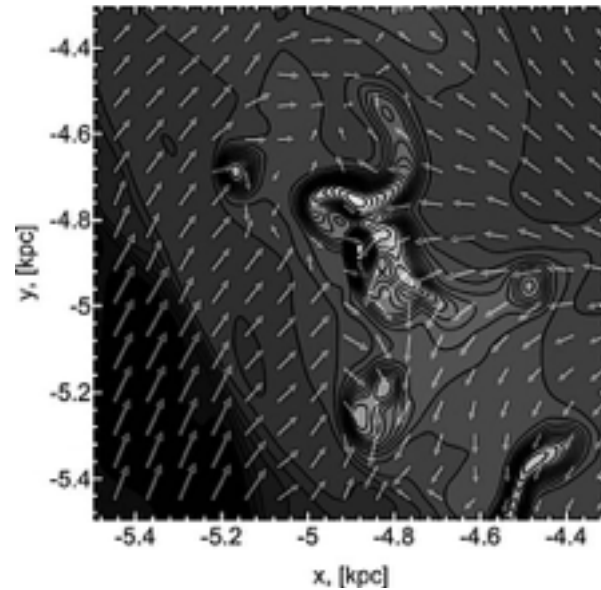


Fig. 45: Jet-induced compression from high-velocity hot gas from the very young, dense cluster NGC 3603 produce filamentary gas–dust clumps that mimic cirrus morphologies.



both high number density ($n = 100\text{--}300 \text{ cm}^{-3}$) and HII molecule abundance of 0.3–0.5). Source: [Khoperskov 2012](#).

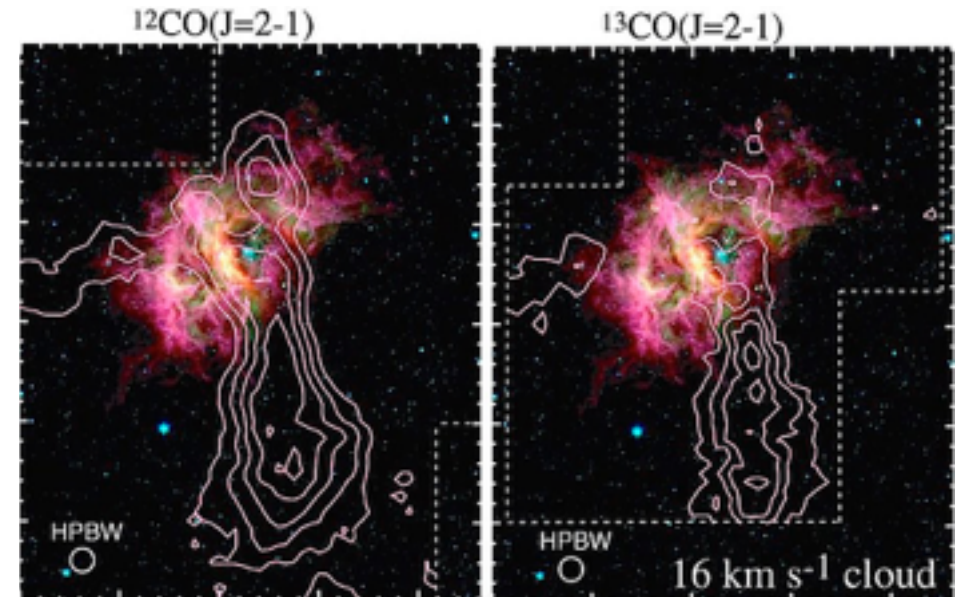


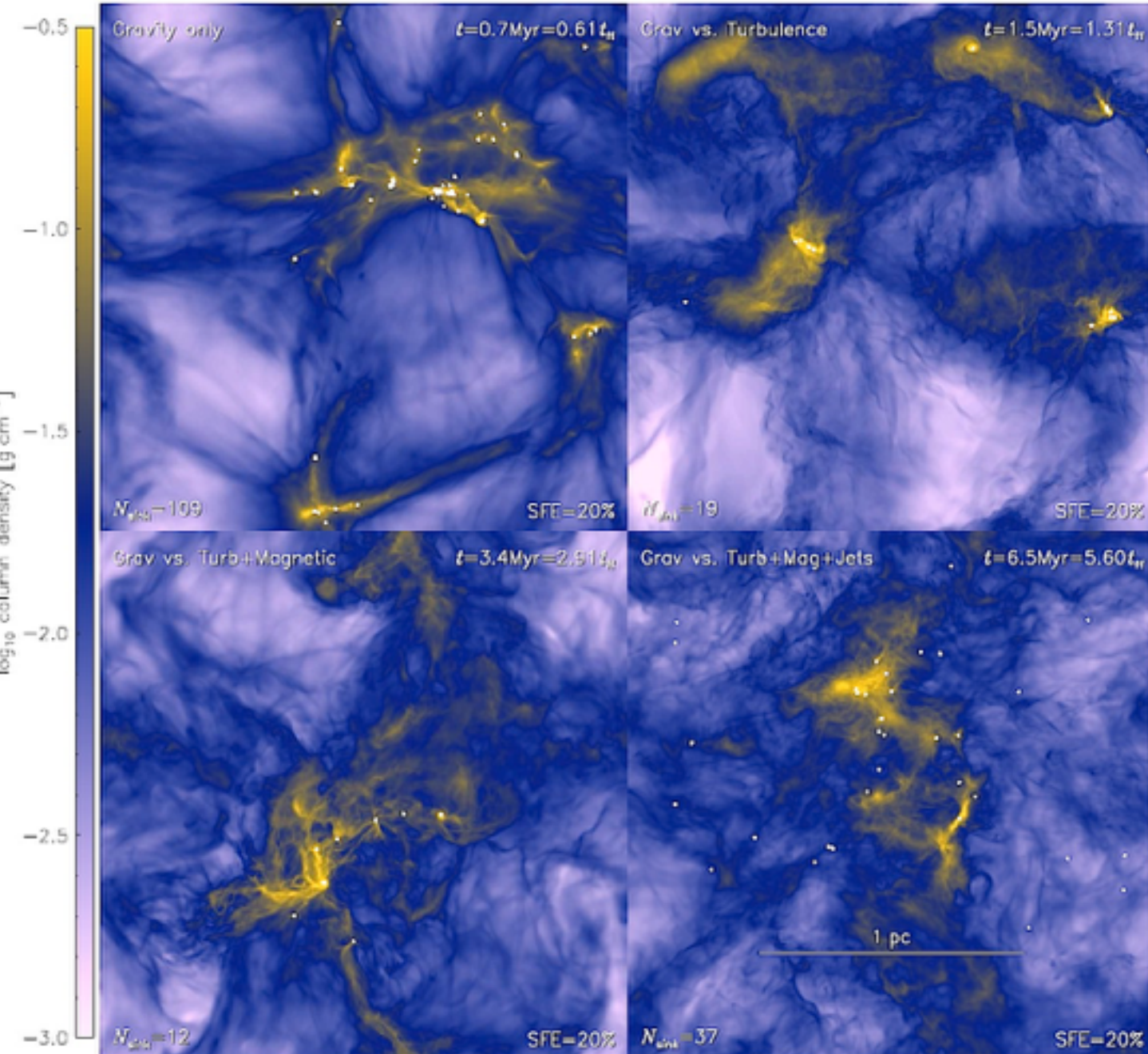
Fig. 46: This high-velocity HI ejection bubble in Westerlund 2 suggests a plausible connection between a fast-moving molecular wind and dust transport.

Fig. 47: The bilobed Homunculus Nebula suggests one transport path removing disc plane gas to the altitude of Galactic cirrus. Up till recently the Homunculus was interpreted as a mottled bipolar ejection nebula which erupted in 1843 from one of the three massive O supergiant stars in the η Carinae triplet system. In 2008, observations with the Mauna Kea Gemini South telescope and the Blanco telescopes in Chile traced η Car's eruptive activity back to an imposter supernova blast a thousand years ago. In this image the outermost flocculent gas clouds from that early blast wave are being overtaken by the expanding shell of η Carinae's 1843 eruption. [See an animated version of this still here.](#) In the animation, the first image shows the original hot blue supergiant (technically a luminous blue variable) before the primordial eruption 1,000 years ago. In 1843, η Carinae produced the explosive outburst which generated the bilobed Homunculus Nebula, plus a faster shock wave propagating ahead of the Homunculus. The 1843 shock wave expanded through the interior of the 1000 year old shell in front of it. As is often the case with multiply erupting shells, younger, faster blast waves overtake the older shells. Such interactions produce a thermal shock lens. The 1843 outburst billowed into the well-known bilobed Homunculus Nebula. A faster high-energy, low-density shock wave propagated ahead of the slower gas-rich Homunculus.

Eventually, the faster blast wave overtook the older shell, producing a bright shock front seen in UV and x-ray that heated the older shell. If any Galactic dust clouds inhabited the region inside the shells shown here, they would have been both thermally and mechanically shocked by the onrushing shock waves. If the clouds were strongly enough bound to avoid disruption, they would have received a kick that pushed them further out into the then disc than normal disc heating may have transported them. The η Carinae event is just one of many shocks produced by the Galactic disc to push GC clouds ever higher into the disc.



The disruptive longevity of stellar outflows



Since 2012 [Christoph Federrath](#) of the [Australian National University](#) has studied the effects of stellar outflow and protostellar jets as a key driver of the dynamics of star cluster evolution and gas distribution in the galactic disc. Federrath's models have significantly advanced our understanding of the long-lived disruptive effects of stellar jets.

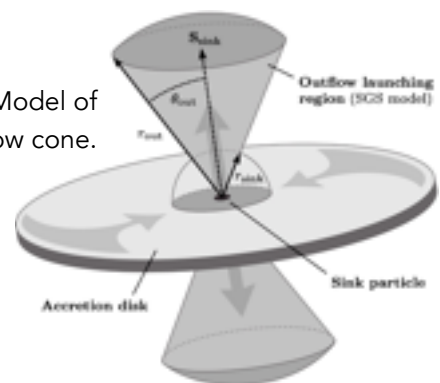
Fig. 48: from [Federrath 2015 Figure 1](#): Column density projections at the end of four simulation models:

- Gravity only (top left)
- Gravity vs. Turbulence (top right)
- Gravity vs. Turbulence + Magnetic Fields (bottom left)
- Gravity vs. Turbulence + Magnetic Fields + Jet/Outflow Feedback (bottom right).

Each box models additional physical processes that resist gravitational collapse. The top right corner of each panel denotes the time it takes for small star clusters to reach a realistic 20% star forming efficiency (SFE). The duration to SFE 20% increases significantly for each box.

The lower right box demonstrates that only the combined effects of gravity, turbulence, magnetic fields, and feedback can produce realistic SFRs.

Fig. 49: Model of polar outflow cone.



Rayleigh–Taylor Instability — the Fifth Horseman of the Galactocirrus Apocalypse?

The “Four Horsemen of the Galactocirrus Apocalypse” might seem bit overenthusiastic when applied to the rather staid context of gas and dust in space. Maybe not. The forces of Gravity, Magnetism, Turbulence, and Jets are as doom-boding to star forming regions today as War, Pestilence, Famine, and Death were to the petrified peasants of long ago.

The plague-harassed bits and pieces of medieval civilisation went on to survive. So do the gas harassed remnants of star clusters. We circle one of them every year.

We also behold — naked eye, no less — a few unorthodox bits lying roughly 240 pc from us in a band of faint light 18° to 24° below the Galactic disc. How did this Galactic cirrus survive the messy goings-on down in the disc to now ride serenely on high with little else to do beyond throw feeble photons at us now and then?

It’s been long suspected that the forces that dissipate star clusters do not inject enough energy to hurl cluster residues 80 to 130 pc into the thin disc, the home of Galactic cirrus anywhere in the sky. Recall from above that the observed SFR_{ff} during cluster formation of 0.04 is

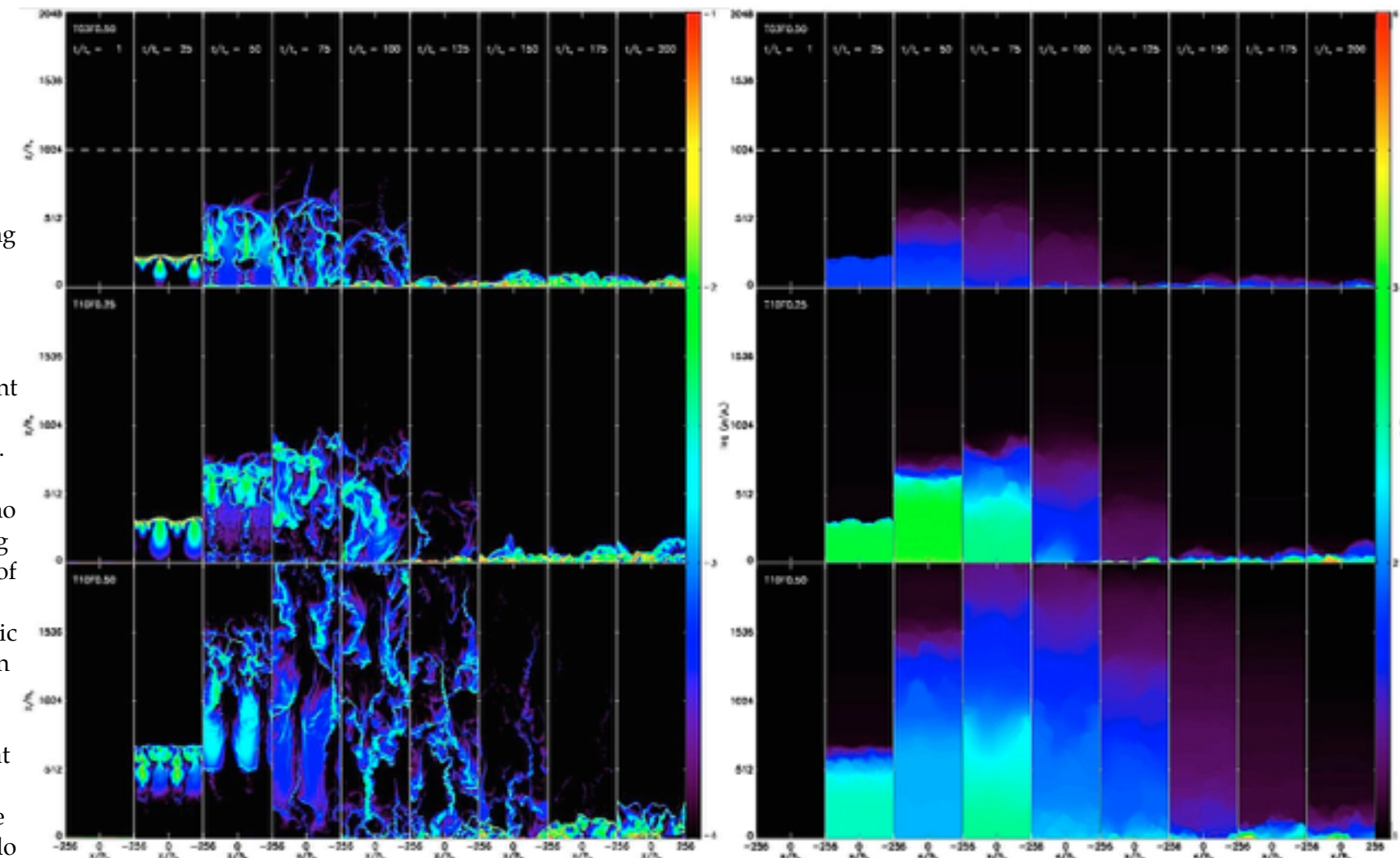


Fig 50: In these simulations from [Krumholz 2014](#) (Figs. 5 & 6), each horizontal row represents a gas parcel within a column whose y-axis is demarcated in time increments. Approx. 95% of the mass in the simulation volume lies within the dynamic range of 10^{-4} to 10^{-1} times the stellar density. The radiation temperature $\Theta_r = T_r/T_*$ and the gas temperature distribution are similar everywhere except at low densities and high altitudes. The [animated version here](#) provides the full-motion version of this static snapshot.

four times greater than observed rates. Perhaps another force has been at work which has eluded the simulations?

Considerable advances have been made along these lines by [Krumholz et al. 2014](#), [Peters et al 2016](#), and a number of others as far back as [Boulanger 1994](#), [Mathis 1999](#), and [Heithausen 2002](#). By their reckoning Radiative Rayleigh–Taylor instability (RRT) becomes a non-localised force when the gravitational field between a sufficiently large low-density radiation-pressure dominated medium (hot gas) in a galactic disc interfaces with a large high-density, less radiatively dominated medium (cool gas) above it. Strong magnetic fields enhance RRT feedback by transferring momentum between parcels of gas, thus redistributing energy momentum throughout the cloud.

RRT is familiar to astronomers studying active star forming regions. Infrared radiation trapped by dust opacity injects energy into mass-loaded winds, producing Rayleigh–Taylor instability. RRT drives the supersonic turbulence seen in Galactic protocluster clouds.

Here our concern is turbulence injected into the disc during and after active star formation, not before. On galactic scales, [Thompson et al. 2005](#) and [Murray et al. 2005](#) proposed that the force exerted by radiation from newly formed stars drives highly supersonic motions observed in these systems. [Zhang & Thompson 2012](#) went further to suggest that radiation pressure is also responsible for launching galactic winds, although at present it is uncertain how much momentum the radiation actually transfers to the gas.

Consider a source of radiation such as a young star surrounded by dusty gas. If every stellar photon is absorbed once, the radiation will deposit its full momentum flux L/c in the gas. But if the medium is optically thick, each photon can be absorbed and re-emitted multiple times. The momentum imparted to the gas would thus be larger, although by an indeterminate amount. If every photon is absorbed many times, much of the energy of the radiation field is transformed into kinetic energy in the gas. The total momentum transfer approaches L/v , where v is the gas characteristic velocity. The exact loading factor depends on the gas's velocity and density. In star clusters the strength and nature of radiation–matter coupling is uncertain because of the unknown mass density distribution.

Radiation passing through complex density regimes results in multiple local instabilities in which radiation exerts forces on the matter. Two examples are *photon bubble instability* (PBI), see [Blaes & Socrates 2005](#); and *Radiative Rayleigh–Taylor* (RRT) instability ([Krumholz et al. 2009, 2014](#)).

In photon bubble instability, a parcel of gas in an optically thick regime is initially flung upward into an optically thin regime by radiation pressure. The parcel compresses into a thin shell with a high radiation temperature beneath it and a low radiation temperature above. The Homunculus Nebula example in [Fig. 47](#) is a good example. The combination of velocity and pressure differentials buckle the parcel shell into blobby “fingers” of gas (as distinct from filaments), some of which are forced back down into the radiation-dominated lower region by the ascending gas around them (e.g., the mushroom-cloud effect).

Somewhat later the still-ascending gas filaments move into the radiation-dominated region. There some of them gradually lose their momentum and settle back toward the disc. The still-rising remnants develop a “clear-channel” morphology, i.e., they turn into dense, nearly vertical filaments while the gas surrounding them stalls as a low-density, slow-moving gas.

In Krumholz’s models most of the ascending gas fingers eventually lose momentum and fall back into the base; a small fraction of the total mass do manage to coast to the top of Krumholz’s computational domain. At that point all upward motion ceases and the remaining gas trickles back to the midplane. Krumholz’s model somewhat resembles a galactic fountain caused by supernova gas clearing, except that the initial impulse is much weaker. The energy directed upwards is not enough to push layers of dust in the mid-disc ahead of the bubble into the lofty upper disc where we find it today.

[Peters et al 2016](#) and the [SILCC Consortium](#) adapted the simple PBI model to widely varying conditions typical of a real-world galactic disc. Two snapshots from the many SILCC models are reproduced on the next page. The SILCC Consortium has modelled too many variations to list here. Some inject many more supernovae than occur in modern galaxy discs but might well represent real-universe conditions of 8 to 10 Gyr ago during the era of peak

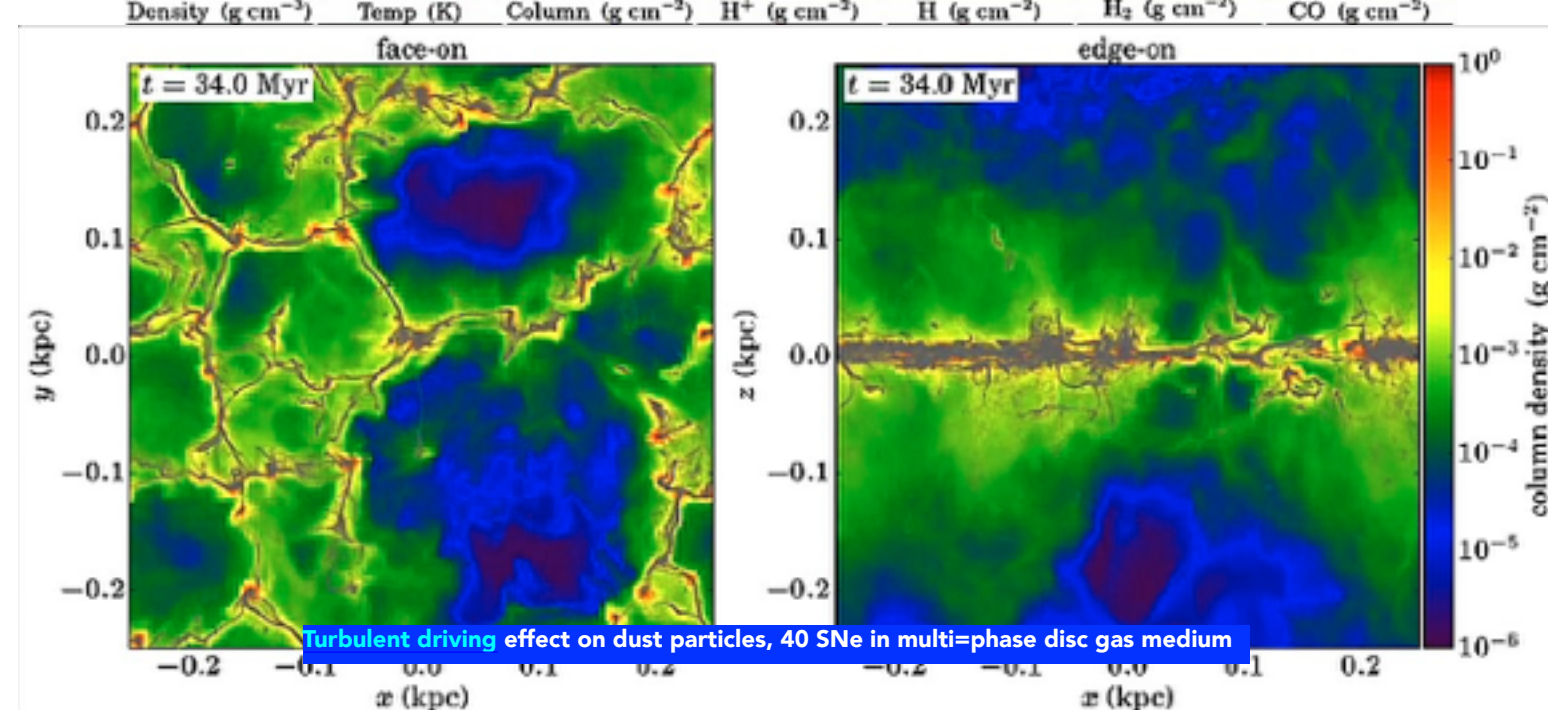
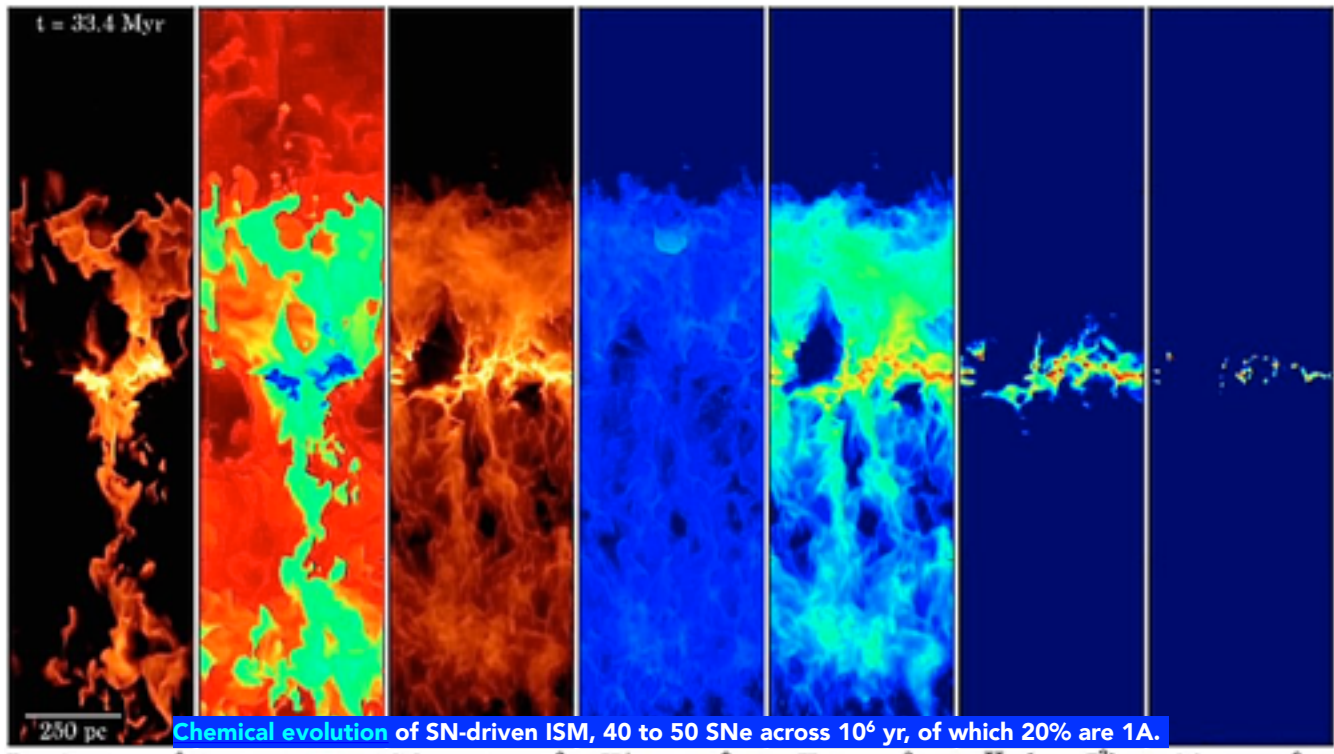
star formation in the universe. Most of these models suggest driving energies sufficient to populate the upper disc of a spiral galaxy with the $0.1 M_{\odot}$ to $3 M_{\odot}$ masses typical of galactic cirrus observed today.

Do they in fact? A 2018 MNRAS paper by [Yaghoobi & Shadmehri](#) suggests a much more abrupt bubble growth-to-instability rate:

In the non-magnetized case, the growth time-scale of the instability for a typical bubble is found to be less than 1000 yr, which is very short compared to the typical star formation time-scale. Magnetic fields with a reasonable strength significantly increase the growth time-scale to more than hundreds of thousand years. The instability, furthermore, is more efficient at large wavelengths, whereas in the non-magnetized case, growth rate at short wavelengths is more significant.

Fig. 51 a & b: In the complex mass–energy exchanges of a galaxy disc, several powerful feedback processes dominate ongoing star formation. In the relative short lifetimes of star clusters (100–500 Myr), feedback can eject enough mass to hinder ongoing star formation. Long-term outflow could halt star formation altogether if there were not compensatory gas replenishment resources.

The [Simulating the Life-Cycle of Molecular Clouds](#) (SILCC) project produced a number of computer simulations to model galaxy disc disruption caused by multiple feedback mechanisms. Click on blue lettering in the callouts to access the original simulations.



FIR emissivity and the chemistry of dust

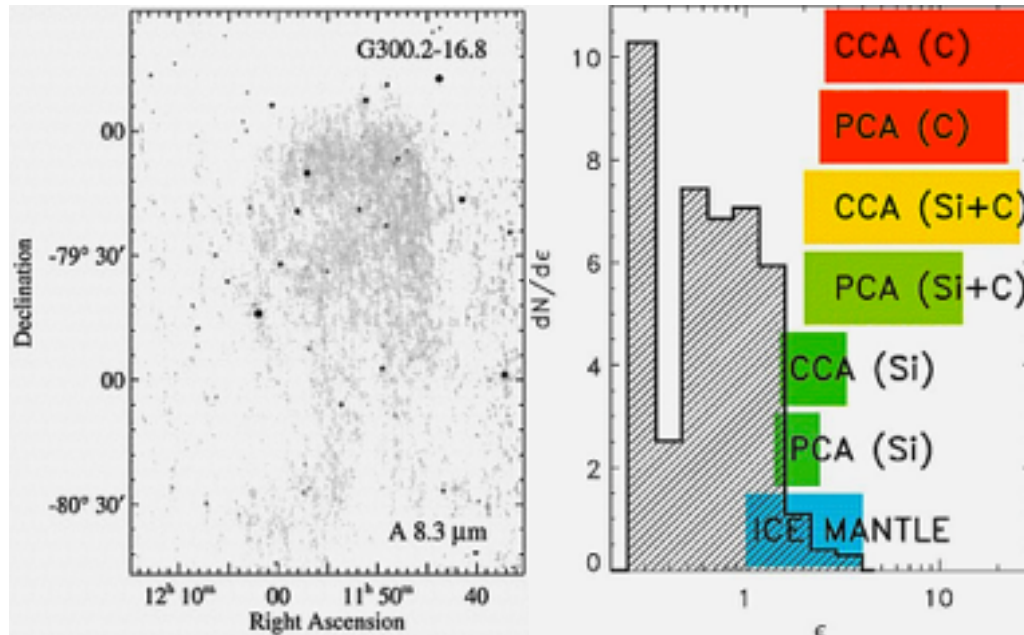


Fig. 52: Chemical composition of a representative Galactic cirrus cloud in Chameleon within a 5° circle of the Ghost region. The data were acquired by the [Midcourse Space Experiment \(MSX\) in 2003](#). This image of the faint diffuse, isolated cloud G300.2-16.8 (mapped on right) reveals the chemistry of dust in the faint patches of emission seen above. The image was acquired at 8.3 μm using 120/200 μm filters in an ISOPHOT photometer. At an average temperature of 14.2 K, the 200- μm surface brightness -vs- visual extinction (A_V) scatter of the faint emission patches shown here was 18.4 and the dust emissivity τ_{200}/A_V was $5.9 \times 10^{-4} \text{ mag}^{-1}$. (Translation, a dim glow.) The coloured boxes on the right list the chemical constituents of the cloud. The hatched vertical bars roughly correspond to the proportions of the following particle types, from numerically fewest up to most frequent: (i) ice mantles, (ii) silicate particle-cluster aggregates, (iii) silicate cluster-cluster aggregates, (iv) mixed (silicate and carbon) particle-cluster aggregates, (v) mixed cluster-cluster aggregates, (vi) carbon particle-cluster aggregates and (vii) carbon cluster-cluster aggregates. The proportion of carbonaceous particles to silicates suggests what we readily see in the MSX image: this cloud is poorly reflective. This is an example why Galactic cirrus has such a low $<26.5 \text{ mag arcsec}^2$ optical surface brightness. The high proportion of silicate content suggests these dust particles are dipolar and will respond to a magnetic field. Source: [Kiss et al 2006](#).

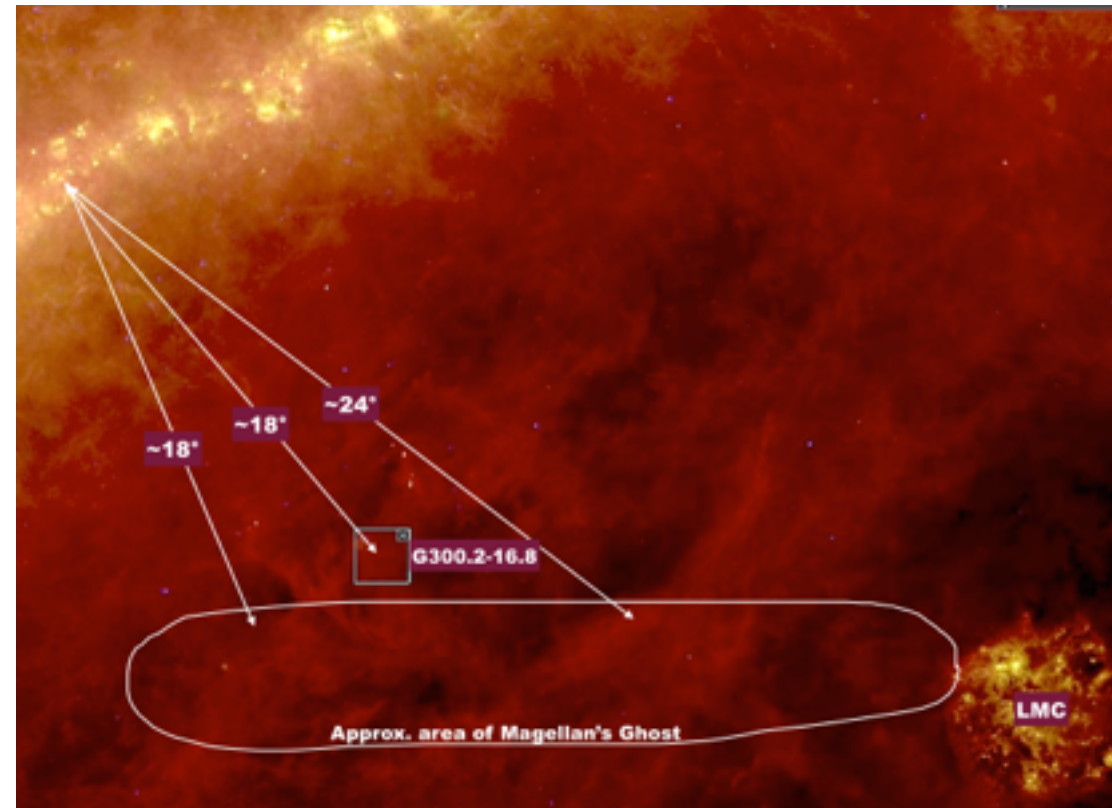


Fig. 53: The molecular cloud G300.2-16.8 is 5° from the dense molecular gas of the Chameleon I, II, & III star-forming region. Its 3D location with respect to the Chameleon SFR is unknown. G300.2-16.8 is likely part of the large cirrus complex which hosts Magellan's Ghost. The scattering angle from the Galactic disc midplane to the "Ghost" region is 18° to 24°. The far-infrared (FIR) emissivity of interstellar grains at 100 – 200 μm can be compared with sub-mm thermal and UV data from massive stars to calculate the HI-to-dust ratio. The low temperature regime of 12 – 14 K in the G300.2-16.8 signifies larger grain sizes. Temperatures below 14.2 K foster ice mantle formation on carbonaceous grains and coagulation of small silicate grains into larger ones. Silicates are more dipole-responsive to magnetic fields, hence will orient their long axes perpendicular to the grains. In effect G300.2-16.8 has aligned its more optically reflective dust grains in such a way that incoming optical light from the disc can act like a shallow-angle forescatter reflection surface. Galactic cirrus in this region can, if aligned normal to the magnetic field, reflect a certain amount of extra light toward the Earth. This is apparently what the nine visual observers report.

The serendipitous location of the Chameleon Galactic cirrus



Fig. 54: Galactic cirrus in Chameleon adjacent to the Magellan's Ghost emission band. Image courtesy of [Gerald Wechselsberger](#).
Unfortunately, there are no similarly detailed images of the Magellan's Ghost nebulosity itself.

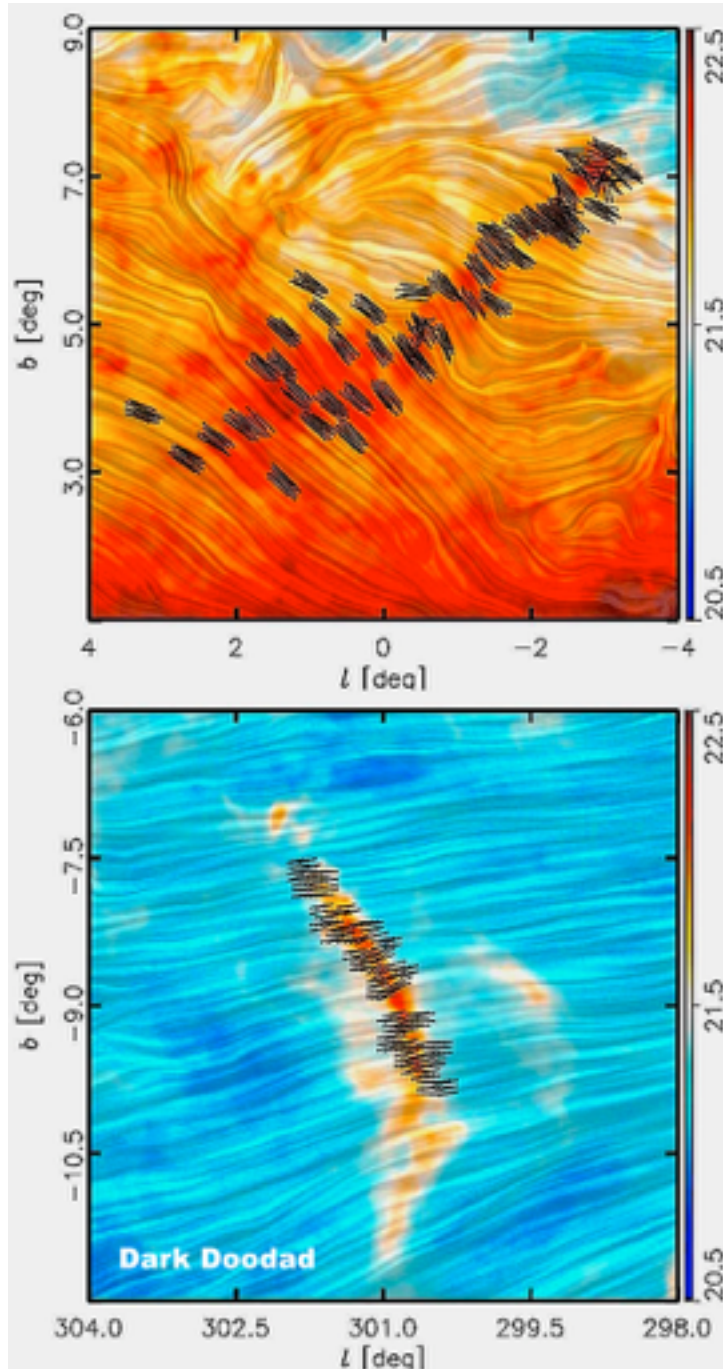


Fig. 55 (I): Dust grains tend to align with their longer axes perpendicular to the local magnetic field of the interstellar gas. Magnetic fields also control the density and distribution of cosmic rays, which can comprise as much as 25% of the local energy density distribution. Synchrotron emission, dust polarisation, and Faraday rotation define the structure of magnetic fields in regions embedded with cold dust clouds. Over time the dipolar long axes of up to 20% the particles align coherently with the magnetic field lines. Although the particles themselves have a low albedo (they're soot after all), the water ices and molecular structures adhering to the grain surfaces reflect incident light if the light arrives at a shallow angle with respect to the grain surfaces.
Source: [Planck Collaboration XX 2016](#).

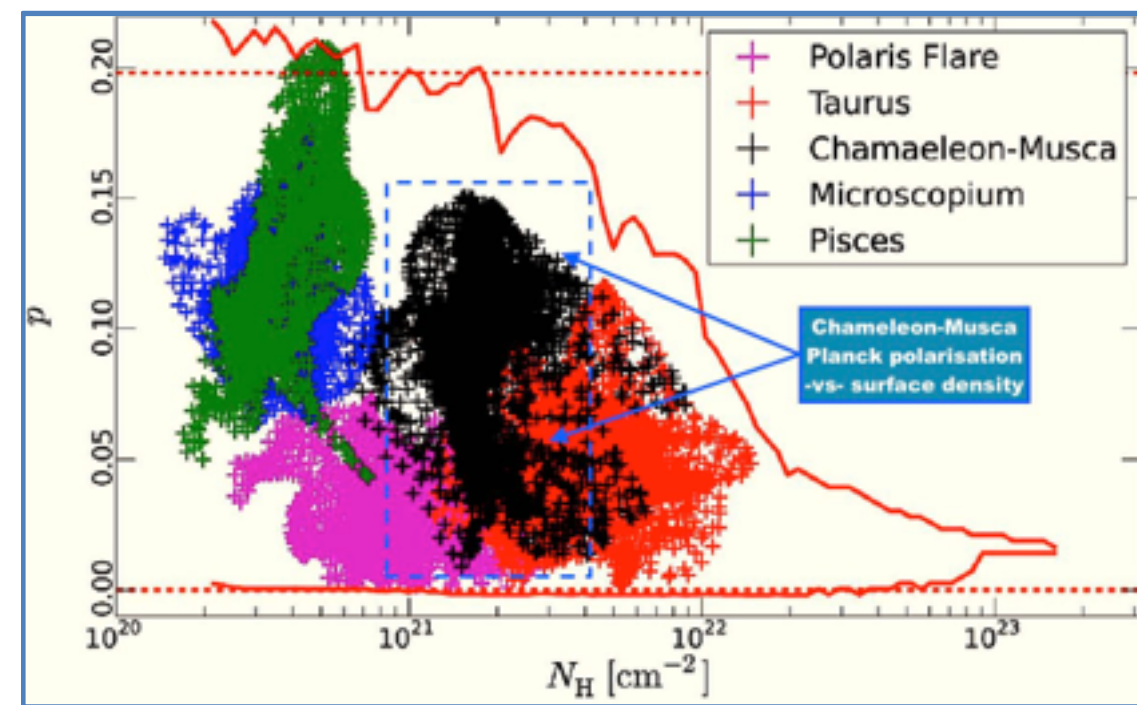


Fig. 56: The Chamaeleon-Musca dust cloud complex lies in a sweet spot for visual observation. Its dust grains have a low polarisation fraction of ≈ 0.02 to 0.15 (i.e., 2% to 15%) while its surface density is $N_H = 10^{21}$ to $10^{21.5} \text{ cm}^{-3}$. High polarisation fractions are reached in the column densities of the Chamaeleon-Musca complex, which, being closer to the Galactic plane, is threaded by the Galactic disc magnetic field. An overabundance of dust alignments in a direction that just happens to reflect more disc light toward observers on Earth is a random accident. [Source: [Planck Intermediate Results XX 2015: Comparison of polarised thermal emission from Galactic dust](#) (A&A 576, Apr 2015, Fig. 2.)]

The competition between gravitational and turbulent pressures in a medium dominated by β fields elongate a cloud either parallel to or perpendicular to the β field. β -field channelled gravitational contraction produces parallel filaments when there are multiple contraction centres. Sub-Alfvénic turbulence (i.e., below the propagation velocity of a magnetic wave) extends the gas distribution lengthwise along the field lines. In Fig 54 (below) the orientations of Galactic cirrus of the Taurus molecular cloud are observed as parallel with the mean field direction of the local ICM. The filaments in the Apus-Musca-Chameleon South Polar Zone tend to be perpendicular to the β field. Source: [Mao 2010](#), p.3.

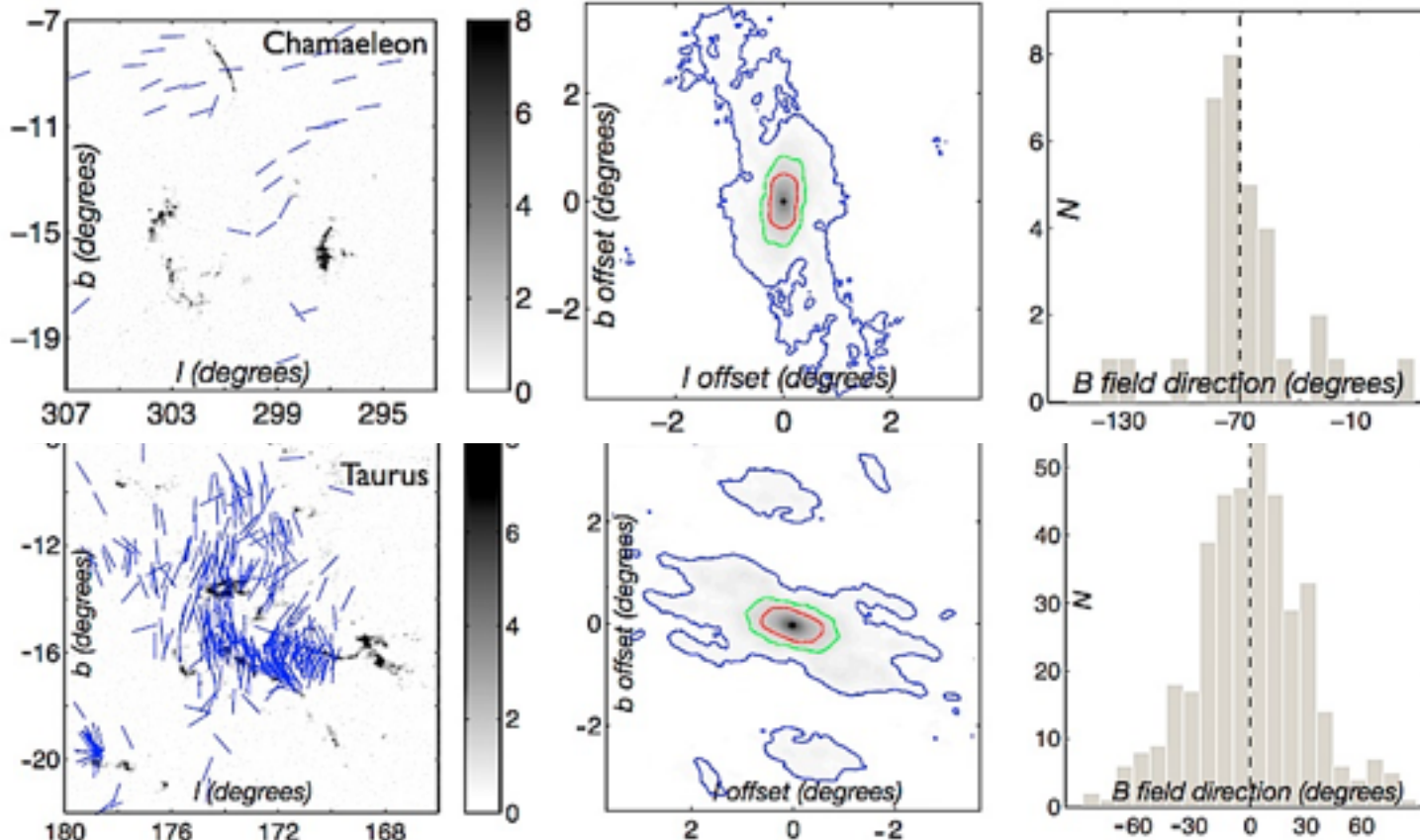


Fig. 53 (r): Filamentary clouds form in dynamically dominant β fields when gravity is magnetically subcritical and the turbulence sub-Alfvénic. Gravitational pressure (P_g) and turbulent pressure (P_t) effectively compete only along the direction of the field lines. When reaching equilibrium ($P_g = P_t$) the dimension of the clouds along the β field are respectively l_1 and l_2 . Projected on the plane of sky, Cloud 1 is parallel with the β field; Cloud 2 is perpendicular to the β field.

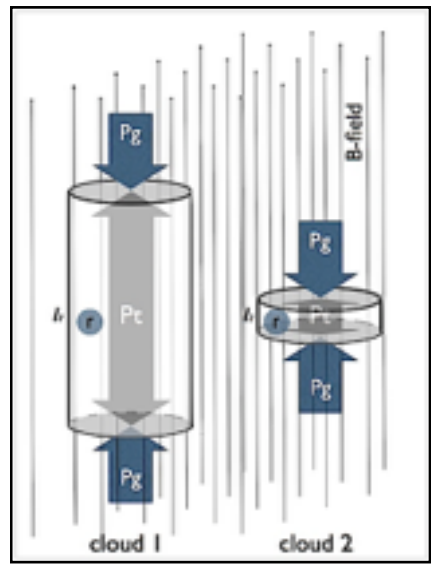


Fig. 54a & b:

Left column: A_V maps from Dobashi (2011) in Galactic coordinates overlapped with optical polarisation vectors from Heiles (2000). Clouds that consist of parallel filaments are indicated by the parallel contours in the middle column.

Middle column: Autocorrelations of the A_V maps with coordinate offsets in degrees. The three contours are 100% (dark shading), 60% (pale shading), and 20% (no shading). The linear fit to the region within a contour defines the direction of the cloud does not vary with the density.

Right column: Distributions of the β -field orientations inferred from the optical polarimetry data in the left column, measured CCW from Galactic North. The dashed line shows mean field direction. Most cloud directions are either nearly parallel with or perpendicular to the mean field directions.

Red sails in the sunset

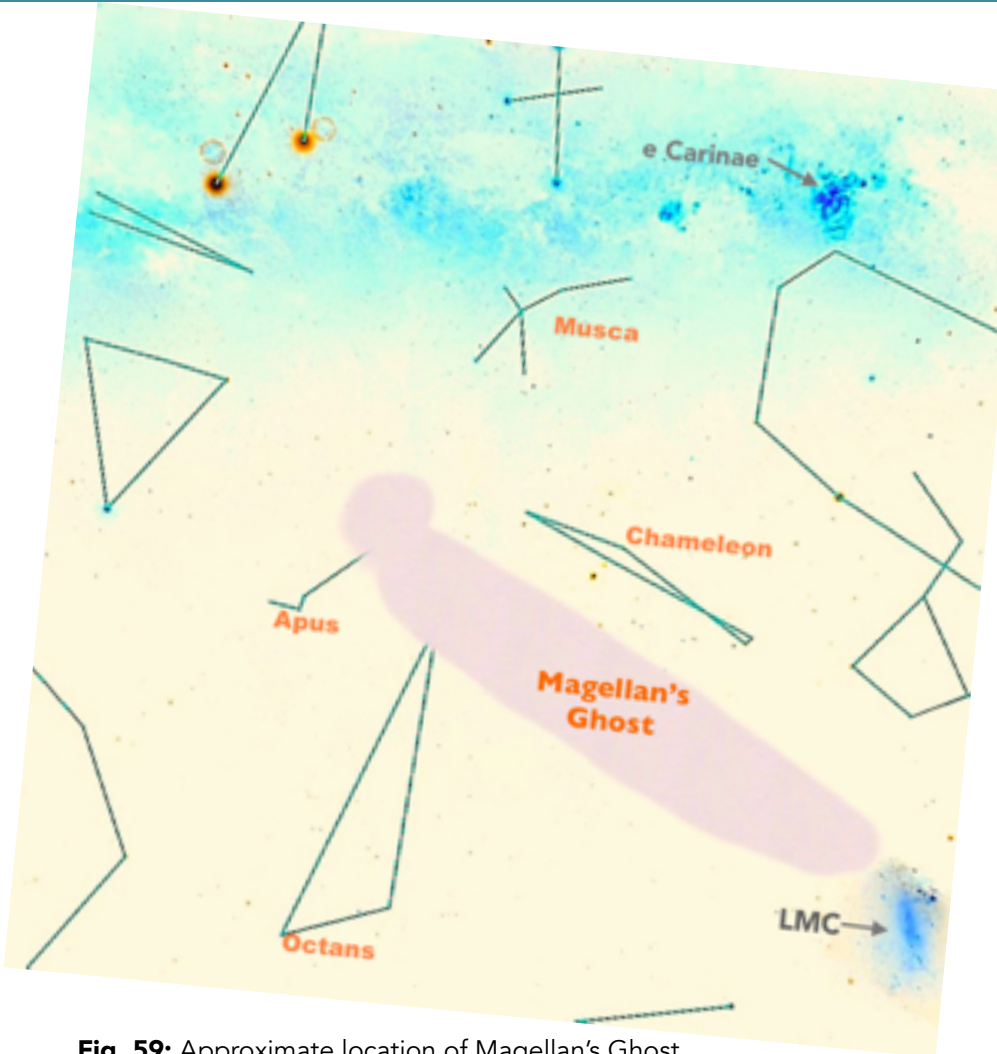


Fig. 59: Approximate location of Magellan's Ghost among the constellations of the South Polar region.

NOTE: There are scale differences between the map projections superimposed on one another. The sky chart above is spherical projection; the Planck images are Molleweide/Aitoff; the [Chromoscope](#) image sets used in this section are Cartesian projections. Some of the constellations look unnaturally warped due to scale-fitting to show the location of the Magellan's Ghost feature.

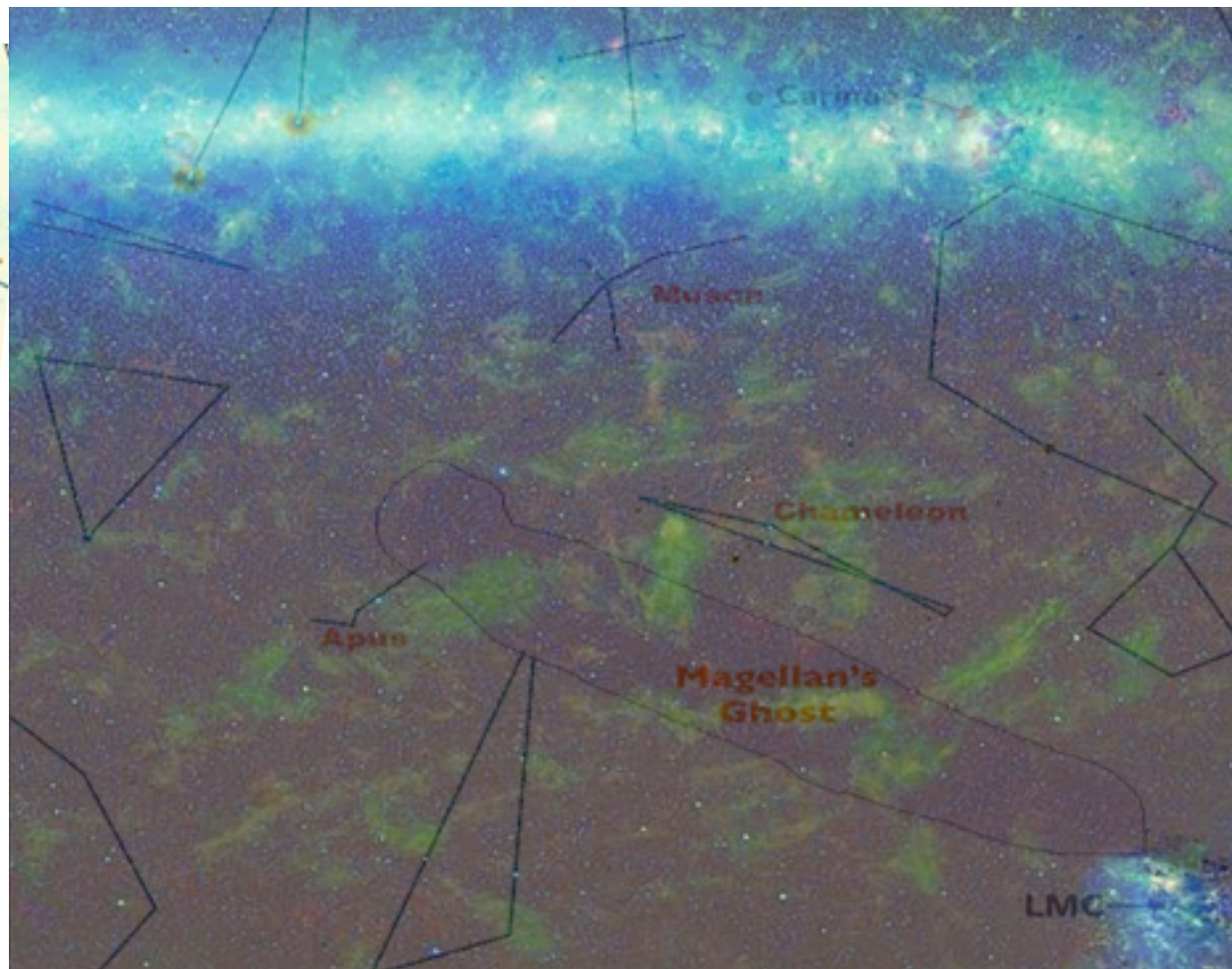


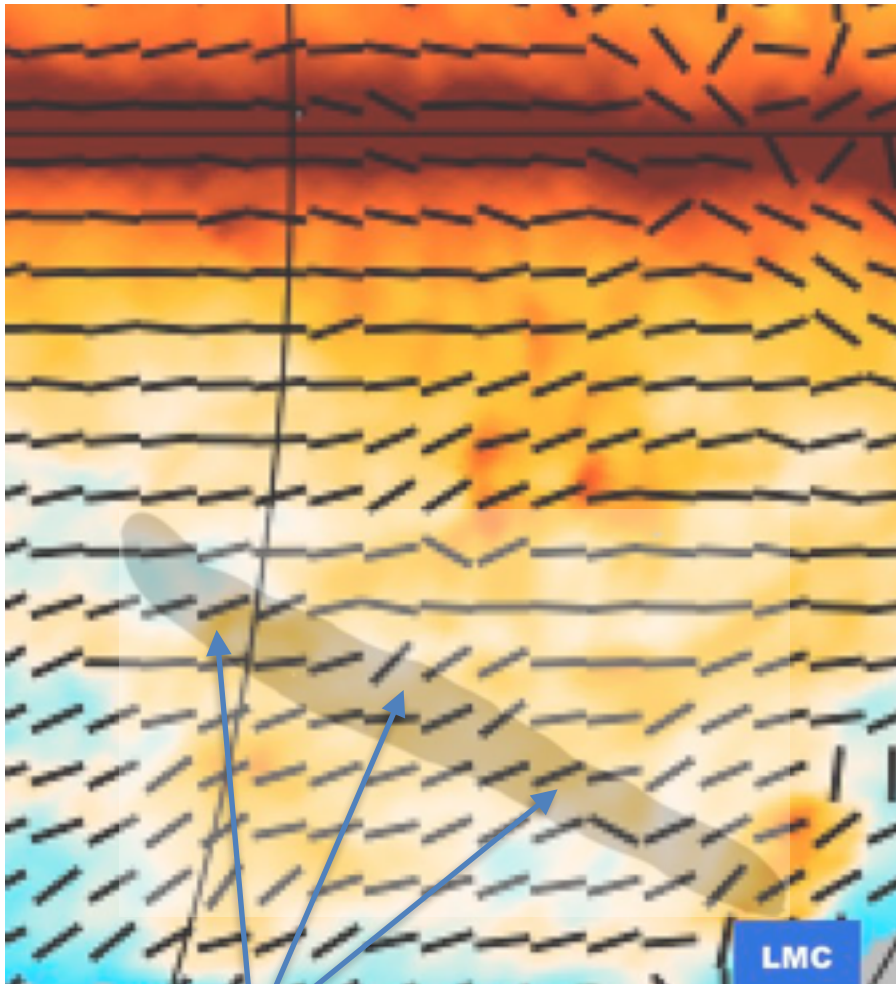
Fig. 60: Approx. location of the Ghost against a [Chromoscope](#) projection of the Near IR sky. The green and red patches show warm dust in the 12 μ m and 24 μ m bands, respectively. Chromoscope is a multiband visualisation utility prepared by the [Cardiff Univ. School of Astronomy and Physics Research](#). Chromoscope sliding-bar interface moves across images from Gamma to 408 MHz radio. The image sets derive from the freely downloadable data from Fermi Gamma ray, ROSAT X-ray, DSS Optical (also used by Wikisky) WHAM-SHASSA-VTSS H-alpha; WISE Near IR; IRAS FIR; Planck Microwave (353-547-847 GHz; HI4PI neutral hydrogen (HI); and 75 cm radio from the Haslam 408 MHz survey by the Parkes 64 m telescope in Australia and Jodrell Bank 76 m dish in the UK.

Chromoscope FIR band

Fig. 61: Far infrared 100 μm emission from the IRAS satellite reveals cold dust between the stars. The brighter clumps are dense regions where stars are forming; the fainter continuum distributed across the sky is Galactic cirrus. Zodiacal light due to dust between the Earth and the Sun has been removed.

Chromoscope microwave band

Fig. 62: A montage of microwave-band emission from the Planck satellite uses blue hues to designate submillimetre wavelengths emitted by cold dust. The pinkish glow is ≈ 1 mm light emitted by hot gas.



Figs 63: There is a noticeable shift in the direction of magnetic field lines in the Magellan's Ghost region. Grains of interstellar dust tend to align their longest axis at right angles to the direction of the Galaxy's magnetic field lines, partly polarising the light. Polarisation patterns enable astronomers to reconstruct the ambient magnetic field. In these two image sets the orientation of the magnetic field lines are indicated by texture lines across the image. **Note:** Images not exactly to scale due to original plate projection differences. Source: [Planck Intermediate XX, Polarization thermal emission](#) Fig. 3, A&A/astro-ph.

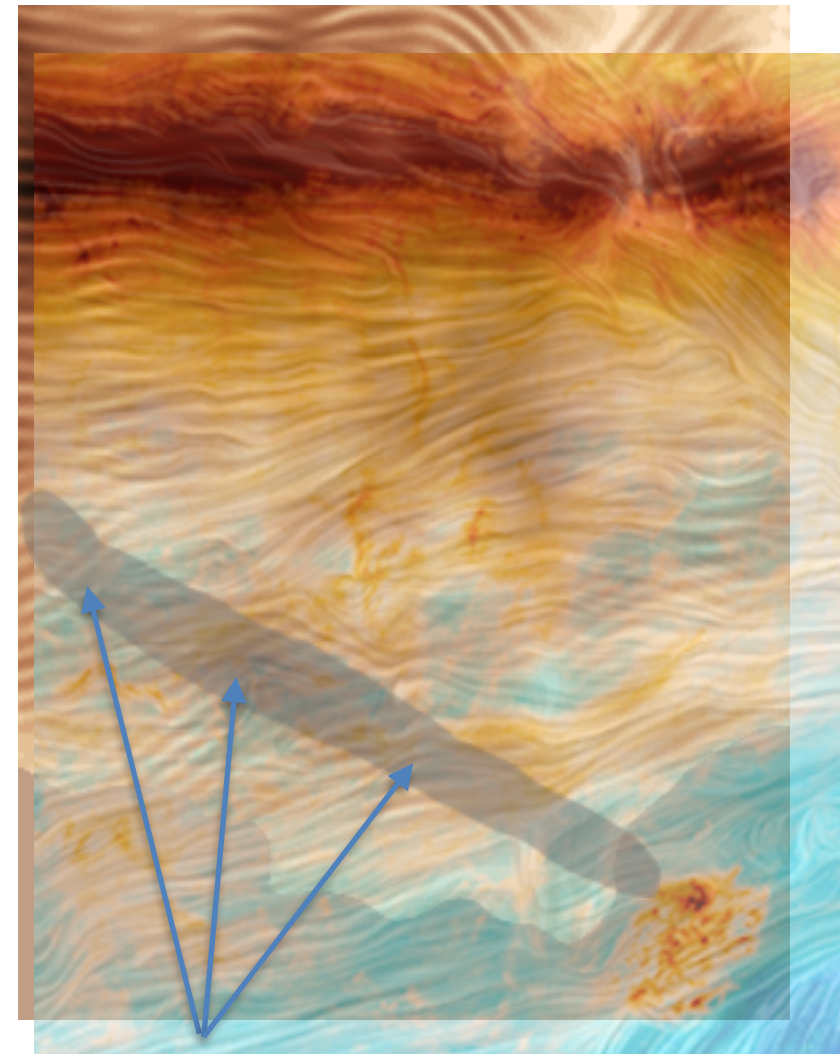


Fig. 64: The most significant unanswered question in these images is the proportion of carbonaceous to silicate particles in the overall dust mix. Carbon-based sooty dust has a low albedo of 5% to 9% from the composition of the molecules adhering to their surfaces, notably H₂I, which is made on carbonaceous dust grains. Silicate grains do not readily attract the simple molecules made in AGB stellar atmospheres, but they are dipolar and respond to the direction of a magnetic field. Their elongated flat, crystalline faces reflect more light if the polarisation angles are serendipitously placed for observers on Earth. We propose that this is the source of the slight enhancement that makes Magellan's Ghost faintly visible to observers under very dark skies. Source: Composite overlay of [Planck XIX Microwave 353-547-847 GHz bands](#).

The expedition took us longer than we expected, but here we are

Magellan's Ghost is an aggregation of many small, wispy, dusty cirrus clumps ± 240 light years away in the direction of Chameleon, Apus, and Octans. Each clump is a loosely bound mass of dust particles of two types: (a) carbonaceous aggregates with significant proportions of HII and PAH molecules on their surfaces, and (b) silicate particle conglomerates with HI, HII, and ice mantles frozen onto the grain surfaces. The striated, chaotic appearance seen in the multiband images and the Planck 353 GHz data are evidence of (a) rapidly spinning elongated dipolar silicate grains aligning their long axes perpendicular to magnetic field lines, (b) parallel Kelvin-Helmholtz waveform structures (Heyer et al., 2016), and (c) legacy pressure discontinuities from gas that rose with Rayleigh-Taylor instabilities and turbulent shock fronts originating near the Galactic disc (Kiss et al 2006). **Fig. 65** to the right shows how Galactic disc light can reflect off magnetically aligned dust dipoles if they are aligned normal to the cloud's magnetic field direction.

Dust clouds in the Galactic disc have been detected from the disc plane to as far 350 pc into the outer thin disc. Normally they are too faint to see visually. But in two regions of the sky, the Polaris Flare and Magellan's Ghost, a fortuitous alignment of flat silicate dust particle surfaces at perpendicular angles to the ambient spiral disc's magnetic β -field create a shallow forescatter zone that reflects the integrated light of the Galactic disc located 18° to 23° above.

It is a lucky accident that a small portion of the forescattered IFN reaches our eyes on Earth — if those eyes happen to be in very dark skies and gazing in the right direction. The tiny enhancement of forescattered light we see provides just enough photons to brighten the cirrus to ± 24.5 MPSAS, just above the luminosity limit of human eyes.

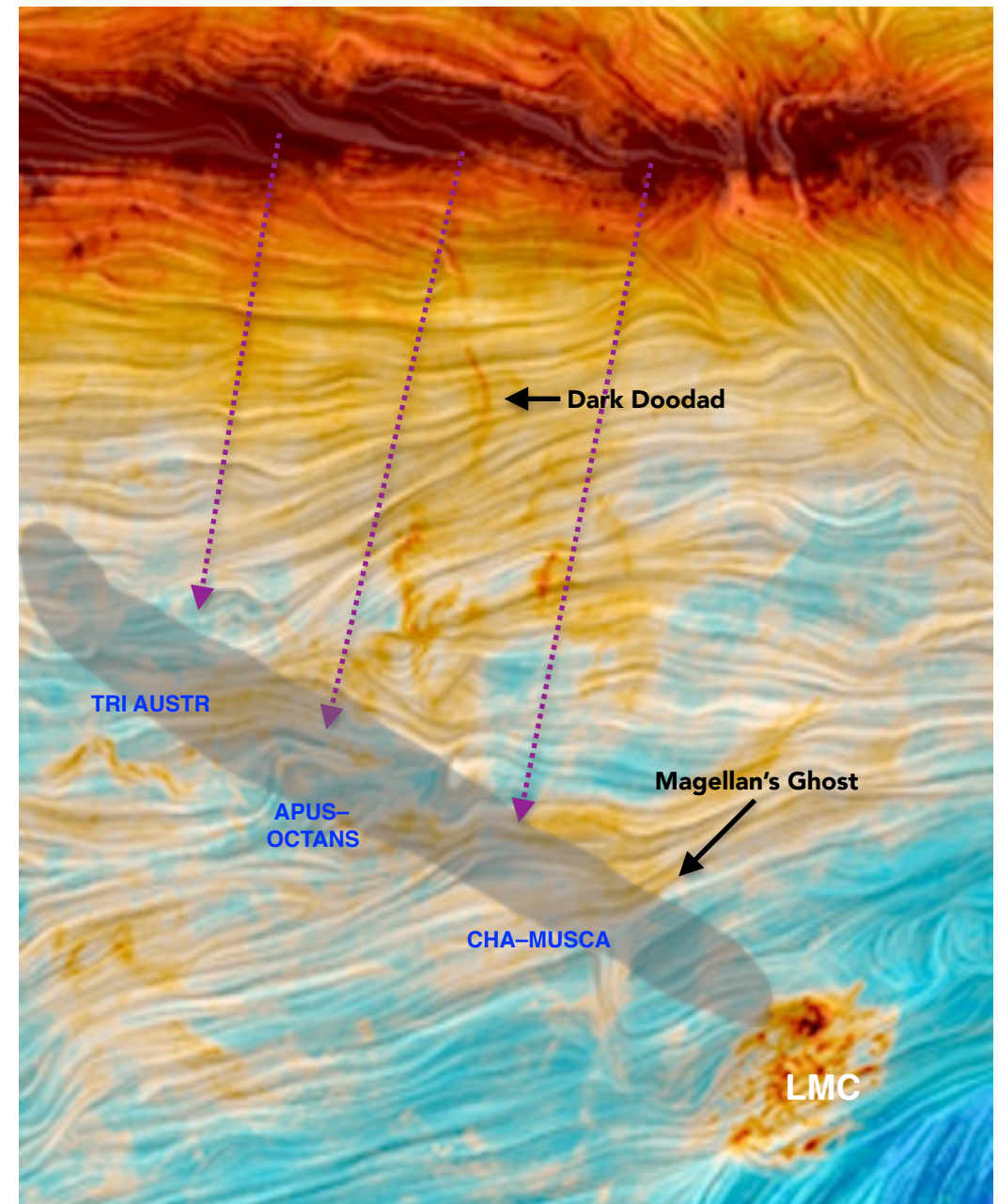
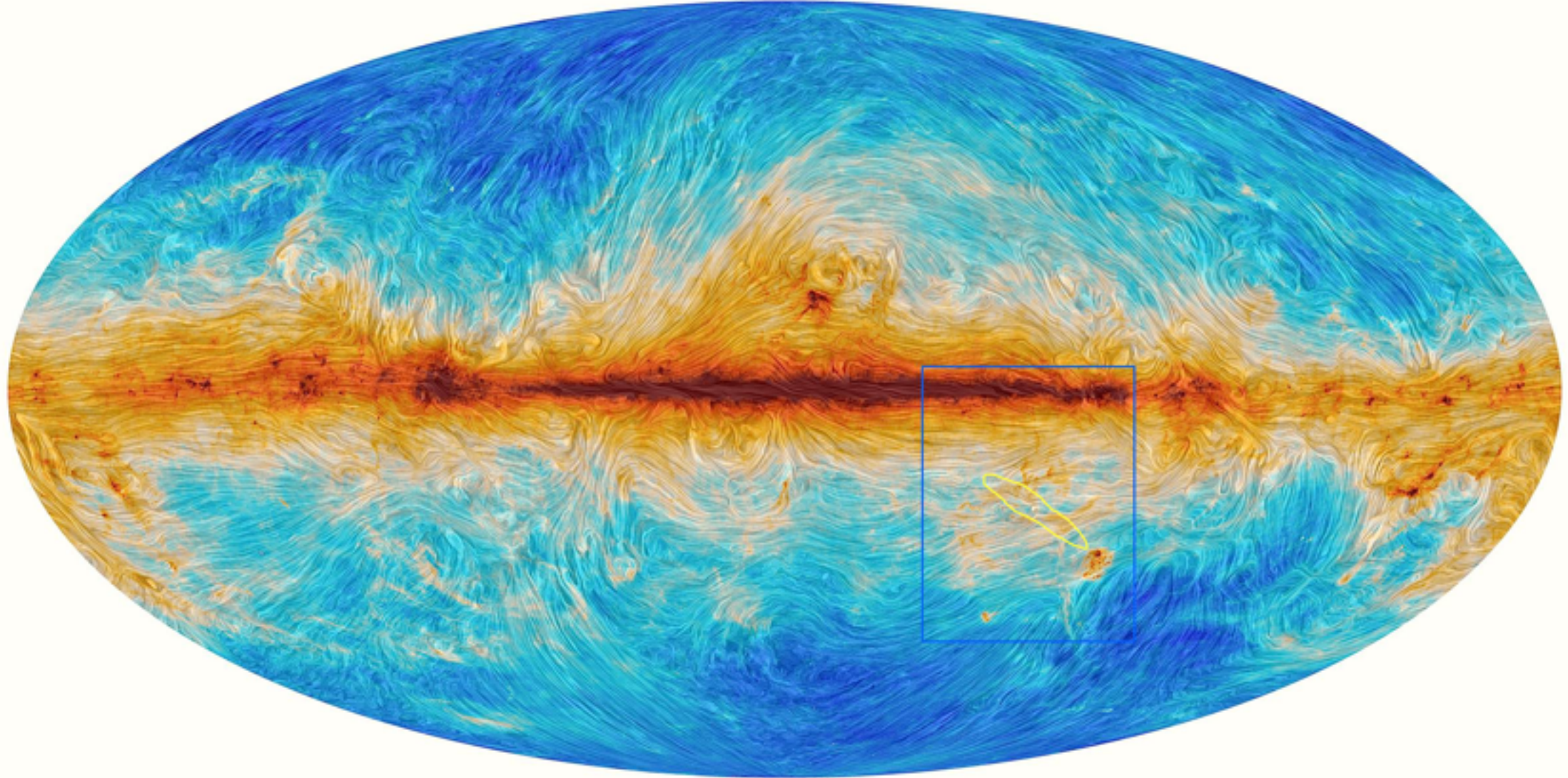


Fig. 65: Shadow image of Magellan's Ghost overlain on the Planck 353 Ghz map of magnetic fields in the South Equatorial Polar region.. The colour scale is **blue** = feeble field strength, **red-yellow** = strongest. Source: [Planck Legacy Archive](#).

All because of a lingering glance



Sherlock would indeed have been impressed by so circuitous a clue.

= Douglas Bullis =